

**The interplay between apoptotic cells and
macrophages: impact on the phenotype and
function of macrophages**

*Wechselwirkungen zwischen apoptotischen Zellen und Makrophagen:
Auswirkungen auf den Phänotyp und die Funktion von Makrophagen*

Dissertation with the aim of achieving a doctoral degree (Dr. rer. nat) at the
Faculty of Mathematics, Informatics and Natural Sciences
Department of Biology
University of Hamburg

Submitted by Imke Liebold from Hamburg,
Hamburg, March 2021

Day of oral defence 14.05.2021

Gutachter: Prof. Dr. Julia Kehr

Gutachter: PD Dr. Thomas Jacobs

Statuary declaration / Eidesstattliche Versicherung

Hiermit erkläre ich an Eides statt, dass ich die vorliegende Dissertationsschrift selbst verfasst und keine anderen als die angegebenen Quellen und Hilfsmittel benutzt habe.



Hamburg, den 14.03.2021

Nachweis über die Korrektheit der Sprache

Hiermit bestätige ich, Madeleine Hamley, geb. 02.10.1991 in London, dass die vorliegende Dissertation „Interplay of apoptotic cells and macrophages: impact on the phenotype and function of macrophages“ sprachlich korrekt ist.

Hamburg, den 01.03.21

A handwritten signature in black ink, appearing to read 'Madeleine Hamley', written over a horizontal line.

(Ort, Datum und Unterschrift)

Danksagung

Mein Dank geht an PD Dr. Thomas Jacobs für die lange und hervorragende Unterstützung meines wissenschaftlichen Werdegangs. Insbesondere möchte ich mich für die Betreuung und die Bereitstellung der Arbeitsmöglichkeit am BNITM bedanken, ohne die es mir nicht möglich gewesen wäre meine Doktorarbeit anzufertigen. Vielen Dank für unsere Diskussionen, deine Ideen und deine immer offene Tür für Hilfe und Fragen.

Des Weiteren möchte ich mich bei Prof. Dr. Julia Kehr ganz herzlich für die Übernahme der Gutachterin bedanken.

Ein besondere Dank geht an Lidia Bosurgi Ph.D. Per il suo grande lavoro di supervisione, le arricchenti discussioni e la libertà nello sviluppo del progetto attraverso le mie idee e ipotesi, vorrei ringraziarvi. Il nostro inizio di laboratorio assieme è stato non solo divertente, ma anche istruttivo e formativo. Grazie per aver sempre avuto una risposta a tutte le mie domande.

Ich möchte mich bei allen Immunologen vom ganzen Herzen für die freundliche und angenehme Arbeitsatmosphäre bedanken. Vor allem möchte ich mich bei Amirah Al jawazneh und Madeleine Hamley für die wunderbare Hilfe an langen Experimenttagen und die wissenschaftlichen Diskussionen bedanken. Zusätzlich möchte ich Rosa Gálvez, Nadine Stetter, Franziska Muscate und Stefan Honoew für ihre Hilfsbereitschaft in jeder nur erdenklichen Situation auch jenseits der Wissenschaft danken, sowie Ulricke Richardt, der ich jede Frage dreimal stellen durfte. Bei Lea Kaminski und Mathias Riehn möchte ich mich für die aufschlussreichen Diskussionen sowie die persönliche Unterstützung danken. Stephanie Leyk danke ich, für ihren Zuspruch und Hilfe besonders in der letzten Phase der Arbeit. Birgit Hüsing danke ich für die Hilfe beim Zell-sortieren.

Ein besonderer Dank geht an Riekje Winzer für das nächtliche Korrekturlesen und die großartige Unterstützung über die gesamte Zeit meiner Doktorarbeit- tausend Dank für alles!

Am Ende möchte ich mich bei meiner Familie, meinem Freund und all meinen Freunden bedanken. Ohne euch wäre diese Dissertation nicht möglich gewesen. Ich danke euch vom ganzen Herzen.

Tablet of content

Abbreviations	VIII
List of figures	X
List of tables	XII
Abstract	XIII
Zusammenfassung	XIV
1 Introduction	1
1.1 The immune system – a short overview	1
1.1.1 Types of macrophages and their development.....	2
1.1.1.1 Macrophages in homeostasis.....	3
1.1.1.2 Polarisation of macrophages during tissue damage und disease	4
1.2 Phagocytosis.....	6
1.2.1 Phosphatidylserine-induced phagocytosis of apoptotic cells	6
1.3 Apoptosis.....	9
1.4 Schistosomiasis.....	11
1.4.1 Life cycle of <i>Schistosoma mansoni</i>	12
1.4.2 Immune response during <i>Schistosoma mansoni</i> infection	14
1.5 Aim of the study	18
2 Materials	19
2.1 Laboratory equipment.....	19
2.2 Glass and plastic consumables	20
2.3 Chemicals and reagents.....	20
2.4 Media and Buffers	21
2.5 Commercially available kits	22
2.6 Software	22
2.7 Antibodies.....	23
2.8 Primer sequences for qPCR	24
2.9 Cell line	25
2.10 Parasite.....	25
2.11 Mice strains	25
3 Methods	26
3.1 Cell culture and <i>in vitro</i> experiments	26

3.2	Hepa 1-6 culture	26
3.3	Cell count	26
3.4	Isolation of bone marrow-derived macrophages	26
3.5	Isolation of neutrophils	27
3.6	Induction of apoptosis	27
3.7	Staining of apoptotic cells	27
3.7.1	Apoptotic cell staining with Annexin V and PI	27
3.7.2	Apoptotic cell staining with TUNEL	27
3.8	Polarisation assay	28
3.9	Phagocytosis assay	28
3.10	Flow cytometry	29
3.11	Fluorescence-activated cell sorting (FACS)	29
3.12	RNA isolation and quantitative real-time PCR analysis	30
3.13	Cytokine detection	31
3.13.1	Enzyme linked immunosorbent assay (ELISA)	31
3.13.2	LEGENDplex™	32
3.14	Mice	32
3.14.1	Genotyping <i>Csf1R-Cre Axl^{fl/fl} Mertk^{fl/fl}</i> -mice	32
3.14.2	Cell isolation from different organs	33
3.14.2.1	Isolation of macrophages from the liver	34
3.14.2.2	Isolation of lamina propria leukocytes	34
3.14.2.3	Isolation of leukocytes from the lymph nodes	34
3.14.3	Thioglycollate-induced peritoneal inflammation	35
3.14.4	<i>Schistosoma mansoni</i> infection	35
3.14.5	Adoptive transfer of macrophages	35
3.14.6	Determination of alanine transaminase levels in the serum	36
3.14.7	Determination of the egg count in liver and colon	36
3.14.8	Histology analysis	36
3.15	RNA-based next-generation sequencing (RNAseq) analysis	36
3.16	Single cell sequencing (ScSeq)	37
3.17	Statistics	37
4	Results	38
4.1	Apoptotic cells with different origins expose similar amounts of PtdSer while being TUNEL negative, and are able to be phagocytosed by macrophages	38

4.2	Macrophages acquire a tissue remodelling phenotype after sensing apoptotic neutrophils, but not after phagocytosis of apoptotic thymocytes or apoptotic hepatocytes	40
4.3	PtdSer alone is not sufficient for the induction of a tissue remodelling phenotype in macrophages nor is a soluble factor released by neutrophils	44
4.4	Apoptotic cells with different identities shape the IL-4-induced response of macrophages	48
4.5	Macrophages' heterogeneity during <i>Schistosoma mansoni</i> infection is a consequence of phagocytosis of different apoptotic cells	51
4.6	Blocking phagocytosis during schistosomiasis reveals its impact on the function of macrophages	53
4.7	The transfer of macrophages treated with apoptotic neutrophils <i>in vitro</i> is beneficial for the <i>Schistosoma mansoni</i> -infected host	59
4.8	Characterisation of phagocytosis receptor expression on human CD14 ⁺ monocytes during schistosomiasis	62
5	Discussion	63
5.1	Induction of the tissue remodelling phenotype is exclusive to apoptotic neutrophils.....	63
5.2	The nature of an apoptotic cell modulates the function of macrophages	68
5.3	The phagocytosis of specific apoptotic cells drives macrophages' heterogeneity during infection with <i>Schistosoma mansoni</i>	70
5.4	AXL and MERTK engagement is necessary for the uptake of apoptotic CD3 ⁺ cells and controls egg deposition and granuloma formation during <i>Schistosoma mansoni</i>	72
5.5	MMP14 and TIMP1 contribute to the egg transition through the liver	75
5.6	Apoptotic cells are able to shape the therapeutic potential of macrophages.....	77
5.7	The role of phagocytic receptor expression in human macrophages during schistosomiasis	79
6	Future perspective	81
6.1	Dissection of the crosstalk between macrophages and apoptotic cells	81
6.2	The therapeutic potential of macrophages.....	82
6.3	The impact of phagocytosis on human macrophages.....	83
7	References	84

Abbreviations

AC	Apoptotic cells
aH	Apoptotic hepatocyte
AM	Axl and MerTK
aN	Apoptotic neutrophil
APC	Antigen presenting cell
Arg1	Arginase 1
ARNT2	Aryl hydrocarbon receptor nuclear translocator 2
aT	Apoptotic thymocytes
ATP	Adenosine triphosphate
BMDMs	Bone marrow derived macrophages
CD	Cluster of differentiation
Chil3	Chitinase-like protein 3
Cre	Cre-recombinase
CSF1/CSF1-R	Colony stimulation factor 1 /-Receptor
DAMPs	Danger-associated molecular patterns
DC	Dendritic cell
DNA	Deoxyribonucleic acid
dNTP	Deoxyribonucleic triphosphate
Ear2	Eosinophil cationic protein 2
EDTA	Ehtylenediaminettetraacetic acid
ELISA	Enzyme-linked immunosorbent assay
f/f	Flox/flox
Fas-L	Fas Ligand (CD95L)
Fc	Fragment crystallisable region
FGF	Fibroblast growth factor
FMO	Flourescence minus one
Fn1	Fibronectin -1
FSC	Forward scatter
g	Gravitational force equivalent
GO-term	Gene ontology term
h	Hours
HRP	Horseradish peroxidase
i.p	Intraperitoneal
i.v.	Intravenous
IFN γ	Interferon gamma
IL	Interleukin
iNOS	Inducible nitric oxide synthase
KC	Kupffer cell
Klf	Kruppel factor like protein
MDMs	Monocyte derived macrophages
MerTk	Mer tyrosine kinase
min	Minutes
mL	Millilitre
mRNA	Messenger ribonucleic acid
MS	Multiple sclerosis

Abbreviations

M ϕ	Macrophage
NE	Neutrophil elastase
NK	Natural killer cell
ns	Not significant
p.i.	Post infection
PAMPs	Pathogen-associated molecular patterns
PBMC	Peripheral blood mononuclear cells
PBS	Phosphate buffer saline
PCR	Polymerase chain reaction
PDGF	Platelet-derived growth factor
PD-L1	Programmed cell death 1 ligand 1
PFA	Paraformaldehyde
PI	Propidium Iodide
PROS1	Protein s1
PRR	Pattern recognition receptors
PtdSer	Phosphatidylserine
PtdSer-R	Phosphatidylserine- Receptor
qPCR	Quantitative real time pcr
Retnla	Resistin-like molecule alpha
RNA	Ribonucleic acid
RNase2	Ribonuclease A family member 2
rpm	Round per minute
s	Seconds
s.c.	Subcutaneous
SEM	Standard error of the mean
SOCS	Suppressor of cytokine signalling
SSC	Side Scatter
TF	Transcription factor
TFG β	Transforming growth factor beta
Th	T helper cell
Thbs1	Thrombospondin 1
TIM-4	T cell immunoglobulin and mucin domain containing 4
TLR	Toll like receptor
TNF α	Tumor necrosis factor α
Treg	Regulatory T cell
Treg	T regulatory cell
UTP	Uracil triphosphate
VEGF	Vascular endothelia growth factor

List of figures

Fig. 1: Sensing of apoptotic cells and IL-4 induces an anti-inflammatory, tissue remodelling phenotype in macrophages.	8
Fig. 2: Distribution of Schistosomiasis in 2014-WHO.	11
Fig. 3: Life cycle of <i>Schistosoma mansoni</i>	13
Fig. 4: Granuloma formation in the liver.	15
Fig. 5: Different apoptotic cell types have similar frequencies of phosphatidylserine and low frequencies of DNA breaks.	39
Fig. 6: Macrophages phagocytose apoptotic cells with different identities.	40
Fig. 7: The phenotype of macrophages is shaped by the origin of apoptotic cells they phagocytose.	42
Fig. 8: <i>In vivo</i> , aN+IL-4 induces higher frequencies of RELM α^+ and YM1 $^+$ macrophages compared to aT+IL-4 injection after peritonitis induction.	43
Fig. 9: PtdSer-provided liposomes are not able to potentiate the expression of tissue remodelling genes in macrophages compared to IL-4.	45
Fig. 10: aN do not release soluble factors during the co-culture with macrophages that are responsible for the induction of a tissue remodelling phenotype in macrophages.	46
Fig. 11: The formation of NETs does not contribute to the induction of a tissue remodelling phenotype in macrophages.	47
Fig. 12: The identity of the apoptotic cell phagocytosed affects the expression of phagocytic receptors in macrophages.	48
Fig. 13: IL-4-induced transcriptional profile of macrophages is dependent on the apoptotic cell they are phagocytosing.	50
Fig. 14: Single cell sequencing (scSeq) of cells isolated from the liver of <i>S. mansoni</i> -infected mice reveals four distinct macrophage clusters.	52
Fig. 15 Macrophage heterogeneity in mice infected with <i>S. mansoni</i> is driven by phagocytosis of different apoptotic cells.	53
Fig. 16: Liver macrophages express high levels of <i>Axl</i> and <i>Mertk</i> in steady stage.	54
Fig. 17: Depletion of <i>Axl</i> and <i>Mertk</i> during the infection with <i>S.mansoni</i> results in accumulation of apoptotic cells in the liver.	55
Fig. 18: Blockage of phagocytosis during the infection with <i>S. mansoni</i> leads to a more severe disease phenotype.	56
Fig. 19: Fibrosis-associated cytokines are enhanced in the serum of <i>Csf1r-Cre⁺AM^{f/f}</i> mice.	57
Fig. 20: Cytokine production from mesenteric lymph nodes is not altered in <i>Csf1r-Cre⁺AM^{f/f}</i> infected mice.	57

Fig. 21: Liver macrophages from *S. mansoni*-infected *Csf1r-Cre⁺AM^{f/f}* mice have an increase in fibrosis markers..... 58

Fig. 22: Transfer of macrophages pre-treated *in vitro* with aN decreases the egg count in the colon of *S. mansoni*-infected mice. 60

Fig. 23: Transfer of macrophages co-cultured *in vitro* with aN increases *Tgfβ* and *Mmp14* expression in the colon of *S. mansoni*-infected mice..... 60

Fig. 24: Recipient mice showed lower amounts of ARG1⁺ macrophages after transfer of macrophages pre-treated with aN *in vitro*. 61

Fig. 25: CD14⁺ cells from patients with *S. mansoni* infection have an increased phagocytosis receptor expression. 62

List of tables

Table 1: Laboratory Equipment and companies	19
Table 2. Plastic and glass consumables	20
Table 3. Chemicals and molecular biology reagents	20
Table 4: Media and Buffers	21
Table 5. Kits	22
Table 6. Programs and purpose.....	22
Table 7: Mouse antibodies with clones, dilution factors and company	23
Table 8: Mouse Primers for qPCR.....	24
Table 9: Eukaryotic cell line	25
Table 10: Mice strains	25

Abstract

Macrophages are a heterogeneous population of innate myeloid cells which appear in every tissue. Depending on their environment, they exert numerous tissue-associated functions as reflected by their transcriptional heterogeneity. The capacity to phagocytose foreign or damaged cells is a common function of macrophages across all tissues and is performed during their whole life span. The constant clearance of apoptotic cells by macrophages is essential for the functionality of the immune system. In particular, phagocytosis of apoptotic cells in the presence of IL-4 and IL-13 drives macrophages towards an anti-inflammatory/tissue remodelling phenotype. Although apoptotic corpses might originate from different cells, up to now they have been defined only by typical morphological changes such as the exposure of phosphatidylserine, membrane blebbing and DNA fragmentation. The data presented in this thesis demonstrate that apoptotic cells are, in fact, a heterogeneous population of cells, which differentially imprint the transcriptome and function of macrophages in dependency of their original identity. Within the IL-4 response, only apoptotic neutrophils were able to induce a tissue remodelling phenotype in macrophages – an ability that was not observed in apoptotic thymocytes or apoptotic hepatocytes. Phagocytosis of apoptotic hepatocytes resulted in a tolerogenic function of macrophages, while apoptotic thymocytes restricted the IL-4 response. Even though the mechanism of how apoptotic neutrophils induce a tissue remodelling response in macrophages has not been fully unravelled, the requirement of a cell-cell contact is suggested. To verify whether these results were relevant in an *in vivo* setting, the *in vitro* experimental approaches were combined with a murine model of *Schistosoma mansoni* infection. It was discovered that during the infection, apoptotic cells with different origins accumulated in the liver. Furthermore, it was shown that the phagocytosis of apoptotic CD3⁺ cells via AXL and MERTK receptors affects granuloma formation and parasite egg deposition. In addition, it was demonstrated that the identity of the apoptotic cell could shape the therapeutic potential of macrophages, because only the adoptive transfer of macrophages that phagocytosed apoptotic neutrophils could reduce the deposition of parasite eggs and thereby ameliorate the immune pathology.

In conclusion, the obtained data provide evidence that the phagocytosis and identity of apoptotic cells actively contribute to the function and phenotype of macrophages. Furthermore, the reprogramming of macrophages driven by apoptotic cells can alter the fate of macrophages *in vivo* and could be used to change the outcome of *Schistosoma mansoni* infection in the future.

Zusammenfassung

Makrophagen sind eine heterogene Population von angeborenen myeloischen Zellen, die in jedem Gewebe vorkommen. In Abhängigkeit von ihrer Umgebung üben sie eine Vielzahl von gewebeassoziierten Funktionen aus, die sich in ihrer transkriptionellen Heterogenität widerspiegeln. Unabhängig von dem Gewebe in dem sie vorkommen besitzen alle Makrophagen die Fähigkeit Pathogene oder geschädigte Zellen zu phagozytieren und dies wird während ihre gesamte Lebensspanne ausgeführt. Die ständige Beseitigung von apoptotischen Zellen durch Makrophagen ist essentiell für die Funktionalität des Immunsystems. Die Phagozytose von apoptotischen Zellen in der Gegenwart von IL-4 und IL-13 induziert einen entzündungshemmenden/gewebsumbauenden Phänotyp in Makrophagen. Obwohl apoptotische Zellen aus unterschiedlichen Zelltypen entstehen können, wurden sie bisher nur durch typische morphologische Veränderungen wie die Freilegung von Phosphatidylserin, Membran-Blebbing und DNA-Fragmentierung definiert. Die Ergebnisse der vorliegenden Arbeit zeigen, dass es sich bei apoptotischen Zellen um eine heterogene Zellpopulation handelt, die das Transkriptom und die Funktion von Makrophagen in Abhängigkeit von ihrer ursprünglichen Identität unterschiedlich prägen. Innerhalb der IL-4-induzierten Makrophagen-antwort waren nur apoptotische Neutrophile in der Lage, einen gewebsumbauenden Phänotyp in Makrophagen auszulösen - eine Fähigkeit, die bei apoptotischen Thymozyten oder apoptotischen Hepatozyten nicht beobachtet wurde. Die Phagozytose von apoptotischen Hepatozyten führte zu einer tolerogenen Funktion der Makrophagen, während apoptotische Thymozyten die IL-4-Antwort einschränken. Obwohl der vollständige Mechanismus, wie apoptotische Neutrophile eine gewebsumbauende Antwort der Makrophagen induzieren, nicht vollständig aufgeklärt werden konnte, deuten die Ergebnisse auf die Notwendigkeit eines Zell-Zell-Kontaktes hin. Die Ergebnisse wurden in ein *murines* Modell der *Schistosoma mansoni* Infektion übertragen. Es wurde festgestellt, dass sich während der Infektion apoptotische Zellen unterschiedlicher Herkunft in der Leber anreichern. Weiterhin konnte gezeigt werden, dass die Phagozytose von apoptotischen CD3⁺ Zellen über die AXL- und MERTK-Rezeptoren, die Granulom-Bildung und die Ablage der Parasiteneier beeinflusst. Darüber hinaus konnte gezeigt werden, dass die Identität der apoptotischen Zelle das therapeutische Potenzial von Makrophagen prägen kann, da nur der adoptive Transfer von Makrophagen, die zuvor apoptotische Neutrophile phagozytiert haben, die Ablagerung von Parasiteneiern reduzieren konnte und damit die Immunpathologie verbesserte. Zusammenfassend zeigen die gewonnenen Ergebnisse, dass die Phagozytose und Identität apoptotischer Zellen aktiv zur Funktion und zum Phänotyp von Makrophagen beitragen. Darüber hinaus kann die, durch apoptotische Zellen gesteuerte, Reprogrammierung die Bestimmung der Makrophagen *in vivo* verändern und könnte in Zukunft zur Verbesserung von Infektionsverläufen eingesetzt werden.

1 Introduction

1.1 The immune system – a short overview

The immune system protects the host from infections with parasites, viruses, bacteria and/or fungi¹. It contains various cellular and soluble components that operate in a complex interplay to ensure a rapid elimination of pathogens without causing harm to the host. Accordingly, the immune system establishes self-tolerance and is able to identify self- and non-self-cells, and distinguishes between normal/healthy and degenerated/abnormal cells. The immune system consists of an innate and an adaptive arm. While the innate response is engaged early after the perturbation occurs and contributes to the non-specific defence of the host, the adaptive immune system, including B and T cells, is known for its high specificity against the invading pathogen. Antibodies are exclusively produced by B cells, which rapidly develop into plasma cells producing IgM as first defense². After activation and presentation of antigens to T cells, B cells receiving signals via the CD40L/CD40 axis undergo an immunoglobulin switch, therefore producing IgA, IgG or IgE^{3,4}. T cells mature in the thymus into CD8⁺ cells, prone to kill or suppress the target cell, or into CD4⁺ cells, known as T helper cells (Th cells)³. T helper cells are able to further specialise into different subpopulations such as Th1, Th2, Th17⁵. Th17 cells are defined by the production of IL-17 and IL-22 and associated with neutrophil and monocyte recruitment, thereby involved in destroying bacteria and fungi³. IFN γ is the defining cytokine of Th1 cells, which are associated in an immune reaction against intracellular pathogens and activation of macrophages. Th1 cells are mainly associated with a pro-inflammatory type 1 immune response in which pro-inflammatory cytokines are produced (e.g. tumor necrosis factor α (TNF α) and IL-2)⁶. Th2 cells are defined by the production of IL-4, IL-5 and IL-13⁷. They activate mast cells, eosinophils and anti-inflammatory/tissue remodelling macrophages and thereby contribute to the elimination of helminths. Th2 cells are highly induced in a type 2 immune response³. To establish an infection, invading pathogens need to overcome the first line of defence of the immune system, which comprises mechanical barriers, including the skin and mucous membranes, and innate immune cells like dendritic cells (DCs), natural killer (NK) cells, and macrophages. DCs appear in many subpopulations. However, besides playing a role in direct pathogen elimination, they mainly function as antigen-presenting cells (APCs). Through presenting antigens to naïve T cells, they initiate the adaptive immune response and directly shape T cell differentiation^{2,3,8}. NK cells are known for their rapid production of toxic granzymes and killing of virus-infected cells⁹. In addition, they are able to limit or exacerbate the immune response of DCs, macrophages, T cells or endothelial cells^{9,10}.

Macrophages are a heterogeneous population of myeloid cells and play a key role in development, defence and homeostasis of the host by reacting to different internal and external stimuli. Macrophages function, in addition to DCs, as professional APCs by presenting antigens to other immune cells, like T cells, and thereby link the innate and the adaptive immune system^{2,3}. Macrophages

are able to activate B and T cells and regulate proliferation and differentiation of lymphocytes¹¹. In addition, macrophages contribute greatly to the immune response against and the clearance of parasites like the helminth *S. mansoni*, highlighting their functional relevance for disease outcome.

1.1.1 Types of macrophages and their development

Macrophages are present in every tissue of adult vertebrates and can be divided into circulating/infiltrating macrophages and tissue-resident macrophages. Infiltrating macrophages derive mainly from monocytes. Monocytes can have multiple origins. They can originate from the foetal liver^{12,13} or hematopoietic stem cells that produce, after BM colonisation, bone marrow monocytes. However, under inflammatory conditions monocytes can differentiate in situ¹⁴. After tissue infiltration, monocytes can develop into monocyte-derived macrophages (MDMs) upon response to tissue specific signals. If resident tissue macrophages are depleted, monocytes with a foetal liver origin are more prone to replenish the niche and fulfil tissue-specific functions compared to monocytes with a BM origin¹². One of the major populations of MDMs is in the liver where they rapidly accumulate after toll-like receptor (TLR) activation. These cells are characterised by the expression of CX3CR1⁺ and Ly6C^{+/-}¹⁵. Macrophages inside the tissue without a monocyte progenitor are tissue-resident macrophages. They are found in essentially every tissue e.g. as Kupffer cells (KCs) in the liver or even inside the epidermis, such as Langerhans cells¹⁶⁻¹⁸, which were historically defined as DCs, but through further transcriptional profiling considered now as tissue-resident macrophages¹⁹⁻²¹. Most of the tissue-resident macrophages derive from the yolk sac and have a long life span. Under homeostatic conditions, they mainly renew themselves by local proliferation and are not replaced by cells from the BM. However, macrophages in the lung and kidney have chimeric origins from hematopoietic stem cells and the yolk sac, and BMDMs replace prenatal-derived macrophages in the gut^{22,23}. Tissue-resident macrophages are known for their heterogeneity, but still share some common features like the expression of the surface markers CD11b, F4/80 and CD64²⁴. Additionally, all macrophages have a core program of transcription factors (TF) like RUNX1 (runt-related transcription factor 1), CEBPs (CCAAT/Enhancer-Binding-Protein) and high levels of the TF PU.1 (SPI1). Tissue-resident macrophages are dependent on signalling via the CSF1-CSF1R-axes (colony stimulating factor 1/- receptor) for their development and proliferation. A deficiency in one arm of CSF1-CSF1R-axes leads to a severe monocytopenia or depletion of tissue macrophages, as seen in mice with a *Csf1r* mutation that have a loss of microglia²⁵⁻²⁷. In addition, granulocyte-macrophages colony-stimulating factor (GM-CSF) and vascular endothelial growth factor (VEGF) contribute to the growth and development of macrophages¹². Besides these common features, specific TF, metabolites, chemokines and other tissue-specific signals are able to modify their phenotype and function, thus contributing to the vast heterogeneity of tissue-resident macrophages. The tissue where they are located determines the

phenotype and nomenclature of resident macrophages. Hence, each resident macrophage population has a unique expression pattern of transcription factors regulated by tissue-specific signals. For instance, microglia, macrophages in the brain, are involved in brain surveillance and development²⁸ and regulate the synaptic pruning or neuronal proliferation. These cells are characterised by the microglia-specific TF, SALL1 (spalt-like transcription factor 1). IL-34, one of the ligands for CSF1R, and transforming growth factor β 1 (TGF β 1) are important for the development and maintenance of microglia²⁰. Intestinal macrophages are responsible for the pathogen elimination in the gut. To this end, they are able to interfere with the host-microbiota and regulate gut inflammation²⁹. In addition, the differentiation of intestinal macrophages depends on TGF β 1 and the TF RUNX3^{30,31}. TGF β is also involved in the development of KCs. KCs are located inside the liver sinusoids and perisinusoidal space³² and one of their main functions is to clear the portal blood flow from small particles, senescent red blood cells and cell debris³³. However, the key regulator for their development is DNA binding 3 (ID3). It regulates TGF β , and a deletion of *Id3* results in reduced numbers of KCs that originate from foetal-derived erythroid myeloid progenitors³⁴. In addition, the TFs LXR α (liver x receptor α) and SPIC are suggested to be involved in the specialisation of KCs³⁵, whereby after loss of KCs, monocytes that are recruited from the BM inside the liver, can acquire a KC-like phenotype, including the expression of transcription factor LXR α and ID3. This process is dependent on TNF and IL-1-induced endothelia and stellate activation respectively³².

1.1.1.1 Macrophages in homeostasis

Macrophages exert a variety of functions that all contribute to maintenance or re-establishment of tissue homeostasis. Besides antigen presentation, immune sentinel functions or phagocytosis, they are responsible for maintaining a constant level of metabolites like glucose, iron, amino acids or lipids^{15,36}. Tissue integrity, for example in the eye, is maintained by macrophages through messenger transport to neighbouring cells³⁷. However, more complex mechanisms to maintain tissue integrity like regulation of matrix metalloproteinase (MMP) expression or VEGF to induce angiogenesis are additionally mediated by macrophages^{38,39}. The phagocytosis of cell debris by macrophages allows the normal function of organs. Moreover, the phagocytosed cells or tissue compartments are often recycled for production of new proteins in an energy-efficient manner⁴⁰. Small injuries are rapidly healed by the tissue-resident macrophages, preventing constant inflammatory responses in the host^{22,41}. Since macrophages are also found in tissues where no blood vessels exist, like the cornea or inside the joints, they are responsible for translating tissue information into daily tissue function. Besides these quotidian functions, macrophages regulate changes in the metabolism of the host. For example, they are able to sense hormone changes during pregnancy and induce an immune-tolerant environment for the embryo. Furthermore, macrophages are important for the homeostasis of the

internal fluid system. Macrophages inside the skin sense electrolyte compositions of the lymphatic system and in response can upregulate TF to induce the production of osmoprotective genes to overcome osmotic stress and to re-establish homeostasis⁴². Furthermore, macrophages are able to communicate with other cell types to maintain homeostasis as e.g. NK cells (via IL-10 or IL-1 β), innate lymphoid cells or T cells (via PD-1/PD-L1, IL-10, IL-4 or IL-13)⁴³. However, macrophages are also able to regulate themselves. They are able to produce factors, like small molecules or nucleotides, to maintain homeostasis after receiving stress signals, like TLR stimulation. In line with this, regulatory mechanisms are also activated simultaneously by macrophages to restrict their own response and to re-establish homeostasis⁴⁰.

1.1.1.2 Polarisation of macrophages during tissue damage und disease

Besides their contribution to the maintenance of tissue homeostasis, macrophages are also highly involved in tissue damage and diseases. After tissue damage, high amounts of infiltrating monocytes are recruited from the blood to the site of injury. Macrophages are highly plastic and able to polarise into different phenotypes, with environmental factors and the surrounding tissue as key factors for the polarisation⁴⁴⁻⁴⁶. Over the last years, many definitions of subpopulations and nomenclatures of macrophages have been proposed. From first distinguishing between interferon γ (IFN γ)/TLR and IL-4 induced macrophages^{44,47}, over M1 (classical activated macrophages by IFN γ) and M2 macrophages (alternative activated macrophages by IL-4/IL-13)⁴⁸, to a more subdivided polarisation nomenclature as M2a, M2b etc.^{49,50} or classifications by the decisive generating agents such as GM-CSF1 or MCSF1^{51,52}. Put simply, macrophages can polarise into a more pro- or anti-inflammatory phenotype.

The pro-inflammatory phenotype is induced e.g. by pathogen-associated molecular patterns (PAMPs) and damage-associated molecular patterns (DAMPs) and characterised by the release of IL-12, IL-1 or TNF α ^{41,53} as well as by the production of reactive oxygen species (ROS) like iNOS (inducible nitric oxide synthase) as an anti-microbial defence mechanism³. Induction of a pro-inflammatory phenotype ensures tissue sterility after bacterial infection or injuries and is often associated with Th1 cell activities that themselves activate pro-inflammatory macrophages through IFN γ and CD40-CD40L interactions³ (see 1.1). This pro-inflammatory response of macrophages is obligatory for the clearance of invading pathogens and thereby advantageous for the host. However, if not controlled, an exacerbated immune response leads to immune pathology. In some individuals, this results in the cytokine storm syndrome and lymphocytopenia, characterised by elevated production of TNF α and IL-6 by macrophages^{13,54}.

To control the pro-inflammatory response, macrophages can polarise into a more anti-inflammatory/tissue remodelling phenotype, which actively suppresses the expression of IL-6 and

TNF α , terminates inflammation and initiates repair mechanisms. This polarisation happens mainly after Th2 cell activation and upon production of IL-4/IL-13/IL-33 from Th2 cells, innate lymphoid cells, B cells, mast cells, basophils, eosinophils or during the course of parasitic infections and allergies⁵⁵. However, in a setting of allergies a more detailed characterisation of the tissue remodelling phenotype of macrophages is needed, since the response of macrophages cannot be described as an anti-inflammatory one in this context. The tissue remodelling/anti-inflammatory phenotype is characterised by the production of cytokines like IL-4, IL-10 and TGF β and growth factors like platelet-derived growth factors (PDGFs), fibroblast growth factors (FGFs) or VEGFs^{17,49,56–58}. A further characteristic of the anti-inflammatory phenotype is the upregulation of tissue remodelling genes like *Cd206 (Mrc1)*, *Resistin-like molecule alpha (Retnla)*, *Arginase 1 (Arg1)*, *Chitinase-like protein 3 (Chil3)* or *Eosinophil cationic protein 2 (Ear2)*. Together these changes result in a tissue remodelling phenotype of macrophages. TGF β , for example, induces collagen synthesis, inhibits NO production and stimulates *Arg1* expression⁴⁸, whereas PDGFs activate fibroblast proliferation³. Consequently, anti-inflammatory macrophages are associated with defence responses against parasites and promotion of wound healing and tissue repair. Besides IL-33 and IL-21 that induce an anti-inflammatory phenotype of macrophages³, the sensing of IL-4 and IL-13 are the prototypical signals that trigger the acquisition of this anti-inflammatory profile in macrophages⁵⁸. Although IL-4R (IL-4 receptor) and IL-13R (IL-13 receptor) are both expressed by macrophages, their activation occurs at different stages of the immune response and their engagement results in the activation of distinct signalling pathways. IL-13R engagement is favoured in settings with persisting anti-inflammatory stimuli and the production of Th2 effector cell cytokines. IL-13 triggers the upregulation of the mannose receptor (CD206) and the depletion of the IL-13R α 1 results in allergen-induced airway hyperactivity in a model of infection with the helminth *Nippostrongylus braziliensis*⁴⁷. In contrast, IL-4R activation induces Th2 cell differentiation at an early stage and at low concentrations of IL-4. Continuous IL-4 signalling is accompanied with increased *Arg1*, *Chil3* and *Retnla* expression. The IL4R α 1 chain signals through a gamma chain and is phosphorylated by Jak2. If IL-13 binds the receptor, this is followed by activation of the STAT6 pathway in type II-mediated signalling. IL-4 binding to the receptor affects SHIP1/2. SHIP1/2 are further involved in macrophage protein phosphorylation by reducing IL-4 production from basophils⁵⁹. Afterwards, downstream triggering of the PI3K/Akt pathway induces type I (mediated mainly by IL-4) and type II (mediated predominantly by IL-13) signalling⁶⁰. Stimulation by the IL4R α 1 is essential for the protection against parasite infections like schistosomiasis⁶¹. During type 2 immune responses, IL-13/IL-4 is responsible for shifting iNOS synthesis towards ARG1 production in activated macrophages. This influences the permeability of the surrounding vessel, enhances cell division and recruitment, tissue integrity and wound healing.

Dysfunction of the activation of the tissue remodelling phenotype leads to enhanced or delayed healing and induces fibrosis when not tightly regulated (see 1.4.2). Additionally, IL-4/IL-13-induced macrophages play a role in tumour development and angiogenesis by producing e.g. VEGF, FGF or PDGF and in autoimmune diseases like asthma or insulin resistance.

1.2 Phagocytosis

The main function of macrophages is to engulf pathogens and altered self-targets (e.g. apoptotic cells and cellular debris, see 1.2.1)⁶². Phagocytosis plays a central role in several immunological processes like host defence, metabolic processes, autoimmunity, tissue remodelling and homeostasis^{63–67}. In general, the term phagocytosis describes the uptake of particles over 0.5 μm ⁶⁸. It is an actin polymerisation-dependent process and a well-orchestrated interplay between the cytoskeleton, membrane rearrangement and signal transduction. Several receptors have been described to be involved in the recognition of invading pathogens. The pathogen-recognition receptors (PRRs) on the surface of macrophages recognise conserved structures of pathogens, the PAMPS or DAMPs. Different classes of PRRs are evolutionarily conserved and expressed on the surfaces of phagocytes. For example, the Fc γ -receptors recognise opsonised coated particles^{69,70}, while TLRs are recognising PAMPS like LPS (TLR4), flagellin (TLR5), or dsRNA (TLR3). They are either expressed on the surface (TLR 1, 2, 4, 5 and 6) or in the endosomal membrane (TLR 3, 7, 8 and 9) of macrophages^{71,72}.

1.2.1 Phosphatidylserine-induced phagocytosis of apoptotic cells

Around one million cells are recycled in the human body every second. This amount of dying cells needs to be removed in order to maintain tissue function and provide space for healthy living cells. Illustrative processes are the elimination of spermatocytes or epithelial cells. In a homeostatic state this process is rapid and only small amounts of apoptotic cells are found inside the tissues⁷³. The process can be divided into three main steps that result in the complete digestion of the target: *i*) Recognition of “find me” and “eat me” signals of apoptotic cells, *ii*) Internalisation, *iii*) Phagosome formation and maturation to a phagolysosome^{68,69,74,75}.

The first step includes “find me” signals. “Find me” signals are soluble factors that attract phagocytes via a chemokine gradient. Chemokines like fractalkine, adenosine triphosphate (ATP) or uridine triphosphate (UTP) are some examples^{76,77}. Besides the “find me” signals, the “eat me” signals play a major role. “Eat me” signals are motifs or proteins exposed on the surface of apoptotic cells like ICAM-1/3, annexin I or calreticulin^{78,79}. The best understood “eat me” signal is the exposure of phosphatidylserine (PtdSer) by dying cells⁸⁰. Cells that go into apoptosis expose PtdSer, which is normally stored intracellularly on their surface in a caspase-dependent mechanism (see 1.3). PtdSer-receptors are a broad family of receptors that recognise the “find me” and “eat me” signals exposed

by apoptotic cells^{78,79}. Apoptotic cells are therefore recognised and internalised by PtdSer-receptor (PtdSer-R)-expressing cells, such as macrophages, which thereby can exert their function. The PtdSer-R family includes the BAI-1 (brain-specific angiogenesis inhibitor), TIM-4 (T-cell membrane protein 4) and CD300f, which are able to directly bind to PtdSer. MerTK, Axl and Tyro3 (TAM receptors, firstly described by Lai & Lemke⁸¹) as well as CD36 are not able to directly bind to PtdSer and require bridging molecules. TIM-4 is able to promote the engulfment of apoptotic cells, but is described as a tether rather than as a phagocytic receptor itself, because of its capacity to work in complexes with integrins or MerTK⁶². Resident cells which normally express the TAM receptors often additionally express TIM-4 in order to enhance apoptotic cell-engulfment^{76,82,83}. MerTK and Axl are tyrosine kinase receptors, which contribute greatly to the clearance of apoptotic cells. Ligand binding activates these receptors by dimerisation. Protein S (Pros1) and growth arrest specific 6 (Gas6) are two of the bridging molecules which close the gap between PtdSer and MerTK or Axl. On the side of the receptor, one of the two N-terminal immunoglobulin (Ig)-like domains binds Pros1 or Gas6. Gas6 has a higher affinity for Axl than MerTK, whereas Pros1 can bind to MerTK but not Axl. Both of these molecules bind to PtdSer in a Ca²⁺-dependent manner and are essential for the induction of phagocytosis⁸⁴⁻⁸⁶. BMDMs that differentiate in the presence of GM-SCF are more prone to express Axl, while in BMDMs differentiated with MCSF abundantly express MerTK but not Axl⁸⁵. However, on KCs MerTK and Axl are co-expressed and act synergistically⁸⁷. Inflammatory stimuli like LPS or TNF potently induce Axl expression in BMDMs. Surprisingly, IL-4 was additionally able to induce Axl expression⁸⁵. *In vivo* studies showed that the activation of Axl leads to a suppression of *Ifnb* and *Ifna4*, revealing that Axl is more relevant in an inhibitory feedback loop in inflammatory or tissue injury settings. Furthermore, Axl is able to cleave itself from the surface of macrophages by activating proteases upon ligand binding. Soluble Axl (sAxl) can be detected alone or as a sAxl-Gas6 complex in the blood. Here, elevated sAxl levels indicate that Axl is used in early stages of phagocytosis and able to act in synergy with another receptor called LRP-1 to enhance the engulfment⁸⁸. The central role of MerTK lays presumably in tolerance⁸⁵. A mild suppressive capacity of MerTK expression is observed after inflammatory stimuli. MerTK expression is upregulated by the addition of dexamethasone, LXR agonist or corticosteroids, while a downregulation of *Axl* mRNA occurs simultaneously in these settings⁸⁹. Moreover, the lack of either Axl or MerTK on macrophages reduced their phagocytic capacity^{85,86,90}.

Besides function as “eat me” signal, PtdSer itself plays a crucial role for the induction of the anti-inflammatory/tissue remodelling phenotype in macrophages. This phenotype is induced by two signals: *i*) the sensing of IL-4 or IL-13 and *ii*) the sensing of apoptotic cells (Fig. 1). PtdSer on the surface of apoptotic cells is sensed by macrophages via the PtdSer-R and if this interaction is inhibited, macrophages do not acquire tissue remodelling gene expression⁹¹. Therefore both signals are essential for macrophages to polarise into an anti-inflammatory/tissue remodelling phenotype⁹¹. Dysfunction in

the clearance of apoptotic cells, like the inhibition of PtdSer sensing by blocking with Annexin V or deletion of Axl and MerTK, leads to a decreased expression of tissue remodelling/anti-inflammatory proteins, apoptotic cell accumulation or the release of proteases from dead cells^{77,91}.

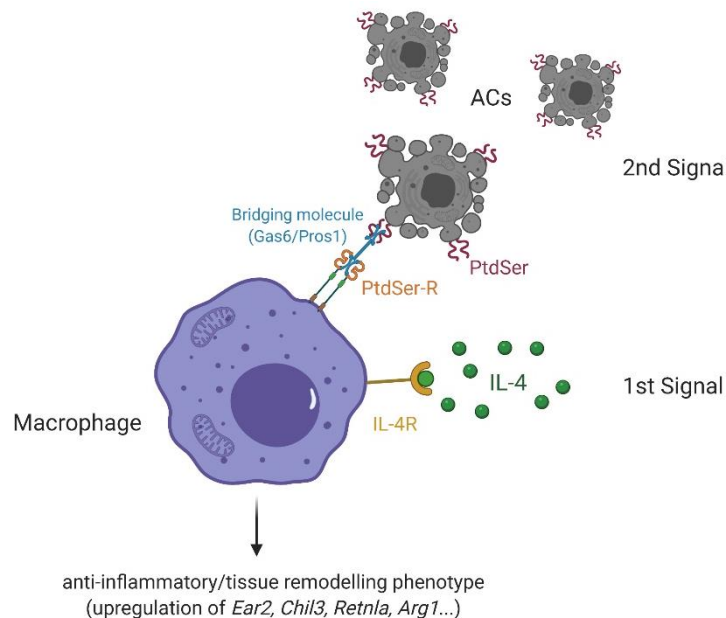


Fig. 1: Sensing of apoptotic cells and IL-4 induces an anti-inflammatory, tissue remodelling phenotype in macrophages.

Phosphatidylserine (PtdSer) is exposed on the surface of apoptotic cells (ACs). Macrophages are able to sense and engulf the ACs via their PtdSer-Receptor (PtdSer-R). If IL-4 is additionally sensed by the IL-4R, macrophages polarise into an anti-inflammatory phenotype. This is characterised by the upregulation of genes like *Arg1*, *Retnla* or *Chil3*. Created with BioRender.com.⁹²

In homeostatic condition, the clearance of apoptotic cells by macrophages takes place without any induction of inflammation or autoimmunity. Since the beginning of the 1990s it has been known that phagocytosis of apoptotic cells is not a silent process, but alters the environment. Indeed, after phagocytosis macrophages are able to induce an immune-suppressive environment⁹³. The engulfment of apoptotic cells, but not necrotic cells, induces the release of anti-inflammatory factors by activation of e.g. LXR α/β or PPAR γ/δ and factors like TGF β , Prostaglandins E2 (PGE2) and IL-10 are produced⁹⁴. In the presence of tissue injury, apoptotic cells can accumulate and provide inflammatory signals. To promote the resolution of this inflammation, apoptotic cells are phagocytosed by macrophages. Therefore, low amounts of endotoxins such as the sensing of DAMPs and PAMPs support the suppression of inflammatory cytokines produced by apoptotic cells. This process is mainly dependent on the ectonucleotidase CD73. Together with CD39, CD73 is involved in the degradation of ATP. CD39 converts ATP to AMP (adenosine monophosphate) and CD73 further dephosphorylates AMP to adenosine. During injury, apoptotic cells are able to release AMP, which is then further degraded to adenosine. Adenosine itself can suppress pro-inflammatory cytokines such as TNF α , favouring an

immune-regulatory phenotype of macrophages^{95,96}. Surprisingly, CD39 is not involved in this process. However, during sepsis, when TLR stimulation occurs, macrophages produce ATP and hydrolyse ATP themselves via CD39. In this way, macrophages regulate their own activation status towards a regulatory phenotype⁹⁷.

After the resolution of inflammation, new signals are needed to compensate for the damage and the loss of the cells. Therefore, removal of these apoptotic cells induces the secretion of regenerative signals. Factors like platelet-activating factor (PAF), hepatocyte growth factor (HGF) and VEGF are released and contribute to healing of the damaged tissue. In addition, macrophages differentiate into a tissue remodelling phenotype with the aim of helping to reconstruct the extracellular matrix (ECM) and favouring the healing process. TGF β secretion by macrophages suppresses' production of e.g. IL-12, IL-8, IL-1 β in an autocrine/paracrine manner. Phagocytosis receptors on the surface of macrophages contribute to the resolution. As an example, a direct anti-inflammatory effect by the suppression of NF- κ B has been described for MerTK⁹⁸. Additionally, regulatory T cells (Tregs) are activated by macrophages and take part in the induced immunosuppressive environment by phagocytosis^{93,99–104}. Ineffective clearance of apoptotic cells and the resulting accumulation contributes to chronic and autoimmune inflammation seen in e.g. systemic lupus erythematosus (SLE), Alzheimer's disease, atherosclerosis, cardiovascular disease and Parkinson's disease¹⁰⁵.

However, cells are able to inhibit their uptake by the exposure of "don't eat me" signals. The most prominent one is the SIRP1 α /CD47 axis¹⁰⁶. SIRP1 α (CD172) is mainly expressed on tissue-resident macrophages and myeloid cells. It contains an immunoreceptor tyrosine-based inhibition motif (ITIM), characteristic for inhibitory receptors. Although the interaction affinity between SIRP1 α and CD47 is low, CD47 is found on many cells of the immune system, like memory T cells. Here, the high amounts of CD47 on their surface favouring their survival, as the binding of CD47 to SIRP α inhibits the phagocytosis of the memory T cell¹⁰⁶. Additionally, the immunological synapses formed between target cells and macrophages could play a role. Neutrophils require the formation of an immunological synapse to kill target cells. However, disruption of the immunological synapse by the CD47-SIRP α interaction favours survival¹⁰⁷. In addition, the loss or dispersed expression of CD47 on the surface of cells induced the engulfment of the cell by macrophages¹⁰⁸.

1.3 Apoptosis

Apoptosis, a programmed form of cell death, is one important mechanism of the body to clear old or abnormal cells without inducing inflammation¹⁰⁹. The induction of apoptosis is a normal process during e.g. development and aging, like the deletion of the webbing between the finger of an embryo^{67,110}. Apoptosis is linked to anti-inflammatory responses when apoptotic cells are recognised and cleared by

phagocytes (see 1.2.1). If apoptosis is impaired, cells likely die via secondary necrosis, thus triggering a pro-inflammatory response. Apoptosis is a tightly regulated process, since apoptosis cannot be stopped easily once it has begun. Characteristic morphological changes during apoptosis are shrinkage of the cell, chromatin condensation, DNA fragmentation, membrane blebbing followed by fragmentation to apoptotic bodies or the exposure of “eat me” signals for phagocytosis (such as PtdSer)^{76,111,112}. Besides that, it is known that apoptosis depends on active protein synthesis since treatment with cyclohexamide and actinomycin D inhibits apoptotic morphological changes¹¹³.

Apoptosis can be induced by an intrinsic/mitochondrial or extrinsic pathway through different factors. Several of these factors have a pleiotropic function in the body. Hormones or growth factors are among these factors. On the one hand they actively block death pathways inside cells to keep them alive, on the other hand hormones such as corticosteroids induce apoptosis in e.g. thymocytes¹¹⁴. Toxins, heat, radiation, hypoxia, inflammation, pathogens and drugs are known to induce apoptosis in cells via the intrinsic/mitochondrial pathway. Under homeostatic conditions, pro-apoptotic proteins (e.g. Bax, Bak, Bid) are inhibited by anti-apoptotic proteins (e.g. Bcl-2, Bcl-xL) of the Bcl family inside the mitochondria. Briefly, the pro-apoptotic molecules induce permeabilisation of the mitochondrial membrane resulting in the release of cytochrome C. Afterwards, a complex consisting of cytochrome C, apoptotic protease activating factor 1 (APAF1) and inactivated caspase 9 is formed - the apoptosome. This complex initiates the final step of apoptosis induction. Here, through activated caspase 9, the effector caspases 3/6/7 are further activated resulting in the death of the cell^{115–117}.

Fas or TNF-receptors (TNF-R) can induce survival of the cells via the NFkB pathway, but more often activate apoptosis in cells after ligand binding. The induction of apoptosis via these receptors is described as the extrinsic pathway¹¹⁸. The best described death-receptors-ligand interactions are FAS-Receptor/FAS-Ligand, TNF-R1/TNF α and TRAIL-R1/R2/TRAIL (TNF-related apoptosis induced ligand-receptor 1 and 2/ TNF-related apoptosis induced ligand)¹¹⁹. FAS-L binding leads to FAS-Receptor clustering and recruitment of adaptor molecules like FAS-associated death domain (FADD) or tumour necrosis factor receptor type 1-associated DEATH domain (TRADD). FADD or TRADD recruit caspase 8, which oligomerises and self-cleaves. Caspase 8 then activates caspase 3, leading to apoptosis of the cell. In the intrinsic pathway the direct activation of caspase 3 always leads to apoptosis. In the extrinsic pathway the amount of activated caspase 8 is not always sufficient to activate caspase 3 and might be need to amplified^{115,116,118–120}. The morphological hallmarks of apoptosis mainly result from caspase activity. Inhibition of caspase activity leads to severe dysfunctions, like reduced life span or malformations. Blocking caspase binding sites in a flippase (ATP11C), which transports PtdSer from the outer membrane to the inner membrane in living cells, leads to the loss of PtdSer exposure on the surface of apoptotic cells and leads to apoptotic cell accumulation¹²¹.

Although apoptosis is a beneficial process (e.g. embryogenesis or clearance of old cells), it can have detrimental effects when induced by parasitic infections¹²². During *Plasmodium spp.* infection the induction of apoptosis in later stages of the disease helps the parasite through inhibition of a proper immune response, while helping the host to limit exaggerated inflammatory responses. At the same time, in the early phase the *sporozoites* are able to induce apoptosis in KCs, reducing the amount of produced cytokines for immune system activation¹²³. In Chagas disease, the apoptosis of cardiomyocytes is one of the most severe characteristics of the pathology. While infected cells seemed to be protected from apoptosis, uninfected neighbouring cells received apoptosis signals from infected cells, which were reprogrammed by the parasite. This indicates that the increased area of dying cells may inducing heart failure¹²². During infection with the parasite *Schistosoma spp.* numerous cells undergo apoptosis. Since for the present thesis the model of Schistosomiasis was used, the immune response against it is described in more detail below (see 1.4.2).

1.4 Schistosomiasis

Schistosomiasis, also known as bilharzia, is a parasite infection caused by the trematode worm *Schistosoma spp.* Over 240 million people worldwide are affected and would need preventive treatment¹²⁴. The majority of cases are located in Africa (around 90 %), but *Schistosoma spp.* are also endemic in Asia, Middle East, South America or South Europe (Fig. 2).

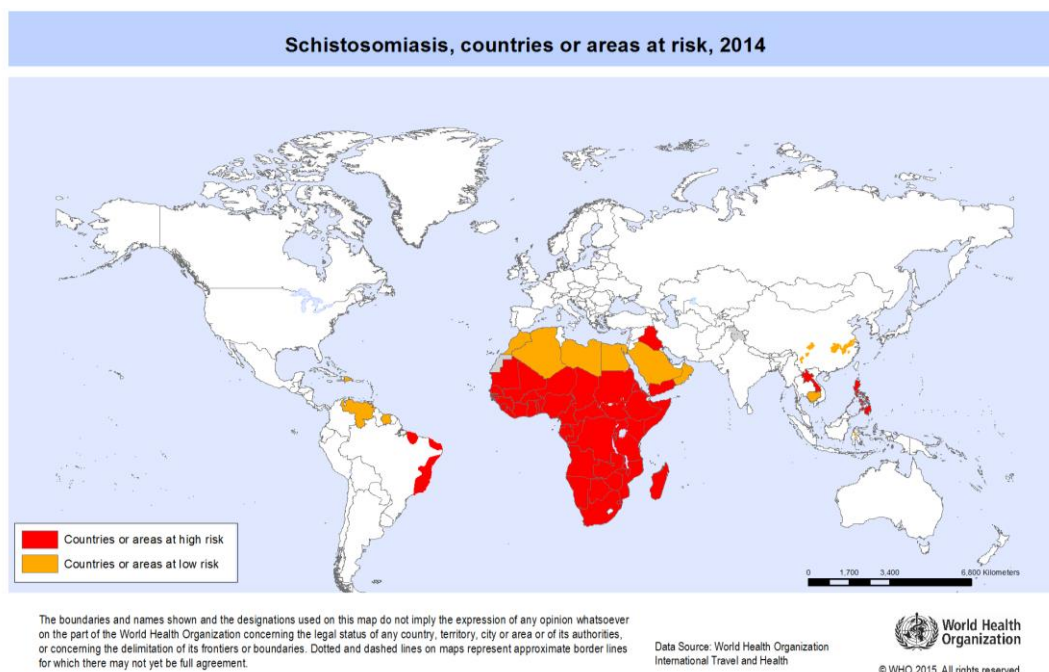


Fig. 2: Distribution of Schistosomiasis in 2014-WHO.

Schistosoma spp. prevalence shown over the world. Orange colour shows countries with low risk for the infection, while red coloured countries have a high risk for the infection. White countries have no risk or risk is not determined. ©WHO 2015.

Six human-pathogen species are known to induce different forms of schistosomiasis: *Schistosoma haematobium* causes urogenital schistosomiasis, while *Schistosoma guineensis*, *Schistosoma intercalatum*, *Schistosoma mansoni*, *Schistosoma japonicum*, *Schistosoma mekongi* cause intestinal schistosomiasis^{125,126}. The focus of this work lays on the most prominent species *Schistosoma mansoni* (*S. mansoni*); therefore the following parts are written with regard to the infection with this species.

The most vulnerable group are children over five years, pregnant women or persons with close contact to water, such as fishermen or people working in agriculture. Infected children are mostly affected by malnutrition or growth/mental defects. Pregnant women are at risk of premature delivery, low birth weight and increased mortality and morbidity rate. First symptoms of schistosomiasis occur 2-12 weeks (peaks 7-8 weeks) post infection. The acute phase of the disease is characterised by symptoms such as katayama fever, headache, myalgia, rash or bloody diarrhoea¹²⁷. Chronic manifestations of the disease can occur after months or years of infection, including symptoms like hypertension, ascites, liver failure or fibrosis. Over 3.3 million people suffer from a disability after infection with *Schistosoma spp.*, affecting their ability to work and acceptance in the community^{128,129}.

The presence of antibodies in the blood or eggs in the stool, detected with e.g. the Kato-Katz method, verifies schistosomiasis and the only available drug to treat schistosomiasis is praziquantel, which is broadly used. Although the WHO planned to eliminate the morbidity caused by schistosomiasis in African countries using praziquantel by the end of 2020, until 2018 more than half of the people requiring treatment had not been reached. In addition to this, praziquantel has several disadvantages: *i)* The drug is not effective against the juvenile worm or chronic forms of the infection. *ii)* Re-infection after treatments have often been reported, leading to long-term drug administrations over years. *iii)* No appropriate paediatric formulation of praziquantel is available for pre-school children, therefore resulting in high infection rates in early childhood and the risk of developmental retardation. Since praziquantel is the only available drug for the treatment of schistosomiasis the risk of drug resistance is high^{126,128}.

1.4.1 Life cycle of *Schistosoma mansoni*

S. mansoni is a soil-transmitting helminth and appears mostly in rural areas. With the rise of tourism, the number of infected tourists and the occurrence in urban areas is increasing. The transmission of the disease starts with an infected mammalian host (humans, dogs or mice) contaminating a freshwater source by releasing faeces or urine including eggs of the parasite. The eggs are hatched, develop into *miracidias* and are ingested by a freshwater snail - their intermediate host (Fig. 3). In the context of *S. mansoni*, a *Biomphalaria* snail represents the intermediate host. The larva asexually reproduce in the snail, as *sporocysts*. Approximately 250-600 *cercariae* are released into the water per day by the snail and need in a period of 48 h to find and actively penetrate their mammalian host.

Inside the host the *cercariae* develop over *schistosomula* to *schistosomes* while migrating through the blood or lymph vessel of the host to the lung¹³⁰. The worm remains there for more than two weeks until it enters the vessels again to reach the hepatoportal circulation. In the hepatoportal circulation, the parasite develops into an adult worm. *S. mansoni* worms then reach the mesenteric vessels of the large or small intestine (mainly colon and caecum). In the mesenteric vessel the worms are able to live up to 10 years, while mating and producing around 100-300 eggs per day^{127,131}. The eggs are released in the capillary walls where they are distributed through the blood flow or translocated into the intestinal lumen. The life cycle completes with the release of the eggs within the faeces or urine into a freshwater source.

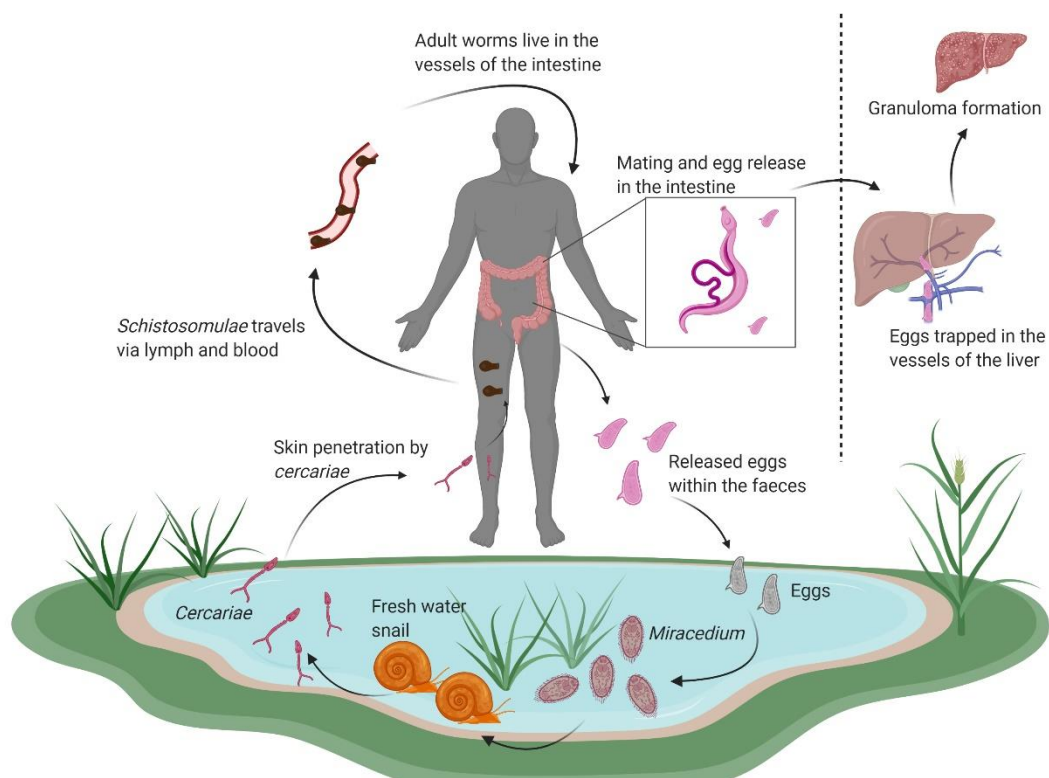


Fig. 3: Life cycle of *Schistosoma mansoni*.

The life cycle of *Schistosoma mansoni* consists of two parts. Eggs are released in the water and hatch into *miracidiums*. This stadium is able to invade fresh water snails, the animal host. *Cercariae*, the infectious stage of the worm, are released from the fresh water snail. Contact with the human host leads to active penetration of the skin by the *cercariae* within minutes. Inside the human host, the cercariae lose their tails and mature into *schistosomulae*. The *schistosomulae* are able to travel through the body via the lymph and the blood stream. The adult worms live in the vessels of the intestine. Here they mate and release eggs. Eggs are released by the faeces to complete the life cycle. Occasionally, these eggs become stuck inside the vessels of the liver, inducing granuloma formation. Created with BioRender.com⁹².

In most of the cases, the eggs are not excreted but swept into other organs. Most of the swept eggs are found in the liver. The eggs induce an inflammatory response due to their high antigenicity followed by the formation of a granuloma around the egg. This rearrangement of the tissue induces

fibrosis, leading to the pathology of the chronic-disease like portal lesion, hypertension and gastrointestinal bleeding up to liver failure¹³¹.

1.4.2 Immune response during *Schistosoma mansoni* infection

The first phase of the infection with *Schistosoma spp.* refers to the acute schistosomiasis while in the later stage chronic schistosomiasis manifests. In the acute phase, migrating *schistosomulae* induce a strong pro-inflammatory type 1 immune response in the host with elevated levels of IL-12, TNF α , IL-6 and IFN γ in the first 4-6 weeks of infection. These cytokines induce the katayama fever and lead to strong intestinal inflammation and death of the host if not restricted. To terminate this response, a type 2 response is induced, triggered by the production of eggs around 6 weeks post infection and the release of soluble egg antigen (SEA). Th2 cell polarisation is induced and accompanied by a decrease of IFN γ levels. The type 2 response increases eosinophils, IL-4, IL-5, IL-10 and IL-13 levels and induces the switch of antibody isotypes towards IgG and IgE. This response peaks 8 weeks post infection. The polarisation of macrophages towards a tissue remodelling, anti-inflammatory phenotype is essential for this switch and for the survival of the host. Furthermore, the polarisation is triggered in a feedback loop. However, IL-10 produced by macrophages plays a dual role during infection. In the acute phase IL-10 suppresses IFN γ and type 1 cytokines via IL-12/IL-12R, while in the later stages IL-10 is essential to control the type 2 response^{127,131}.

As described before (see 1.4.1), not-excreted eggs are trapped in the liver or intestine. The immunogenicity of the egg induces the formation of the granuloma around the egg guided by a fibrotic response¹³¹⁻¹³³. The response to the *schistosoma* egg can be separated into five steps: the weakly reactive, exudative, exudative-productive, productive and involutinal stages¹³². Around the eggs, accumulation of neutrophils and eosinophils leads to the early formation of a micro-abscess. This abscess matures into a granuloma. Epithelioid cells and macrophages surround the neutrophil eosinophils layer in the periphery. Hepatic stellate cells (HSC) are located in the Disse space of the liver and are responsible for maintaining the ECM. These cells are activated in response to the egg and trans-differentiate into a myofibroblast, producing high amounts of collagen^{127,129,134,135}. In the productive stage, myofibroblasts and collagen are present in the outer layer of the granuloma. B and T cells are infiltrating the granuloma during this stage. The closure line of the granuloma to the healthy tissue is formed by hepatocytes. In the involutinal stage, the degeneration of the egg leads to increased numbers of fibrocytes, an increase in collagen production and the formation of a new outer zone layer comprised of eosinophils, leukocytes and plasma cells. This formation involves a lot of remodelling of the surrounding tissues. In the last step, collagen necrosis induces shrinking of the granuloma and egg calcification. The chronic phase response decreases around three months post

infection, including reduced granuloma inflammation and hyporesponsiveness through increased levels in Tregs and B cells^{127,131,132}. The size of newly formed granuloma decreases over weeks 8-20 post infection, but are unresolved and stable in size at least till 32 weeks post infection¹³¹.

The composition of the granuloma differs in dependency of the tissue. The intestinal granuloma composition is more similar to the early stages of a liver granuloma. It consists of fewer eosinophils, T and B cells but more macrophages compared to a grown liver granuloma. It helps to translocate the egg into the gastrointestinal lumen and is mostly temporally restricted¹³⁶. Liver granulomas, on the other hand, are not able to shed, becoming fibrotic and inhibiting the release of hepatotoxic secretions from the eggs. Eosinophils, neutrophils, T and B cells are frequently found inside¹³¹.

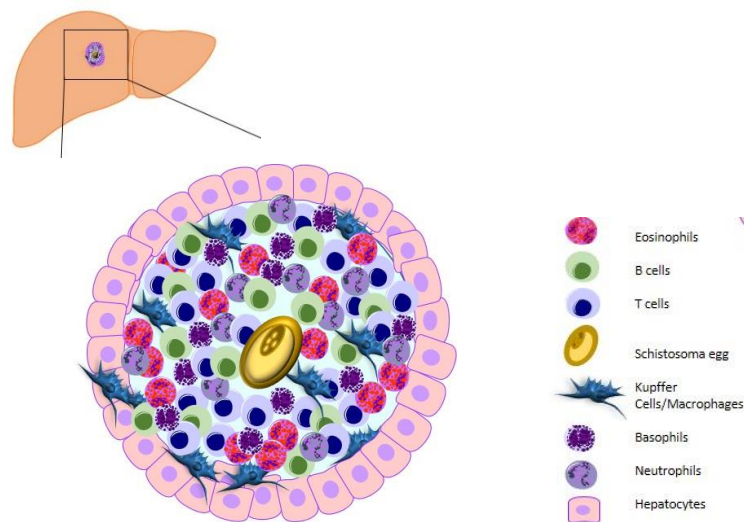


Fig. 4: Granuloma formation in the liver.

The granuloma encloses the egg, restricting its antigenicity. Besides the egg, the granuloma consists of different immune cells such as T cells, B cells or eosinophils. During the chronic phase of the disease, the collagen content increases over time.

Macrophages play a crucial role during the immune response, since high levels of IL-4 and IL-13 have a profound impact on their phenotype and function. Already in the early stage, when the *cercariae* are actively penetrating the human skin, Langerhans cells are activated (macrophages of the skin) and produce IL-10¹³⁷. Furthermore, macrophages phagocytose and present *cercariae* antigens, promoting IL-4 production by CD4⁺ T cells through binding of released *cercariae* material via CD206. In addition, signalling through the CD206 receptor induces an anti-inflammatory response in macrophages. Infection of mice with deletion of the CD206 receptor was accompanied by CD4⁺ T cell polarisation towards Th1, instead of Th2, and increased production of IFN γ and lower IL-4 levels¹³⁸. Multiple exposure to *S. mansoni cercariae* shapes skin-macrophages towards a tissue remodelling phenotype through IL-4 and IL-13 enrichment in the skin, but also induce T cell hyporesponsiveness¹³⁹. After

maturing into *schistosomulae*, the worm seems to be highly susceptible to cellular immune attack in the first days after developing, but not later on¹⁴⁰. Here, vaccine studies using Sm-p80 showed enhanced macrophage antibody-dependent cell-mediated cytotoxicity (ADCC) against the *schistosomulae*¹⁴¹. After reaching the intestine, the worm further matures and activates tissue remodelling macrophages through TLR activation or histamine release. In line with this, tissue rearrangement occurs through MMPs or collagenase release by eosinophils or macrophages¹⁴². Released alarmins like IL-33 and IL-25 from the damaged tissue stimulate IL-4, IL-5 and IL-13 release, favouring further macrophage activation towards a tissue remodelling phenotype^{143,144}.

If the worm reaches the adult stage, it is less likely that macrophages are able to eliminate the parasite and therefore the immune response focuses on limiting collateral damage induced by the parasite. Although necessary for the survival of the host, this induces the chronic progression of the disease; the formation of granulomas to reduce immunogenicity of the trapped egg¹⁴⁵ and induction of fibrosis in the late stage¹⁴⁶. This dual role of macrophages could be observed through depletion of macrophages (CD11b⁺F4/80⁺) during the chronic phase of *S. mansoni*, which reduced granuloma-induced inflammation and liver fibrosis¹⁴⁷. The induced anti-inflammatory/tissue remodelling macrophages are characterised by expressing e.g. *Arg1* and *Reln1a*. ARG1 metabolites proline and polyamine induce collagen synthesis and thereby favour fibrogenesis in the chronic phase of the disease. During the early acute phase of the disease, ARG1 is beneficial for the host. It inhibits cachexia, endotoxemia, mortality and egg accumulation in the intestine as seen in *Arg1*^{-/-} mice where these symptoms are accompanied with low levels of IL-10 and TGFβ¹⁴⁸. In addition, macrophages lacking *Arg1* expression were in particular associated with increased susceptibility, liver fibrosis and granuloma inflammation¹⁴⁹. RELMα (gene name *Reln1a*) activates fibroblast and collagen organisation in the liver, and therefore contributes to the progression of liver fibrosis. However, mice lacking *Reln1a* expression showed enhanced fibrosis, granuloma size and pulmonary inflammation during the infection¹⁵⁰. Thus, RELMα and ARG1 restrict Th2-induced pathology, which is accompanied by IL-4 and IL-13 production. Here, IL-4 determines the granuloma response, including the size, activation of Th2 proliferation, IL-5 and IL-13 production. IL-13 is the key cytokine during schistosomiasis for the induction of liver fibrosis and activates fibrotic pathways in target cells, TGFβ independently¹⁵¹. High levels of IL-13 are correlated with disease severity and progression¹⁵². Both cytokines enhance the immune response respectively and both cytokines signal via the IL-4Rα.

The recruitment of macrophages in the liver during schistosomiasis is mainly IL-4Rα-independent. Most of these macrophages have a blood-monocyte origin and it is controversially discussed whether IL-4Rα is directly linked to the protective response from macrophages during infection¹⁵³. LysM-restricted IL-4Rα depletion increases the mortality with less dense but larger granulomas¹⁵⁴. Depletion of IL-4Rα specifically in macrophages has no direct impact on the mortality but increases liver

inflammation¹⁵⁵. However, signalling via IL-4R α enhances the production of IL-10 and TGF β in macrophages with a tissue remodelling phenotype¹⁵⁶. Stimulation of macrophages with *Schistosoma* antigen increases IL-10 production and inhibits pro-inflammatory polarisation of macrophage after IFN γ or LPS stimulation. However, delayed antigen presentation was observed¹⁵⁷. Although IL-10 production by macrophages reduced morbidity¹⁵⁸ and high levels promote anti-fibrotic-processes¹⁵⁹, IL-10 is not able to compensate loss of tissue remodelling macrophages¹⁵⁴. Furthermore, IL-10 is additionally produced by CD4⁺Foxp3⁺ regulator T cells and tissue remodelling macrophages promote Treg differentiation during the infection. They are recruited to the liver and limit granuloma-induced inflammatory responses and suppress pro-inflammatory cytokine production¹⁶⁰.

During the chronic phase of the disease monocytes infiltrate the liver and polarise into CD206⁺PD-L2⁺ macrophages in a T cell dependent manner, contributing to the tissue remodelling process¹⁶¹. However, monocytes are in general involved in the response to the infection. Numbers of Ly6C⁺ monocytes rise during the infection and acquire CX3CR1⁺ expression in the infected liver. Depletion of these monocytes resulted in loss of the protective Th2 response with an increase in weight loss, controversially accompanied by smaller granulomas¹⁴⁵. Transfer of monocytes reduced liver fibrosis, pro-fibrogenic mediators (e.g. TGF β or IL-1 β) and M1 markers with simultaneous upregulation of M2 markers¹⁶². In addition, studies using mice lacking CD18 (α/β integrin responsible for leukocyte trans-endothelia migration) resulted in monocytopenia. Higher worm burden accompanied with increased granuloma formation, egg deposition and mortality was the consequence¹⁶³. Furthermore, in patients with schistosomiasis monocytes contribute to the liver fibrosis. Here, human monocytes increased the expression of TGF β and liver fibrosis¹⁴⁶, presumably a response of monocytes to SEA as observed *in vitro*. Additionally, SEA induce monocytes to produce high levels of suppressor of cytokine signalling 1 (SOCS1), IL-10, TNF α and IL-12¹⁶⁴. KC numbers decline simultaneously with the rising numbers of monocytes during infection. Although KCs are not responsible for the disease outcome, since depleting KCs resulted in no changes in the survival rates, they constantly recruit new monocytes to the liver that acquire tissue resident macrophage characteristics.¹⁶⁵

During the infection, many factors induce apoptosis in the host cells. While on the one hand the migrating worm is harming the host, on the other hand the translocation of the egg through the intestinal wall and the formation of the granuloma are accompanied by cell death. Hypoxia and toxic substances released by the eggs are responsible for induction of apoptosis within the granuloma. In addition, the formation of the granuloma leads to apoptosis of the enclosed cells in the long term. The SEA is able to specifically induce apoptosis in T cells and hepatic stellate cells, modifying the immune response of the host¹⁶⁶. Studies demonstrated that Th1 cells are more susceptible than Th2 cells to apoptosis during infection and apoptotic CD4⁺ cells are found in high numbers inside the granuloma

and spleen in the acute stage of the disease. An increase in SEA-induced Fas-L expression could be found in B cells and favours apoptosis of these cells^{167,168}. Importantly, all dying cells are able to be phagocytosed by the neighbouring macrophages, within both the intestine and the liver granuloma.

1.5 Aim of the study

The crosstalk between macrophages and apoptotic cells has been broadly investigated, however, many unanswered questions still remain. In the presence of IL-4/IL-13, the phagocytosis of apoptotic cells commits macrophages towards an anti-inflammatory/tissue remodelling phenotype. The full dissection of this interplay is crucial to understand how apoptotic cells shape the response of macrophages. Up to now, apoptotic cells have only been described by their characteristic morphological changes. Although they can originate from various cell types, a contribution of the apoptotic cell identity to the polarisation of macrophages has not been investigated so far.

The aim of the study was to investigate whether the phagocytosis of different apoptotic cells affects the functional heterogeneity of the corresponding macrophages in dependency of the original apoptotic cell identity. In particular, the influence of apoptotic cells on the IL-4 response of macrophages was analysed. Furthermore, *Schistosoma mansoni* infection of mice with a genetic ablation in macrophages allowed investigation of the effect of phagocytosis on the immune pathology. In addition, these findings could be used to improve the therapeutic potential of macrophages in the context of *Schistosoma mansoni* by pre-treatment with apoptotic cells.

2 Materials

2.1 Laboratory equipment

Table 1: Laboratory Equipment and companies

Name	Company
Accuri C6™	BDBiosciences, Heidelberg, Germany
Agarose gel electrophoresis chamber	BioRAD, Munich, Germany
Analytical scale	Satorius AG, Göttingen, Germany
Benchtop centrifuge	Eppendorf, Hamburg, Germany
Cell sorter FACSaria III	Becton Dickinson, Heidelberg, Germany
Centrifuge	Eppendorf, Hamburg, Germany
ChemiDoc Touch Imaging System	BioRAD, Munich, Germany
Dissection instruments (forceps & scissors)	Neolab, Heidelberg, Germany
ELISA Photometer	MRX-II Dynex Technologies, Berlin, Germany
FACSaria II	BD Biosciences, Heidelberg, Germany
Freezer -20°C /-70°C	Liebherr, Biberach an der Riss, Germany
Fridge Comfort	Liebherr, Biberach an der Riss, Germany
Incubator	Heraeus instruments, Hanau, Germany
Laminar flow FlowSafeB-(MacPro) ³ -130	Brener, Elmshorn, Germany
LSR II	BD Biosciences, Heidelberg, Germany
MACS Magnet	Miltenyi Biotec, Bergisch Gladbach, Germany
Microscope Keyence	Nikon GmbH, Düsseldorf, Germany
Multichannel pipettes	Eppendorf, Hamburg, Germany
NanoDrop 2000C	ThermoScientific, Waltham, USA
PCR machine (Piqstar 96x Universal Gradient)	Peqlab, Erlangen, Germany
Pipettboy Acujet pro	Brand, Wertheim Germany
Pipettes (10 µL, 20 µL, 200 µL, 1000 µL)	HTL, Wertheim, Germany
Power supply	BioRAD, Munich, Germany
Thermomixer MM	B Braun, Melsungen, Germany
Vortexer Genie 2	Bender & Hobein AG, Zürich, Switzerland
Water bath	Haake, Karlsruhe, Germany

2.2 Glass and plastic consumables

Table 2. Plastic and glass consumables

Name	Company
Cannula, Sterican, 2 G, 14 G , 21 G	B. Braun Melsungen AG, Melsungen, Germany
Cell culture plate (6/24/96 U/R bottom)	Greiner bio-one, Frickenhausen, Germany
Cell Strainer (100, 70, 40µm)	Pluriselect, Leipzig, Germany
Cryo tubes	Nunc, Wiesbaden, Germany
ELISA plate (microplate high binding)	Greiner bio-one, Frickenhausen
FACS tubes	Sarstedt, Nürmbrecht, Germany
Falcons (15, 50 mL)	Sarstedt, Nürmbrecht, Germany
Glass-pipettes (2, 5, 10, 20 mL)	Brand GmbH, Wertheim, Germany
Glass-bottle (50, 100, 200, 500, 1000 mL)	Schott AG, Mainz, Germany
LS-MACS columns	Miltenyi Biotec, Bergish Gladbach, Germany
Neubauer Chamber (0.1 x 0.0025 mm ²)	Hecht-Assistent, Sondheim, Germany
Omnican 500 / 1000 µL	B Braun Melsungen AG, Melsungen, Germany
Pasteur pipettes glass	Fisher Scientific GmbH, Schwerte, Germany
Petri dish 15 cm	Sarstedt, Nürmbrecht, Germany
Pipette tips (10,20,200,1000 µL)	Sarstedt, Nürmbrecht, Germany
Plastic pipettes (5, 10, 25 mL)	Sarstedt, Nürmbrecht, Germany
Single-use hypodermic needles (Gr 1, 2, 16, 18)	B Braun Melsungen AG, Melsungen, Germany
Syringes (5 mL, 10 mL, 20 mL)	B Braun Melsungen AG, Melsungen, Germany
Tubes (0.5 mL, 1.5 mL, 2 mL)	Sarstedt, Nürmbrecht, Germany
Venofix A 21 G butterfly	B. Braun Melsungen AG, Melsungen, Germany

2.3 Chemicals and reagents

Table 3. Chemicals and molecular biology reagents

Name	Company
Agarose	Biomol, Hamburg, Germany
Ampuwa, water	Fresenius, Graz, Austria
Click's Medium	Merck , Darmstadt, Germany
Collagenase IV	Stem Cell, Köln, Germany , Worthington, USA
Collagenase VIII	Worthington, NJ, USA
Disinfection spray incidin Liquid	Ecolab, Düsseldorf, Germany
DMEM	PAA Laboratories GmbH, Pasching, Austria

DNase I	Quagen, Hilden, Germany, Roche, Germany
DPBS 10 x	Capricon, Ebsdorfergrund, Germany
Fetal calf serum (FCS)	Capricon, Ebsdorfergrund, Germany
Generuler 100 bp DNA Ladder	ThermoFisherScientific, Waltham, USA
Gentamycin	Capricon, Ebsdorfergrund, Germany
Heparin	Rathiofarm, Ulm, Germany
L-Glutamine	Capricon, Ebsdorfergrund, Germany
Lugol Solution	Carl Roth, Karlsruhe, Germany
Percoll	Sigma Aldrich, Darmstadt, Germany
RPMI 1640 without L-Glut	PAA Laboratories GmbH, Pasching, Austria
Tetramethylbenzidine (TMB)	Carl Roth, Karlsruhe, Germany
Trizol	Merck, Darmstadt, Germany
Trypan blue solution 0.4%	Invitrogen, Gibco, Auckland, New Zealand
Trypsin-EDTA (1x)	PAA Laboratories GmbH, Pasching, Austria
β -Mercapthoethanol	Invitrogen, Gibco, Auckland, New Zealand

All other, not listed chemicals or molecular biology reagents were purchase at Merck (now including Sigma-Aldrich) or Roth.

2.4 Media and Buffers

Table 4: Media and Buffers

<p>cRPMI + 10 % FCS + 2.5 % L-Glutamine + 0.5 % Gentamycin</p> <p>Click's Medium + 10 % FCS + 2.5 % L-Glutamine + 0.5 % Gentamycin</p> <p>FACS Buffer PBS + 2 % FCS</p> <p>Macrophage Media RPMI + 20 % FCS + 30% L929 sup. + 2.5 % L-Glutamine + 0.5 % Gentamycin</p>	<p>Digestion Buffer Liver 10 mL DMEM/ sample + 1mg /mL Collagenase IV + 100μL MgCl₂ (0.2M) + 40μL CaCl₂ (0.5 M) + 50μL DNase I (150 U/mL)</p> <p>Digestion Buffer colon I 5 mL HBSS /per sample + 2 % FBS + 3μL DNase I + 5 mg Collagenase VII</p> <p>Digestion Buffer colon II 20 mL HBSS /sample + 200 μL EDTA (0.5 M)</p> <p>TBE Buffer (in H₂O) for Agarose-gel + 89 mM Tris base + 89 mM boric acid + 2mM EDTA</p>
--	--

Apoptotic neutrophil aging Buffer RPMI + 5 % FCS + 2.5 % L-Glutamine + 0.5 % Gentamycin	Digestion Buffer Biopsies 0.1 M Tris·Cl pH 8.0 + 0.005 M EDTA + 0.2 M NaCl + 0.2% SDS
cDMEM + 10 % FCS + 2.5 % L-Glutamine + 0.5 % Gentamycin	Substrate Buffer (ELISA) + 0.1 M NaH ₂ PO ₄ + TMB 30 mg/5mL DMSO + 30 % H ₂ O ₂
MACS Buffer PBS PH 7.2 + 0.5 % BSA + 2 mM EDTA	Blocking Buffer (ELISA) PBS + 1% BSA

2.5 Commercially available kits

Table 5. Kits

Name	Company
10x Permeabilisation Buffer	BD Bioscience, Heidelberg, Germany
Chromium Single Cell3' Reagent Kits v3	10x Genomics, Fell, Germany
Chromium Single Cell 3' GEM librabry &Gel Bead Kit v3	10x Genomics, Fell, Germany
DreamTaq	ThermoFisherScientific, Waltham, USA
ELISA	R&D System, Abingdon, UK
FITC Annexin V Apoptosis Detection Kit with PI	BioLegend, San Diego, USA
<i>in situ</i> cell death detection Kit, Fluorescein (Roche)	ThermoFisherScientific, Waltham, USA
Intracellular Fixation/Permeabilisation Buffer Set Foxp3	ThermoFisherScientific, Waltham, USA
iScript™ cDNA synthesis Kit	BioRAD, Munich, Germany
LegendPlex mouse 8-Plex Th1/Th2	Biolegend, Fell, Germany
Maxima SYBR™ Green qPCR Master Mix with separate ROX™ vials	ThermoFisherScientific, Waltham, USA
QiaShredder	Quiagen, Hilden, Germany,
RNeasy Mini Kit	Quiagen, Hilden, Germany

2.6 Software

Table 6. Programs and purpose

Software	Purpose
Adobe Reader DC	Reading PDF files
BD FACS DIVA 6.2	Acquire FlowJo data

BioRender	Graphic processing
Flow Jo Version 10.01	Analysis of flow cytometry data
Graphpad Prism 8 for Windows	Statistical analysis
Inkscape 0.92.3	Graphic processing
LEGENDplex v8.0	Analysis of LEGENDplex data
Mendeley Desktop 1.16.3	Citations
Microsoft Office 2013	Word and graphic processing

2.7 Antibodies

Table 7: Mouse antibodies with clones, dilution factors and company

Epitope	Fluorochrome	Clone	Dilution	Company
Anti-goat IgG	FITC	Poly4606	1:300	BioLegend
Anti-rabbit IgG	BV421, BV510	Poly4064	1:300	BioLegend
ARGINASE I	APC	A1exF5	1:500	Invitrogen
AXL	FITC	MAXL8DS	1:200	ThermoFischer
CD11b	APC/Cy7	M1/70	1:400	BioLegend
Cd11c	PerCP	N418	1:400	BioLegend
CD163	PE	TNKUPJ	1:400	BioLegend
CD206	PE/Dazzle	Co68C2	1:600	BioLegend
CD3 ϵ	BUV395	145-2C11	1:200	BD Biosciences
CD45	PE/Cy7	30-F11	1:1300	BioLegend
CD45.1	PerCP	A20	1:150	BioLegend
CD45.2	Pe/Cy7	104	1:150	BioLegend
CD68	BV421	FA-11	1:400	BioLegend
F4/80	AF700	BM8	1:400	BioLegend
LY6C	PerCP-Cy5.5	HK1.4	1:300	BioLegend
LY6G	PerCP-Cy5.5	IA8	1:300	BioLegend
MERTK	PE	2B10C42	1:200	BioLegend
MHC II	BV510, BV421	M5/114.15.2	1:400	BioLegend
RELM α	Purified	Polyclonal rabbit IgG	1:200	Peptotech
SIGLEC F	BV421	E502240	1:300	BD Biosciences
YM1	Purified	Polyclonal Goat IgG	1:200	R&D

2.8 Primer sequences for qPCR

All oligonucleotides were synthesised and purchased by Eurofins.

Table 8: Mouse Primers for qPCR

Name	Sequence 5'->3'
<i>Arg1_fw</i>	CATTGGCTTGCGAGACGTAGAC
<i>Arg1_rev</i>	GCTGAAGGTCTCTTCCATCACC
<i>Axl_fw</i>	TGCCAGTCAAGTGGATTGCT
<i>Axl_rev</i>	CACACATCGCTCTTGCTGGT
<i>CD163_fw</i>	GGTGGACACAGAATGGTTCTTC
<i>CD163_rev</i>	CCAGGAGCGTTAGTGACAGC
<i>Chil3_fw</i>	CTGGAATTGGTGCCCCTACA
<i>Chil3_rev</i>	CAAGCATGGTGGTTTTACAGGA
<i>Ear2_fw</i>	AACATCACCAGTCGGAGGAGAA
<i>Ear2_rev</i>	GCAGATGAGCAAAGGTGCAAA
<i>Fn1_fw</i>	GATGTCCGAACAGCTATTTACCA
<i>Fn1_rev</i>	CCTTGCGACTTCAGCCACT
<i>Gapdh_fw</i>	TCCCACTCTCCACCTTCGA
<i>Gapdh_rev</i>	AGTTGGGATAGGGCCTCTCTT
<i>Ifny_fw</i>	TCAAGTGGCATAGATGTGGA
<i>Ifny_rev</i>	TGAGGTAGAAAGAGATAATCTGG
<i>Il-13_fw</i>	TGAGGAGCTGAGCAACATCACACA
<i>Il-13_rev</i>	TGCGGTTACAGAGGCCATGCAATA
<i>Il-4_fw</i>	AGATGGATGTGCCAAACGTCCTCA
<i>Il-4_rev</i>	AATATGCGAAGCACCTTGGGAAGCC
<i>Mertk_fw</i>	GTAGATTACGCACCCTCGTCAAC
<i>Mertk_rev</i>	GCCGAGGATGATGAACATAGAGT
<i>Mmp14_fw</i>	GCTTCTACCACAAGGACTTT
<i>Mmp14_rev.</i>	CAATTAGGGACTGAGAAGGG
<i>Retnla_fw</i>	CCAATCCAGCTAACTATCCCTCC
<i>Retnla_rev</i>	CCAGTCAACGAGTAAGCACAG
<i>Serpinb9b_fw</i>	CAAGCCCACATCCCTTTGAA
<i>Serpinb9b_rev</i>	TGTTGGCAGATGACTCAGTTCCTTTC
<i>Socs2_fw</i>	GGTTGCCGGAGGAACAGTC
<i>Socs2_rev</i>	GAGCCTCTTTTAATTTCTCTTTGGC

<i>Tgfβ fw</i>	GGTTCATGTCATGGATGGTGC
<i>Tgfβ rev</i>	TGACGTCCTGGAGTTGTACGG
<i>Timp1 rev</i>	GCGGTTCTGGGACTTGTGGGC
<i>Timpf1 fw</i>	GCATCTCTGGCATCTGGCATC
<i>Tnfa fw</i>	TAGCTCCCAGAAAAGCAAGC
<i>Tnfa rev</i>	TTTTCTGGAGGGAGATGTGG

2.9 Cell line

Table 9: Eukaryotic cell line

Name	Origin
Hepa 1-6	Hepatoma

2.10 Parasite

S. mansoni cercariae were grown, isolated and purchased from Helmuth Haas (Research Center Borstel).

2.11 Mice strains

Table 10: Mice strains

Name	Origin
C57BL/6	BNITM, Hamburg, Germany
<i>Csf1R-Cre⁺Axl^{f/f}Mertk^{f/f}</i>	Rothlin Lab Yale, USA, breeding at BNITM, Hamburg, Germany
<i>Csf1R-Cre⁻Axl^{f/f}Mertk^{f/f}</i>	Rothlin Lab Yale, USA, breeding at BNITM, Hamburg, Germany

3 Methods

3.1 Cell culture and *in vitro* experiments

All cell culture experiments and *in vitro* experiments were handled under sterile conditions. All cells were cultured in 37°C 5 % CO₂, except the Hepa 1-6 cell culture.

3.2 Hepa 1-6 culture

For the Hepa 1-6 culture, serial dilutions were performed for maintenance of the cells. Detaching of the cells during the culture was performed with trypsin for 5 min at 37°C, followed by adding complete media to stop the reaction, washing and seeding into fresh media. Cells, which were harvested for the experiment, were washed with PBS and detached using a cell scraper. Hepa 1-6 cells were cultured in 37°C 9 % CO₂. In the following chapters, this cell line will be referred to as hepatocytes.

3.3 Cell count

The cell count of a cell suspension was determined with a Neubauer Chamber. The following formula was used to calculate the cell concentration:

$$\frac{\text{cell count}}{\text{big squares}} \cdot \text{dilution factor} \cdot 10^4 = \text{cells/mL}$$

3.4 Isolation of bone marrow-derived macrophages

Bone marrow-derived macrophages (BMDMs) were obtained from wild type (WT) mice. For the isolation, the femur and tibia were removed as one whole, disinfected for 1 min in 70 % Ethanol (EtOH) and cut open at one end. To remove the bone marrow, the bones were transferred into a 0.5 mL tube with a hole and placed in a 1.5 mL tube and centrifuged at 13000 rpm for 2 min. The isolated bone marrow was resuspended in 200 µL RPMI, filtered through a 40 µm cell strainer and seeded into a 15 cm dish in 10 mL RPMI containing 20 % FCS, 30 % L929-cell line supernatant, 2.5 % L-Glutamin and 0.5 % Gentamycin (macrophage media). For the differentiation of macrophages from the bone marrow precursor, half of the media was changed at day 3 by removing 5 mL media, centrifugation at 300 xg for 5 min and resuspending cells in 5 mL fresh macrophage media. The suspension was then transferred back into the cell dish. At day 5, cells were split and plated into two new 15 cm dishes with 10 mL fresh media. At day 7, the fully differentiated BMDMs were harvested, counted and 0.33·10⁶ cells/well were seeded into a 24-well plate to perform the experiments in fresh macrophage media.

3.5 Isolation of neutrophils

Neutrophils were obtained by harvesting the bone marrow of old (≥ 11 weeks old) WT (as described before; see 3.4) mice and isolated with the negative MACS-selection Kit for Neutrophils (Miltenyi) according to the manufacturer's protocol. Briefly, an antibody cocktail labelled with streptavidin was added to the bone marrow cell suspension to bind to all cells except neutrophils and incubated for 10 min at 4°C. After washing away the unbound antibodies, cells were incubated with biotin-conjugated beads (15 min 4°C) and the neutrophils were isolated by obtaining the flow-through fluid from the magnetic column separation. The purity of neutrophils was determined by Ly6G and CD11b staining and was set above 90 %.

3.6 Induction of apoptosis

Apoptosis was induced by aging of neutrophils for 24 h in cRPMI media containing a reduced amount of FCS (5 % FCS) at 37°C 5 % CO₂ in a 15 cm dish.

The thymus were harvested from the same mice the neutrophils were obtained from. For the isolation, the thymus were mashed over a 40 μ m cell strainer, washed and plated in a 15 cm dish with 3 mL cRPMI per thymus. Apoptotic thymocytes (aT) were generated by aging for 24 h at 37°C 5 % CO₂.

Hepatocytes (Hepa 1-6 cell-line) were detached and suspended in PBS with a cell scraper. Apoptotic hepatocytes (aH) were generated by heating the cell suspension for 1 h at 40 °C in PBS with 0.5 % FCS while shaking.

3.7 Staining of apoptotic cells

3.7.1 Apoptotic cell staining with Annexin V and PI

For all three cell types, the cell numbers were determined and the apoptosis levels were verified by Annexin V and PI staining. To this end, 10 μ L of each cell suspension was transferred into a FACS tube containing 100 μ L of Annexin V binding buffer and 2 μ L Annexin V was added to stain the PtdSer on the surface of the apoptotic cells. After 15 min incubation at room temperature (RT) in the dark, 200 μ L Annexin V binding buffer was added to the cell suspension together with 1 μ L PI staining solution and the samples were directly measured at the LSR II.

3.7.2 Apoptotic cell staining with TUNEL

In some experiment a TdT-mediated dUTP-biotin nick end labelling (TUNEL) staining to determined apoptotic DNA fragmentation was performed. The TUNEL dye is marking the 3'OH end of DNA breaks.

The *in situ* cell death detection Kit, Fluorescein (Roche) was used by following the manufacturer's instructions. Briefly, apoptotic cells were pre-stained for surface markers (see 3.10) and fixed afterwards with 2 % PFA for 1 h at RT, followed by permeabilisation with a 0.1 % Triton-X100-PBS solution for 2 min on ice. After washing two times with 200 μ L PBS, 25 μ L of freshly prepared TUNEL-reaction-mix (enzyme + labelling solution 1:10) was added and incubated for 1 h at 37°C. Afterwards samples were measured at the LSR II. Living cells were used as negative control. For the positive control, cells were treated for 10 min with DNase I. A technical control was performed by preparing the TUNEL-reaction-mix without the enzyme solution.

3.8 Polarisation assay

For the polarisation apoptotic neutrophils (aN), apoptotic thymocytes (aT) and/or apoptotic hepatocytes (aH) were harvested, washed and co-cultured with $0.33 \cdot 10^6$ pre-plated BMDMs (2 h earlier) in 500 μ L macrophage media per well in a ratio of 5:1, 5:1 or 2:1, respectively,. After 45 min the apoptotic cells were washed out with PBS (5 times). 1 mL macrophage media and 10 ng/mL murine recombinant IL-4 (eBioscience) was added to the BMDMs. After 48 h the cells were gently detached with cold PBS on ice, blocked, stained and analysed by flow cytometry for e.g. tissue remodelling proteins. In some of the experiments, the indicated genes were detected on mRNA level by qPCR. To this end, the cells were directly lysated with the Qiashtredder Kit and the RNA was isolated (see 3.12). In addition, the polarisation assay was performed with FITC-labelled liposomes in a ratio of 5:1 (liposomes : BMDMs). The liposomes were kindly provided by Andrea Schromm, Research Center Borstel.

All data obtained from the polarisation assays are displayed as fold change related to the IL-4 sample.

3.9 Phagocytosis assay

$0.33 \cdot 10^6$ BMDMs/well (24-well plate) were pre-plated 2 h before the experiment in duplicates in two separated plates. Before starting the phagocytosis assay, one plate was incubated for 30 min at 4°C on ice. The assay was performed at 37°C and 4°C simultaneously, whereby at 37°C, the apoptotic cells can be bound and phagocytosed by macrophages and at 4°C, the macrophages are only able to bind to the apoptotic cells but are not able to uptake them. Apoptotic cells were pre-labelled with CFSE in a final concentration of $10 \cdot 10^6$ cells/mL. To this end, apoptotic cells were washed twice with PBS to remove any serum and resuspended in pre-warmed PBS at a concentration of $20 \cdot 10^6$ cells/mL. A CFSE solution of 20 μ M was prepared in a final volume of 1 mL and mixed with the apoptotic cell solution while vortexing. The cells were incubated for 10 min at 37°C in the dark. The labelling-process was stopped

by adding 10 mL of cold cRMPI and incubating for 5 min on ice. Apoptotic cells were washed 3 times and co-cultured with BMDMs for 1 h (see 3.8). Afterwards, apoptotic cells were washed out (5 times with PBS) and BMDMs were harvested, stained and analysed at the LSR II. The ratio between BMDMs positive for the apoptotic cells at 37°C and 4°C were calculated and displayed as phagocytosing macrophages.

3.10 Flow cytometry

The flow cytometer allows the analysis of the granularity and size of cells by sideward scatter (SSC) and forward scatter (FSC). The cells are separated into a single cell solution by squeezing through a capillary tube before passing the laser. In addition to the morphological investigation, expression levels of extra-(surface) and intracellular proteins/molecules can be analysed. To this end, the cells are labelled with fluorescence-conjugated antibodies. To investigate different molecules at the same time, antibodies that are excited by different wavelengths are used. Cells derived from mice as well as from *in vitro* assays were stained using the following protocol. To block unspecific binding of antibodies to the Fc-receptor, $2\text{-}6\cdot 10^6$ cells were incubated with anti-CD16/CD32 (1:10000 in PBS/2 % FCS) for 15 min at 4°C. Washing steps for the surface staining with 200 μL PBS/2 % FCS were repeated 3 times and included after each antibody incubation to remove unbound antibodies. For the surface staining, antibodies were diluted in 50 μL or 25 μL PBS/2 % FCS per FACS-tube or well of a 96-well plate, respectively, and incubated for 35 min at 4°C in the dark. If intracellular epitopes were analysed, cells were fixed and permeabilised before staining. For the fixation, 100 μL of 1 % paraformaldehyde (PFA) were added to the wells or tubes and incubated for at least 20 min at 4°C in the dark. To permeabilise the cells, 100 μL permeabilisation buffer (BD Bioscience) was slowly added and incubated for 15 min at RT. The cells were stained intracellularly for 45 min afterwards. To this end, the intracellular antibodies were diluted in permeabilisation buffer to ensure the membrane permeability and cells were washed at least twice with permeabilisation buffer to remove unbound antibodies. If liver samples were analysed, cells were fixed and permeabilised using the Foxp3 staining Kit (eBioscience™). Antibodies used for the cell-staining are listed in Table 7. The samples were measured at the LSR II.

3.11 Fluorescence-activated cell sorting (FACS)

To obtain specific cell populations fluorescence-activated cell sorting (FACS) was used. Surface-stained cells are separated as described above (see 3.10) and enclosed by liquid droplets that are labelled with an electric charge. Passing an electric field, cells are sorted into different populations depending on

their charge. Cells of the liver were isolated for sorting and stained extracellularly for molecules of interest (see 3.10 and Table 7). Sorting of the cells was performed by the core facility of the BNITM using a BD FACSAria. Cells were diluted in PBS/2 % FCS and filtered through a 30 μm strainer before sorting. A 70 μm nozzle was used to sort macrophages out of the cell suspension and sorted cells were collected in cold PBS/2 % FCS.

3.12 RNA isolation and quantitative real-time PCR analysis

To obtain RNA from BMDMs or sorted cells the Qiagen RNeasy mini Kit was used by following the manufacturer's instructions. Briefly, cells were lysated by adding 350 μL RLT buffer containing β -mercaptoethanol and spun down over the shredder column for 2 min at maximum speed. The suspension was mixed in a ratio of 1:1 with 70 % EtOH, transferred to the RNeasy mini column and briefly centrifuged (21 s) at 13000 rpm. RW1 buffer was added afterwards and a DNase I digestion was performed on the column for 15 min at RT. After a second RW1 washing step, two washing steps with 500 μL RPE2 solution were performed by applying the solution to the column and centrifuging them for 2 min at 13000 rpm. RNA was eluted with 32 μL RNase-free water and RT incubation for 5 min. For sorted cells, RNA was eluted using 28 μL RNase-free water. The purity and the amount of RNA was verified with the NanoDrop.

To obtain RNA from tissue stored in *RNAlater*, RNA isolation were performed using TRIzolTM. A 1 cm^2 piece of tissue was transferred into a 1.5 mL Tube with 200 μL TRIzolTM. Using a homogeniser, the tissue was disrupted and 800 μL TRIzolTM added to the homogenised sample. After 5 min incubation at RT, 200 μL chloroform were added, mixed for 15 s and incubated for 3 min at RT. The samples were centrifuged at 12000 xg for 15 min at 4°C and 500 μL of the supernatant carefully transferred into a new tube containing 500 μL isopropanol and incubated at RT for 10 min. The samples were centrifuged (at 12000 xg for 15 min at 4°C), the supernatant discarded and 500 μL of 80 % EtOH added. After mixing, the suspension was centrifuged for 5 min at 7500 xg at 4°C, the supernatant discarded and the RNA air-dried. The RNA was dissolved in 150 μL Ampuwa water and the concentration determined by Nanodrop.

cDNA Synthesis was performed with the iScriptTM cDNA synthesis Kit from BioRad (see cDNA cycles). Afterwards a quantitative Real-Time polymerase chain reaction (qPCR) was performed using the MaximaTM SYBRTM Green qPCR Master Mix (2X), with separate ROXTM vial from Thermo Fischer. By using a qPCR, the quantification of a specific DNA-sequence can be performed in real time. Here, a fluorescence dye (SYBRTM Green) is intercalating in the amplified PCR product during the reaction (see qPCR cycles below) and measured by the Rotor-gene 6000 machine. All reactions were performed in duplicates in a final volume of 12 μL per reaction including 40 ngcDNA and analysed using the Rotor-

gene 6000 Series Software 1.7. All runs were performed with *Gapdh* as reference gene. The used primers are listed in Table 8.

Reaction-Mix cDNA- iScript™ cDNA Synthesis Kit

- 1 µL iScript Reverse Transcriptase
- 4µL 5x iScript Reaction Mix
- X µL Nuclease-free water
- X µl RNA template (200-400 ng)

cDNA cycles

- Priming 25°C for 5 min
- Reverse transcription 46°C for 20 min
- RT inactivation 95°C for 1 min

Reaction Mix for qPCR – Maxima™ SYBR™ Green qPCR Master Mix

- 6 µL Master Mix
- 0.15 µL per Primer (forward and reversed)
- 4.7 µL Ampuwa water
- 1 µL RNA template (40 ng)

qPCR cycles

- | | | |
|----------------------|-----------------|-------------|
| UDG pre-treatment | 50°C for 2 min | |
| Initial denaturation | 95°C for 10 min | |
| Denaturation | 95°C for 15 s | repeat 40 x |
| Annealing | 60°C for 30 s | |
| Extension | 72°C for 30 s | |
-

3.13 Cytokine detection

3.13.1 Enzyme linked immunosorbent assay (ELISA)

The sandwich ELISA-Kit from RnD was used according to the manufacturer’s protocol to perform the quantitative determination of the cytokines produced by stimulated mesenteric lymph nodes. Before performing the assay, culture supernatant was tested at different dilutions to obtain the best results. Briefly, the ELISA plates were coated overnight at RT with a specific antibody for the cytokine of

interest. The day after, before blocking free binding sites (1 % BSA in PBS for 2 h), two washing steps were included to minimise background signals. The plate was incubated overnight at 4°C after transferring the serial diluted standard and the samples into the plate. The next day, the detection antibody was added for the specific cytokine for 2 h at RT and the development started by the addition of horseradish peroxidase (HRP) to start the catalysis of the supplied substrate. To stop the enzyme reaction 2M H₂SO₄ was supplemented. The intensity of the colour reaction was measured at 450 nm. A higher OD (optical density) means a higher catalytic activity and therefore a higher amount of cytokines that are bound to the enzyme-linked antibody, which can be used to calculate the quantitative cytokine levels.

3.13.2 LEGENDplex™

To determine the cytokine levels in the serum the LEGENDplex™-Kit (BioLegend) was used. The assay was performed according to the manual, whereby the volume of reagents and samples were reduced to 1/3 of the original volume. Overall, the method is based on the detection of the antigen by two different antibodies, also known as the sandwich-ELISA method. Briefly, cytokines of interest are bound to beads coated with the corresponding antibody. To distinguish between the different cytokines that are able to bind to the beads, the beads differ in size and intensity of the bound fluorochrome for each cytokine. The beads are detected by the use of a second antibody, which is linked to biotin. By adding a streptavidin-bound fluorochrome, the fluorescence intensity can be used to determine the amount of cytokine inside the sera. The LEGENDplex™ was measured at the Accuri C6 and analysed with the LEGENDplex™ software v8.0.

3.14 Mice

All experiments were approved by the office for consumer protection of the city of Hamburg (N66/17, N042/2019 and T_18_006). Mice were bred and kept in a SPF facility at the BNITM.

3.14.1 Genotyping *Csf1R-Cre Axl^{fl/fl}Mertk^{fl/fl}*-mice

Mice were earmarked and the ear tissue sample was used for genotyping. For the lysis, proteinase K (10 µL) was added to 90 µL digestion buffer per sample and stored at 37°C at 200 rpm overnight. The next day the genomic DNA (gDNA) was harvested by stopping the reaction with 200 µL Ampuwa water and incubating for 10 min at 95°C. Samples were roughly vortexed in between the steps. gDNA was amplified by PCR using the DreamTaq™-PCR Kit from Thermo Fisher. The PCR was performed for each gene separately. To validate the specific amplification an agarose gel electrophoresis was performed

using 1.5 % agarose in TBE buffer. The expected band size as well as the PCR-Primer and PCR cycles are depicted below.

Primer sequence:

Mertk-SC1: ATG TGA CCT TCA GAG ATT CCC AGG

Mertk-PRPL4: TGA CGA AGC ACA CAG AGC TGG

Mertk-flox: 437 bp

Mertk-WT: 367 bp

Axl-PINK3: CTG TTG TAC CAT GTC CAC TGT GG

Axl-SDL2: CCC TTG TCT CTA CAT TTG TCT CCA

Axl-flox: 472 bp

Axl-Wt: 406 bp

Csf1r- Cre fw.: CTGGCTGTGAAGACCATC

Csf1r-Cre rev.: CAGGGCCTTCTCCACACCAGC

Csf1r-Cre: 393bp

PCR cycles

Denaturation: 94°C for 3 min

Denaturation 94°C for 30 s repeat 35 x

Annealing 60°C for 30 s

Elongation 72°C for 1 min

Final elongation 72°C for 10 min

3.14.2 Cell isolation from different organs

The mice were sacrificed by application of CO₂/O₂. To ensure sufficient anaesthesia, cornea and foot reflexes were checked twice and death ensured by cervical dislocation. The harvested organs were collected and stored in PBS/2 % FCS, in RNA \textit{later} for RNA analysis or formaldehyde for histology. Blood was collected in tubes containing 20 μ L heparin, centrifuged for 15 min at RT at 13000 rpm and the sera stored at -20°C.

3.14.2.1 Isolation of macrophages from the liver

To isolate the lymphocytes from the liver, a liver perfusion was performed after cervical dislocation of the mice. A Venofix 27 G butterfly needle was inserted in the vena cava and the blood from the liver removed by perfusion with 20 mL PBS by hand. The liver was collected and stored in 2 mL PBS/2 % FCS on ice. The gallbladder was removed and the liver minced into pieces before 10 mL of digestion buffer (DMEM, 1mg/mL Collagenase IV, 150 U/mL DNaseI, 0.2 M MgCl₂, 0.5 M CaCl₂) were added and the suspension incubated for 45 min at 37°C while shaking. The digested suspensions were mashed over a 70 µm cell strainer and the strainer was washed twice to obtain a single cell suspension. The suspensions were centrifuged at least twice at 300 xg 5 min 4°C and washed with 20 mL of cRPMI until the supernatant, which was discarded, was clear. To obtain non-parenchymal cells (NPC) the suspension was centrifuged at 50 xg for 4 min, the supernatant transferred into a new falcon, washed again and resuspended in 6 mL 37 % Percoll. After centrifugation for 10 min at 400 xg (dec.1 acc.9) a red blood cell-lysis was performed (1 mL for 3 min). After washing, the cells were used for RNA analysis, cell sorting at the FACSaria or phenotypical investigations at the LSR II.

3.14.2.2 Isolation of lamina propria leukocytes

The colon was harvested, the mesenteries removed, and cut longitudinally before being transferred into a tube to wash the colon multiple times with cold PBS to remove remaining faeces. The colon was cut into pieces and digested in HBSS containing 200 µL EDTA (0.5 M) for 20 min at 37°C while shaking. After another washing step, to remove epithelial cells, the colon was minced into a thin paste in a petri dish and a second digestion step (HBSS, 2 % FCS, 3µL DNase I per 5 mL HBSS and 5mg Collagenase VIII) was performed for 45 min at 37°C while shaking. The cell digest was filtered through a 100 µm cell strainer followed by a 40 µm cell strainer. After centrifugation (5 min, 300 xg, 4°C) the cells were counted and used for cell staining.

3.14.2.3 Isolation of leukocytes from the lymph nodes

The three mesenteric lymph nodes were harvested and cleaned before being stored in cold PBS/2 % FCS on ice during all the isolation processes. The lymph nodes were mashed through a 100 µm filter and centrifuged at 420 xg for 5 min at 4°C. The cells were resuspended in Clicks Media, counted and seeded in a 96 well plate with a concentration of 6·10⁶ cells/well in duplicates. Half of the cells were stimulated with 1 µg/mL of anti CD3ε (BioLegend) for 48 h. The supernatant was harvested, centrifuged and stored at -20°C until an ELISA was performed.

3.14.3 Thioglycollate-induced peritoneal inflammation

Female mice were injected intraperitoneal (i.p.) with 600 μ L 4 % Thioglycollate (Merck) on two sides, each 300 μ L, of the peritoneum. Two days later mice were treated i.p. with complexed IL-4 (cIL-4) and $3 \cdot 10^6$ aN, cIL-4 and $3 \cdot 10^6$ aT or with 200 μ L PBS as vehicle control. For the cIL-4 a solution of 5 μ g recombinant mouse IL-4 (Peprtech) and 25 μ g anti-IL-4-murine antibody (clone 11B11, BioxCel) was prepared and incubated for 5 min on ice. At day four, the peritoneal cells were isolated. To this end, mice were sacrificed with CO₂/O₂ following cervical dislocation and the fur carefully removed. 5 mL PBS/2 % FCS was injected into the intact peritoneum and the peritoneum was massaged for at least 30 s to detach the macrophages. Without puncturing the organs, the fluid was reobtained with a syringe. Afterwards a red blood cell-lysis was performed, the cells stained and analysed by flow cytometry.

3.14.4 *Schistosoma mansoni* infection

For the infection with *Schistosoma mansoni*, WT (C57BL/6), *Csf1r-Cre⁻ Axl^{fl/fl} Mertk^{fl/fl}* and *Csf1r-Cre⁺ Axl^{fl/fl} Mertk^{fl/fl}* were separately injected subcutaneously (s.c.) with 20-35 *cercariae* diluted in 200 μ L distilled H₂O (dH₂O). The *cercariae* were grown by Helmuth Haas from the Research Center Borstel. For counting the *cercariae* 10 μ L *cercariae*-solution was diluted in 100 μ L dH₂O in a 48-well plate with a grid. By supplementing 1 mL Lugol solution the *cercariae* were immobilised and counted under the microscope. A male to female *cercariae* ratio of 1: 1.2 was used for infection. After sacrificing the mice at different time points as indicated in the figures with time post infection (p.i.), liver, mesenteric lymph nodes and the colon were collected and leukocytes, in particular macrophages, were isolated as described below (see 3.14.2.1-3.14.2.3). To investigate mRNA levels of specific genes, a piece of the right renal fossa loop of the liver and piece of the left loop of the lung tissue were harvested in *RNAlater*. For histology, liver samples (right loop) were fixed in formaldehyde.

3.14.5 Adoptive transfer of macrophages

Macrophages were differentiated from the BM as described earlier (see 3.4) and plated in an untreated 6-well plate in a concentration of $1.2 \cdot 10^6$ cells/well. aN, aT and aH were generated (see 3.4) and co-incubated with the macrophages (see 3.8). Afterwards, macrophages were treated with recombinant mouse IL-4 (eBioscience) for 24 h. Cells were harvested, washed and counted. 1 Mio cells per mouse in 200 μ L PBS were injected intravenously (i.v.) in the lateral tail vein at week 6 and 7 p.i. Control mice were injected with 200 μ L PBS. Mice were sacrificed at week 8 p.i. and liver and colon harvested for further investigations.

All data provided from the adoptive transfer experiment are normalised, except the mRNA expression. The data obtained from mice that received macrophages, were normalised to the mice that was infected but did not receive cells (control mice). The average of the obtained data of the control mice was set to 1 and the fold change compared to the control is depicted for the other samples.

3.14.6 Determination of alanine transaminase levels in the serum

The quantification of the alanine transaminase (ALT) levels in the serum from the naïve and infected mice were determined using the Reflotron™ from Roche. The measurement of ALT levels is used to obtain information about the health status of the liver, where high ALT levels indicate liver damage. 32 µL of the Sera were added to a test strip, without touching the barcode, and inserted in the Reflotron™. Measurements were performed at 25°C.

3.14.7 Determination of the egg count in liver and colon

A piece of the left loop of the liver or a piece of the colon were harvested, weighed and stored in 2 % KOH for 8 h or 16 h, respectively, at 37°C in a 24 well plate with a grid. The tissue was further disrupted by resuspending with a 1 mL pipette and the eggs counted on a bright field microscope using 4 x magnification. The eggs per gram liver/colon were calculated.

3.14.8 Histology analysis

Histology slides and staining were performed by the Diagnostic department of the BNITM. For liver section, sirius Red (siRed) staining was performed to visualise deposition of collagen and to investigate fibrosis or granuloma formation inside the liver. Histology pictures were taken with a Keyence microscope. Analysis of the histology was performed with ImageJ. siRed-positive granuloma-structures were determined.

3.15 RNA-based next-generation sequencing (RNAseq) analysis

RNA from three independent *in vitro* samples were pooled and the RNA transcriptome sequenced using 100 base/paired-end reads performed on a BGISEQ platform. For RNA-seq analysis genes which were at least 3-fold increased by IL-4 compared to untreated samples were selected. For these 444 genes the counts per million (CPM) in the sample aN+IL-4, aT+IL4 and aH+IL-4 were analysed and visualised in a heatmap. For visualisation, the CPMs were logarithmised (log10) and scaled by calculating the average of the gene and subtracting it from each sample, followed by dividing through

the SED. Scaled values higher than zero indicate a higher expression of these genes compared to the other samples. For GO analysis, a threshold for the most highly expressed genes in each sample was set at the scaled value of ≥ 1 . All genes above, while having a negative score in the two other samples were included in the GO analysis, which was performed with the software DAVID 6.7 (Database for Annotation, Visualization and Integrated Discovery) and the modified Fisher exact score (EASE) was plotted. A dotted line was set to an EASE score of 0.05 (logarithmised (-log₁₀)). Higher -log₁₀ values indicate a lower p-value.

RNAseq analysis were performed together with Christian Casar, University Hospital Eppendorf

3.16 Single cell sequencing (ScSeq)

For single cell sequencing (scSeq), liver cells were isolated from *S. mansoni*-infected mice, stained for CD45, CD11b, Ly6G and CD11c and sorted at the FACS Aria. Dead cells and doublets were excluded. Neutrophils were excluded by CD11b⁺Ly6G⁺ staining and DCs with CD11c⁺ staining. CD11b⁺ cells were stained and used for scSeq. Library preparation was performed using the Chromium Single Cell 3' GEM, Library & Gel Bead Kit v3 from 10x genomics. Library preparation was performed according to the manufacturer's protocol in cooperation with Jenny Krause, AG Gagliani and AG Krebs. Two-lanes DNBseq PE100 sequencing was performed on a BGISEQ platform generating about 300-350 mio reads per sample. Index Primer (Chromium i7 Sample Index Platte well ID) that were used are:

Sample 1: SI-GA-F4,CCCAATAG,GTGTCGCT,AGAGTCGC,TATCGATA

Sample 2: SI-GA-F5,GACTACGT,CTAGCGAG,TCTATATC,AGGCGTCA

ScSeq analysis were performed by Christian Casar, University Hospital Eppendorf.

3.17 Statistics

Detailed information on the statistical analyses is supplied in the figure legends. Briefly, all data were analysed for normal distribution before running statistical tests. All of the provided data did not reach normal distribution. If, within one graph, comparisons of one treatment were only made to one other treatment, without interest in its relation to another sample, a Mann-Whitney U test (two groups) was performed. For comparison among different treatments inside one graph, a Kruskal-Wallis-test was used to determine statistically differences followed by pairwise comparisons analysis using Dunn's test, as indicated in the legend or graph respectively. Statistical significance is indicated for $p \leq 0.05$. Non-significant results ($p > 0.05$) are marked as "ns". All data are shown as mean \pm SEM; each data point indicates one independent sample/mouse. Numbers of samples are indicated in the figure legends.

4 Results

Constant clearance of apoptotic cells by macrophages is essential for the functionality of the immune system. How apoptotic cells influence the immune response of macrophages has become more and more important in the last years. This work aims to understand the impact of phagocytosis of apoptotic cells with different origins on the function and phenotype of macrophages. The polarisation status of macrophages after co-culture with apoptotic cells *in vitro* was analysed by flow cytometry, RNAseq and qPCR analysis. *In vivo*, the impact of phagocytosis on the heterogeneity of macrophages was investigated during the infection with *S. mansoni*, using mice with *Axl* and *Mertk* receptor deficiency on macrophages. Besides evaluating the clinical outcome of the infection, macrophages' phenotype was analysed by flow cytometry and scSeq. In addition, the therapeutic potential of macrophages imprinted by different types of apoptotic cells on parasite clearance during infection was evaluated. To translate the murine results obtained to human samples, the phagocytic receptor expression in PBMCs from patients with schistosomiasis was analysed.

4.1 Apoptotic cells with different origins expose similar amounts of PtdSer while being TUNEL negative, and are able to be phagocytosed by macrophages

To investigate the influence of apoptotic cells with different original identities on macrophages, apoptosis was induced in a sterile way in neutrophils, thymocytes and hepatocytes. For this, isolated primary neutrophils and thymocytes were aged over night with low amounts of FCS. Hepatocytes were heated for the induction of apoptosis. Afterwards, apoptotic neutrophils (aN), apoptotic thymocytes (aT) and apoptotic hepatocytes (aH) were characterised. When cells go into apoptosis, PtdSer is exposed on the cell surface (see 1.3)^{121,169}. During later steps of apoptosis, dying cells undergo DNA fragmentation and membrane blebbing followed by apoptotic body formation. Based on that, apoptotic cells were characterised by their PtdSer exposure with Annexin V staining, as well as by the amount of DNA breaks detectable by TUNEL staining. Early apoptotic, but not late apoptotic cells are important for this study, since PtdSer is one of the known factors that modulates the tissue remodelling response of macrophages. The magnitude of this response is dependent of the amount of early apoptotic cells in the culture and is not induced by late or necrotic cells^{91,170}. To this end, cells with increased membrane permeability to propidium iodide (PI) were excluded from the analysis. PI is a dye that enters the nucleus when the membrane disintegrates and marks either necrotic cells (single positive) or late apoptotic cells (double positive for PI⁺ and Annexin V⁺). All three apoptotic cell types, aN, aT and aH, showed similar frequencies of Annexin V⁺ PI⁻ cells (20 % to 25 %) (Fig. 5). After the exclusion of doublets, the TUNEL staining revealed low levels of DNA breaks in all three apoptotic cell

types with frequencies of TUNEL⁺ cells varying from 1.1 % to 2.1 %, only slightly above the negative control (1.05 %) (Fig. 5B).

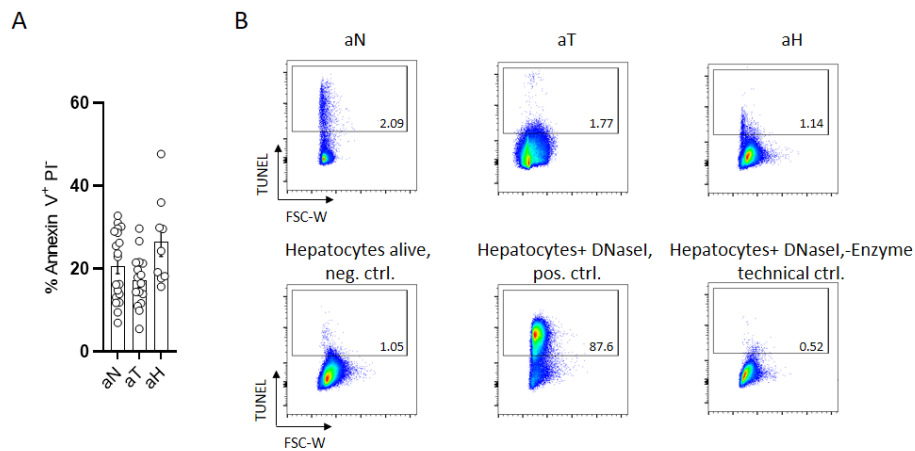


Fig. 5: Different apoptotic cell types have similar frequencies of phosphatidylserine and low frequencies of DNA breaks.

(A) Frequencies of early apoptotic (Annexin V⁺ PI⁻) neutrophils (aN), thymocytes (aT) and hepatocytes (aH). Each data point indicates one independent sample. n= 10-19. Mean \pm SEM. Kruskal-Wallis test, differences did not reach statistical significance. (B) Representative flow cytogram shows frequencies of cells with DNA breaks, detected by TUNEL staining. For the negative control living hepatocytes were used. Positive control shows hepatocytes treated with DNaseI. Technical control is represented by hepatocytes treated with DNaseI, undergoing TUNEL staining in the absence of the staining-enzyme.

The apoptotic cells from different sources here analysed do not differ in their apoptotic characteristics with regard to the exposed PtdSer or the amount of large DNA breaks.

To investigate the impact of apoptotic cells on the phenotype and function of macrophages, the capacity of macrophages to phagocytose aN, aT and aH was analysed (Fig. 6). To this end, the apoptotic cells were stained with a cell tracker-dye (CFSE) and the phagocyte with antibodies against the macrophage markers CD11b and F4/80. This allowed the discrimination of macrophages that phagocytosed (positive for CFSE and macrophage markers) and macrophages that did not phagocytose (negative for CFSE and positive for macrophage markers). Both markers, CD11b and F4/80, are used consistently in this work to identify macrophages by flow cytometry. The assay is performed on two conditions simultaneously. At 4°C, the cytoskeleton rearrangement of macrophages is inhibited and they can bind the apoptotic cells, but are not able to uptake them (Fig. 6 upper row). At 37°C, macrophages bind and uptake the apoptotic cells (Fig. 6 lower row). A representative dot plot is shown. Here the incubation of macrophages with aT leads to the highest frequency of bound and uptake apoptotic cells (56.2 %). By subtracting the percentages of CD11b⁺F4/80⁺CFSE⁺ macrophages that bound apoptotic cells (measured at 4°C) from the percentages of macrophages that bound and uptake apoptotic cells (measured at 37°C), the frequencies of phagocytosing macrophages were

determined and are shown on the right. These results indicate that macrophages phagocytosed all three apoptotic cell types. aH and aT are phagocytosed to a significantly higher extent compared to aN. However, aN are bound, but not phagocytosed, to a greater extent compared to aT and aH by macrophages. This is reflected by smaller differences between CD11b⁺F4/80⁺CSFE⁺ macrophage frequencies at 4°C and 37°C (cumulative data not shown).

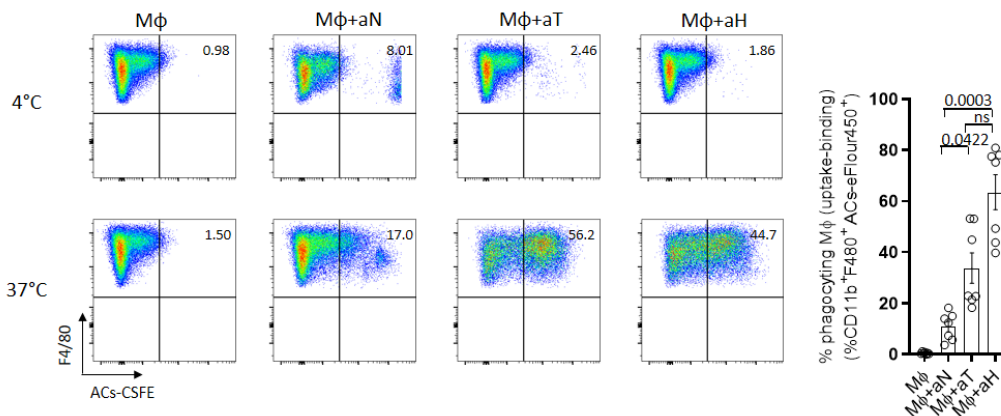


Fig. 6: Macrophages phagocytose apoptotic cells with different identities.

Representative flow cytogram (left) depicts BMDMs phagocytosing different apoptotic cells (ACs) (aN, aT and aH), detected as frequency of cells positive for the CSFE-labelled AC dye. A summary of the data is shown on the right. Data display frequencies of phagocytosing macrophages (Mφ). Phagocytosis is defined by the difference of the frequency of macrophages binding and uptaking ACs at 37°C and the frequency of macrophages binding ACs at 4°C. Each data point indicates one independent sample. n=6. Mean ± SEM, Kruskal-Wallis test resulted in $p < 0.0001$, followed by pairwise comparisons conducted with Dunn's test between indicated samples, ns: $p > 0.05$.

The apoptotic cell types analysed do not differ in their apoptotic characteristics and macrophages are able to phagocytose all of them.

As described in the introduction (see 1.2.1), clearance of apoptotic cells induces the release of anti-inflammatory factors by macrophages. Whether the induction of the anti-inflammatory/tissue remodelling phenotype depends on the origin of the apoptotic cells was investigated by analysis of the polarisation status of macrophages after phagocytosis of aN, aT or aH in an IL-4-enriched environment.

4.2 Macrophages acquire a tissue remodelling phenotype after sensing apoptotic neutrophils, but not after phagocytosis of apoptotic thymocytes or apoptotic hepatocytes

IL-4 is a prototypical trigger of an anti-inflammatory/tissue remodelling phenotype in macrophages⁵⁸. This dogma has been extended, as in the last years, studies have shown that not IL-4 alone, but rather the synergistic sensing of IL-4 and apoptotic cells polarises macrophages towards an anti-inflammatory/tissue remodelling phenotype. Increasing the amount of apoptotic cells, which are

normally found in every cell culture, by adding exogenous apoptotic cells, potentiated the IL-4 response in macrophages⁹¹. To investigate if all of the three apoptotic cell types (aN, aT and aH) are able to potentiate a tissue remodelling signature in macrophages, compared to the IL-4 stimulation alone, tissue remodelling-associated gene expression (*Ear2*, *Retnla*, *Chil3*) in macrophages isolated from the BM was analysed. To this end, macrophages were stimulated with IL-4 after exposure to apoptotic cells from different cellular origins.

Only macrophages co-cultured with aN (red bars) showed a significant enhancement of the IL-4-induced transcripts *Ear2*, *Retnla* and *Chil3* (Fig. 7A). Macrophages co-cultured with aT did not show any potentiation of the IL-4-induced phenotype, while aH even reduced the expression of *Ear2*, *Retnla* and *Chil3*. Flow cytometry analysis of macrophages stained for RELM α (protein encoded by *Retnla*) or YM1 (protein encoded by *Chil3*) confirmed the results at protein level, here a representative dot plot and the cumulative data are shown (Fig. 7B and C). The frequencies of RELM α ⁺ and YM1⁺ macrophages (CD11b⁺F4/80⁺) were significantly higher after co-cultivation with aN (red bar) compared to macrophages treated with IL-4 alone (Fig. 7C). Co-culture of macrophages with aT did not alter the frequencies of IL-4-induced RELM α ⁺ or YM1⁺ macrophages, while co-culture with aH reduced the amount of RELM α ⁺ or YM1⁺ macrophages compared to IL-4 stimulation alone. Due to the absence of commercially available antibodies against *Ear2* that can be used for flow cytometry, its expression at protein level was not evaluated.

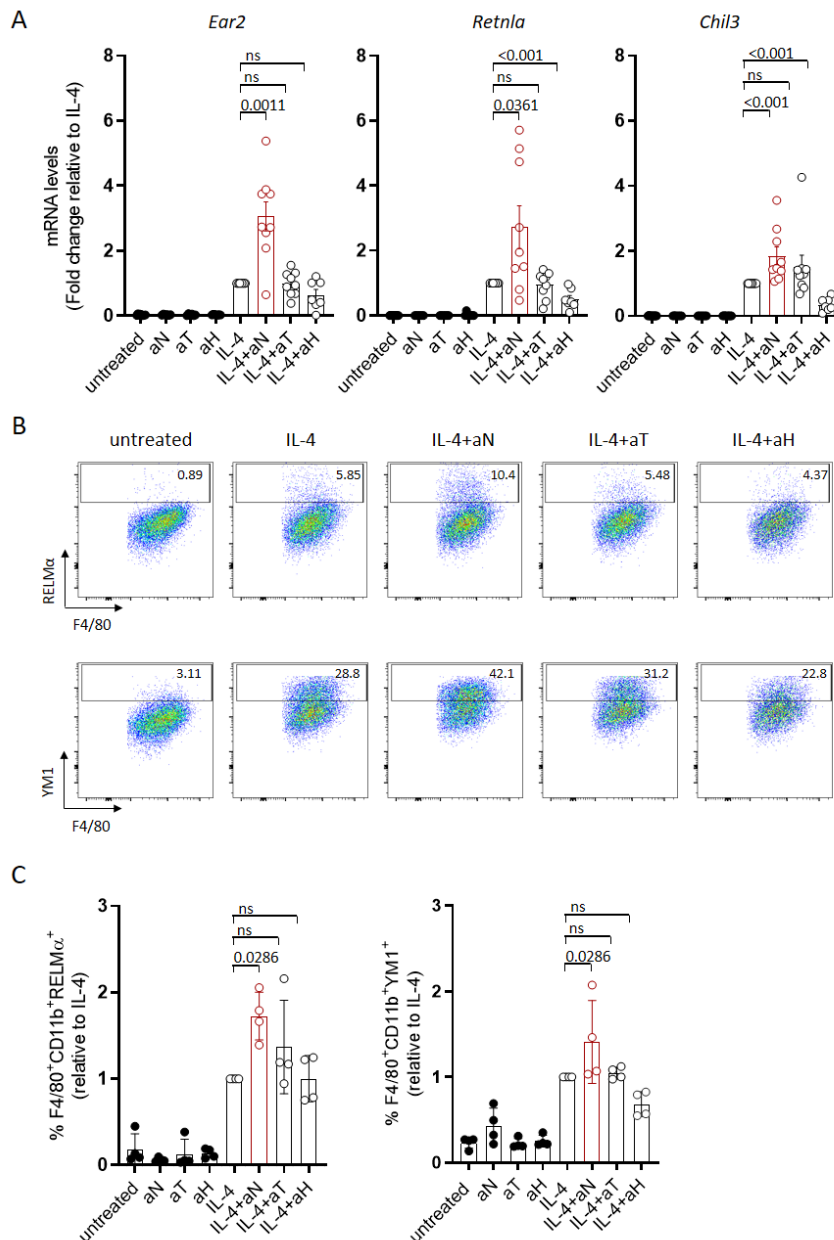


Fig. 7: The phenotype of macrophages is shaped by the origin of apoptotic cells they phagocytose.

(A) mRNA levels of *Ear2*, *Retnla* and *Chil3* in BMDMs either untreated or treated with apoptotic neutrophils (aN), apoptotic thymocytes (aT) or apoptotic hepatocytes (aH) alone, or prior to stimulation with IL-4 for 48 h, as detected by qPCR. (B) Representative flow cytograms and (C) pooled data reporting the frequencies of macrophages expressing RELM α and YM1 when exposed to different apoptotic cells in combination with IL-4, as described in A. Each data point indicates one independent sample. n = 4-9. Mean \pm SEM, Mann-Whitney U test. Test was exclusively performed between indicated samples, ns: p > 0.05.

These results demonstrate that not all apoptotic cells are able to shape macrophages towards a tissue remodelling phenotype. aN induced the tissue remodelling response in macrophages, which could not be observed after the uptake of aT or aH; on the contrary, macrophages decreased their expression of tissue remodelling genes after the sensing and uptake of aH.

To confirm that apoptotic cells from different origins imprint the phenotype of macrophages *in vivo*, macrophages were primed either with aN+IL-4 or aT+IL-4. Beforehand, peritonitis was induced in the mice by the inoculation of thioglycollate, which induces a non-microbial-induced inflammation in the peritoneum that resolves through the recruitment of macrophages with a tissue remodelling function¹⁷¹. Afterwards, aN+IL-4 or aT+IL-4 were injected and two days later macrophages were isolated from the peritoneum. To evaluate whether the apoptotic cells are able to alter the frequency of tissue remodelling-associated macrophages *in vivo*, the frequencies of RELM α ⁺ or YM1⁺ macrophages were analysed by flow cytometry. Mice treated with aN+IL-4 showed significantly higher frequencies of RELM α ⁺ or YM1⁺ macrophages compared to mice treated with aT+IL-4 (Fig. 8). The injection of aH+IL-4 was omitted because the size of the cells might lead to unpredictable health problems for the mice, which could result in enhanced recruitment of neutrophils and macrophages followed by the priming of macrophages by dying neutrophils and not by the injected aH.

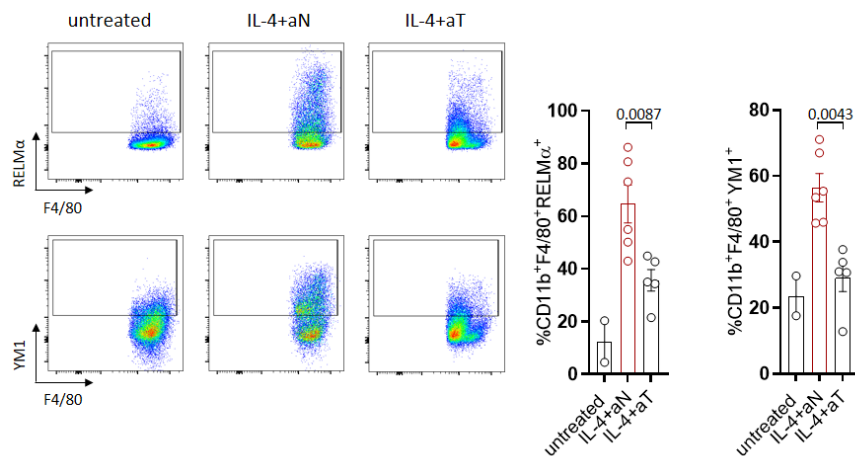


Fig. 8: *In vivo*, aN+IL-4 induces higher frequencies of RELM α ⁺ and YM1⁺ macrophages compared to aT+IL-4 injection after peritonitis induction.

Representative flow cytograms (left) and independent data of the frequencies of RELM α ⁺ and YM1⁺ macrophages (CD11b⁺F4/80⁺) (right) isolated from the peritoneal cavity of mice treated with thioglycollate and two days later injected with aN+IL-4 or aT+IL-4. Two independent experiments are shown. Each data point indicates one independent sample. n=2-5. Mean \pm SEM, Mann-Whitney U test. Test was exclusively performed between indicated samples, ns: p>0.05.

In summary, only aN induce the expression of tissue remodelling markers at mRNA and protein level *in vitro* and *in vivo* and thereby alter the phenotype of macrophages towards a tissue remodelling phenotype. However, the reason for the specific macrophage-modulation by aN, that was not observed by aT or aH, was further investigated.

4.3 PtdSer alone is not sufficient for the induction of a tissue remodelling phenotype in macrophages nor is a soluble factor released by neutrophils

Further studies of the macrophage - apoptotic cell interaction revealed that the sensing of PtdSer exposed on the surface of apoptotic cells induces the tissue remodelling phenotype in macrophages, as indicated by experiments in which blocking the sensing of PtdSer via Annexin V reduced their tissue remodelling signature¹⁷². Since all three apoptotic cell types exposed similar levels of PtdSer (Fig. 5A), the specific impact of PtdSer on the response of macrophages was investigated via the use of liposomes provided with different amounts of PtdSer, which mimics the exposure of PtdSer on apoptotic cells. These liposomes were labelled with FITC fluorochromes to track them by flow cytometry. Similar to the results obtained with the phagocytosis assay performed with different apoptotic cell types (Fig. 6), the capacity of macrophages to phagocytose liposomes provided with different concentration of PtdSer was investigated. Additionally, their impact on the tissue remodelling gene transcripts was analysed. Phagocytosing macrophages are defined, as described previously, by the difference between macrophages positive for the liposome dye at 37°C and 4°C. The frequency of liposome-phagocytosing macrophages (CD11b⁺F4/80⁺FITC⁺) was dependent on the amount of PtdSer presented by the liposomes (Fig. 9A). Liposomes provided with the highest amount of PtdSer (30 %) were phagocytosed the most. However, a significant difference between phagocytosis of liposomes with 30 % PtdSer or 10 % PtdSer was not observed. Gene expression analysis of *Ear2*, *Retnla* and *Chil3* after treatment with either IL-4 alone or after co-culture with aN or PtdSer-liposomes in combination with IL-4 showed that BMDMs treated with IL-4+aN were able to potentiate the IL-4 response significantly for all the three genes analysed, as shown previously. Importantly, this was observed to a lesser extent for the BMDMs treated with liposomes prior to IL-4 stimulation (Fig. 9B). Liposomes provided with a reduced concentration of PtdSer were also not able to potentiate the IL-4 response (data not shown).

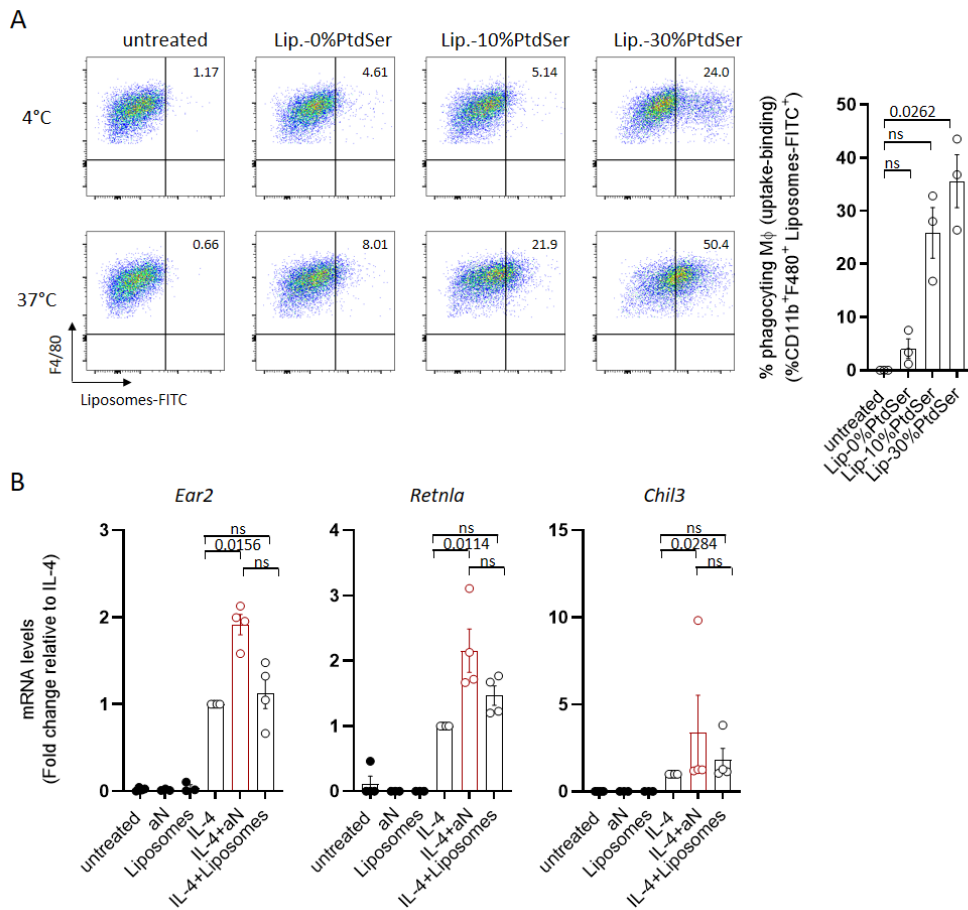


Fig. 9: PtdSer-provided liposomes are not able to potentiate the expression of tissue remodelling genes in macrophages compared to IL-4.

(A) Representative flow cytogram (left) depicting BMDMs phagocytosing liposomes provided with different amounts of PtdSer detected as cells positive for the FITC-labelled liposomes, CD11b and F4/80. Independent data are shown on the right. Data display frequencies of phagocytosing macrophages (M ϕ). Phagocytosis is defined by difference of the frequency of macrophages binding and uptaking liposomes at 37°C and the frequency of macrophages binding liposomes at 4°C. (B) mRNA levels of *Ear2*, *Retnla* and *Chil3* in macrophages either untreated or treated with apoptotic neutrophils (aN) or with liposomes provided with 30 % PtdSer (Liposomes) or with aN or Liposomes prior to stimulation with IL-4, detected by qPCR. Each data point indicates one independent sample. n=3-4 Mean \pm SEM, Kruskal-Wallis test resulted in (A) p= 0.0006 (B) p= 0.0026; p= 0.0019; p= 0.0087 (left to right) and followed by multiple comparisons conducted with Dunn’s test between indicated samples. If not revised differently no significant changes were observed, ns: p>0.05.

The obtained data revealed that PtdSer alone is not sufficient to induce a tissue remodelling phenotype as a post-engulfment consequence in macrophages, independent of its amount. The involvement of an additional factor, besides the exposure of PtdSer, in the polarisation of macrophages towards a tissue remodelling phenotype was further investigated.

Soluble factors released during the co-culture of apoptotic cells and macrophages could interfere with the polarisation of macrophages¹⁷³ and were therefore analysed. However, a transfer of the supernatant from the co-culture of macrophages with aN (aN-med) to the co-culture of macrophages

with aT (Fig. 10A) did not amplify the tissue remodelling response in macrophages compared to the co-culture with aT without the aN-med (Fig. 10B).

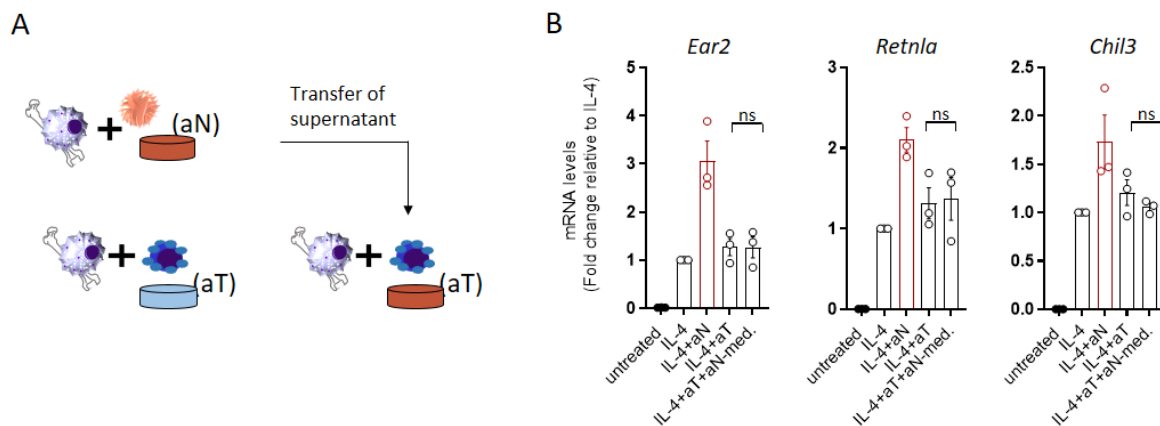


Fig. 10: aN do not release soluble factors during the co-culture with macrophages that are responsible for the induction of a tissue remodelling phenotype in macrophages.

(A) Experimental scheme. Supernatant of the co-culture of BMDMs with aN (aN-med) were transferred to the co-culture of macrophages with aT. (B) Expression of *Ear2*, *Retnla* and *Chil3* in BMDMs, detected by qPCR. Macrophages are either untreated, or treated with IL-4 or with aN or aT prior to IL-4 stimulation or treated with aT prior to IL-4 stimulation in the presence of conditioned media harvested from macrophages in co-culture with aN (aN-med.). Each data point indicates one independent sample. n=3. Mean \pm SEM, Mann-Whitney U test was exclusively performed between indicated samples, ns: p>0.05.

To further investigate the involvement of a soluble factor, cytokine productions during the co-culture of macrophages with aN, aT or aH were evaluated. No production of the analysed cytokines IL-2, IL-4, IL-5, IL-6, IL-10, TNF α and IFN γ during the co-culture of macrophages with different apoptotic cells could be observed (therefore no data shown). Another possibility is that different cytokines are produced during the induction of apoptosis, and that this contributes to the aN-induced macrophage phenotype¹⁷⁴. However, none of the analysed cytokines (IL-4, IL-5, IL-6, IL-10, TNF α or IFN γ) were detected either after induction of apoptosis in neutrophils, hepatocytes and thymocytes (therefore no data shown). These data suggest that the capacity of aN to induce a tissue remodelling response in macrophages is not mediated by soluble factors that are released while undergoing apoptosis or during the co-culture of apoptotic cells with macrophages. To this end, specific neutrophil characteristics were further investigated.

A unique function of neutrophils is to kill invading pathogens by the formation of neutrophil extracellular traps (NETs), without damaging the host itself¹⁷⁵. One of the responsible proteins in the activation process of NETs is myeloperoxidase (MPO)^{176,177}. To assess whether NET formation contributes to neutrophil capability to induce a tissue remodelling phenotype in macrophages, aN from *Mpo*^{-/-} mice were co-cultured with macrophages. mRNA expression of *Ear2*, *Retnla* and *Chil3* were

compared to macrophages treated with aN isolated from WT mice (Fig. 11C). Differences in the gene expression between macrophages treated with either aN from WT mice or aN from *Mpo*^{-/-} mice was not observed.

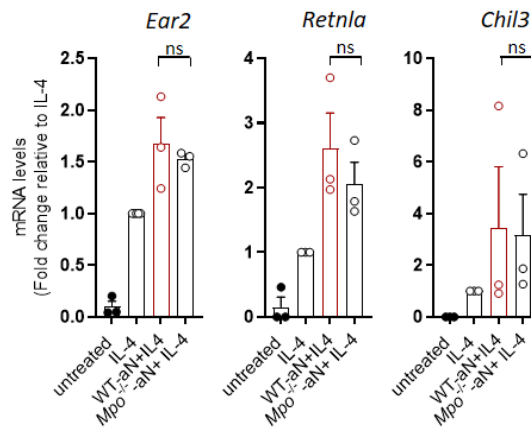


Fig. 11: The formation of NETs does not contribute to the induction of a tissue remodelling phenotype in macrophages.

mRNA levels of *Ear2*, *Retnla* and *Chil3* in BMDMs either untreated or treated with IL-4 or aN prior to IL-4 stimulation. aN are obtained either from WT or *Mpo*^{-/-} mice. Each data point indicates one independent sample. n=3. Mean ± SEM, Mann-Whitney U test was exclusively performed between indicated samples, ns:p>0.05.

With the conducted experiments a contribution of NETs, or more specifically, a contribution of MPO to the specificity of aN to commit macrophages towards a tissue remodelling response, could be excluded as well as the involvement of a soluble factor. This favours the possibility that a cell-cell contact between aN and macrophages is needed for the tissue remodelling response of macrophages, like the interaction of the phagocytic receptors on the macrophages and their ligands on the surface of the apoptotic cell.

To investigate whether the sensing and uptake of a selective apoptotic cell can affect the expression of phagocytic receptors in macrophages, mRNA levels of the PtdSer- dependent phagocytic receptors *Axl*, *Mertk* and *Cd36* (see 1.2.1) in macrophages were compared after the co-culture with aH, aT and aN prior to IL-4 stimulation. In addition, the bridging molecules *Pros1* and *Gas6*, necessary for the binding of AXL and MERTK to PtdSer, were analysed. Macrophages that phagocytosed aH showed significantly less expression of *Mertk* compared to the untreated sample, which was not observed in macrophages that engulfed aT or aN. In addition, *Cd36* expression was decreased in macrophages that phagocytosed aH compared to all other conditions analysed except the untreated control. *Axl* expression was not changed (Fig. 12A). The expression of both bridging molecules, *Gas6* and *Pros1*, are significantly decreased in macrophages that sensed and phagocytosed aH, which was not observed for macrophages co-cultured with aN or aT (Fig. 12B).

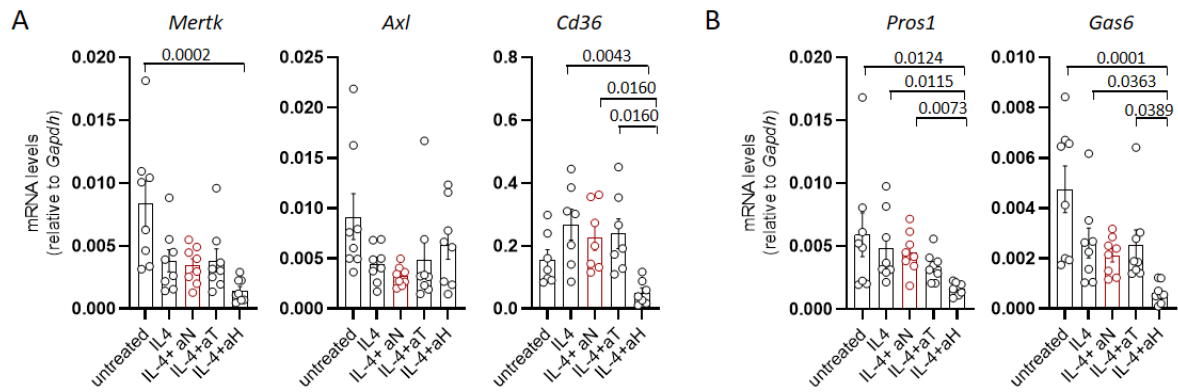


Fig. 12: The identity of the apoptotic cell phagocytosed affects the expression of phagocytic receptors in macrophages.

(A) mRNA levels of the PtdSer-R *Mertk*, *Axl* and *Cd36* in BMDMs either untreated or treated with IL-4 or aN, aT or aH prior to IL-4 stimulation. (B) mRNA levels of the bridging molecules *Pros1* and *Gas6* either untreated or treated with IL-4 or aN, aT and aH prior to IL-4 stimulation. Each data point indicates one independent sample. n=8. Mean \pm SEM, Kruskal-Wallis test resulted in (A) $p=0.0010$; $p=0.0485$; $p=0.0021$ (B) $p=0.0027$; $p=0.0004$ (left to right), followed by pairwise comparisons conducted with Dunn's test between indicated samples. If not revised differently no significant changes were observed, ns: $p>0.05$.

The obtained results showed that the phagocytosis of apoptotic cells with different origins modulates the expression of the phagocytic receptors *Mertk* and *Cd36* and the bridging molecules *Gas6* and *Pros1*. However, a specific expression profile of the genes analysed for aN was not observed.

Accordingly, the mechanism behind the specificity of aN to induce a tissue remodelling response of macrophages could not be fully revealed. Nonetheless, whether aT or aH are able to shape the phenotype and function of macrophages differently, apart from a tissue remodelling signature, was further dissected.

4.4 Apoptotic cells with different identities shape the IL-4-induced response of macrophages

To verify that the identity of an apoptotic cell imprints the transcriptional heterogeneity of macrophages within the IL-4 response after phagocytosis, RNAseq analysis of macrophages co-cultured either with aN, aT or aH prior to IL-4 stimulation *in vitro* was performed. It has been shown that RNA from internalised apoptotic cells dissolves after 6 h¹⁷⁸. To affirm that the transcriptional heterogeneity in macrophages is not affected by RNA contaminants from apoptotic cells, RNAseq was performed 48 h after exposure of macrophages to apoptotic cells. Genes that showed at least a 3-fold induction in macrophages stimulated with IL-4 compared to the untreated samples were selected. The differential expression of these 444 genes in macrophages co-cultured with either aN, aT or aH prior to the IL-4 stimulation was investigated with a hierarchical cluster analysis. The results are displayed

in the heatmap (Fig. 13A). Red colour indicates upregulation of genes, while blue colour depicts downregulated genes in each of the three conditions analysed. The sequencing results revealed distinct gene profiles for macrophages that phagocytosed either aN or aT or aH prior to IL-4 stimulation.

To investigate the enrichment in gene functions in each of the three conditions analysed, gene ontology (GO) analysis on differentially expressed genes was performed (Fig. 13B). GO-term assessment for the macrophages co-cultured with aN+IL-4 showed the induction of GO-terms associated with tissue remodelling like response to wounding, wound healing or coagulation, and genes like *Chil3*, *Ear2* and *Arg1* (Fig. 13B-red bars). Macrophages treated with aH+IL-4 upregulated pathways which are more associated with a tolerogenic or homeostatic function of macrophages, like inflammatory and defence response, regulation of cytokine production, regulation of cell proliferation and genes like *Programmed cell death 1 ligand 1 (Pdl-1)* or *Socs2* (Fig. 13B orange bars). Interestingly, the GO-term “response to wounding” was also associated with the aH+IL-4 sample. Evaluation of the genes included in this category revealed the presence of transcripts associated with the recognition and antigen-presentation capacities of macrophages, like *TLR* and *C-type lectin domain family 7 member A (Clec7a)*, rather than genes associated with a macrophage wound healing response. In contrast, in the aN+IL-4 sample the same pathway (“wound healing”) comprised genes that are known to be induced specifically in macrophages that acquire a tissue remodelling phenotype, like *Arg1* or *Fibronectin-1 (Fn1)*. Although the GO-term indicated the same pathways for both samples, analysis of the genes inside the categories confirmed a disparity between the samples. GO-term assessment for the genes specifically induced after aT+IL-4 treatment showed no significantly enriched functional pathway. Genes like *Serpinb9b*, *ribonuclease A family member 2 (Rnase2)*, *Ahnak* and *Aryl hydrocarbon receptor nuclear translocator 2 (Arnt2)* are upregulated inside this group. W

Within the 444 genes which were altered by the IL-4 treatment, only a small proportion of transcripts were specifically induced when macrophages were exposed to aT+IL-4 (46 genes). Sensing of aH+IL-4 induced changes in 121 of the genes that are upregulated by IL-4 specifically, the highest number of genes among the three cell types. Nevertheless, most of the IL-4 induced genes were not altered exclusively by only one of the apoptotic cell types and were instead changed by two or all of the apoptotic cells (199 genes) (Fig. 13C).

To verify the sequencing data, mRNA expression of one of the highly induced genes in each group was analysed (Fig. 13D). *Arg1*, a tissue remodelling gene¹⁷⁹ is significantly upregulated in macrophages co-cultured with aN+IL-4 and to a lesser extent in macrophages treated with aT+IL-4. In addition, *Arg1* is decreased significantly in macrophages that were co-cultured with aH+IL-4 compared to the IL-4 treatment. In macrophages treated with aH+IL-4 a significant increase of *Socs2* expression, a

tolerogenic/suppressive gene¹⁸⁰, was observed compared to the IL-4 stimulation alone. However, this was also seen after co-culture with aN+IL-4, although to a much lesser extent. Sensing of aT prior to IL-4 stimulation was not able to upregulate *Socs2* expression in macrophages compared to IL-4 alone. *Serpinb9b*, a proteinase inhibitor involved in DNA binding and apoptosis¹⁸¹, is slightly induced in macrophages co-cultured with aT prior to IL-4 treatment. This trend towards increased expression of *Serpinb9b* was also observed in macrophages treated with aN prior to IL-4 stimulation.

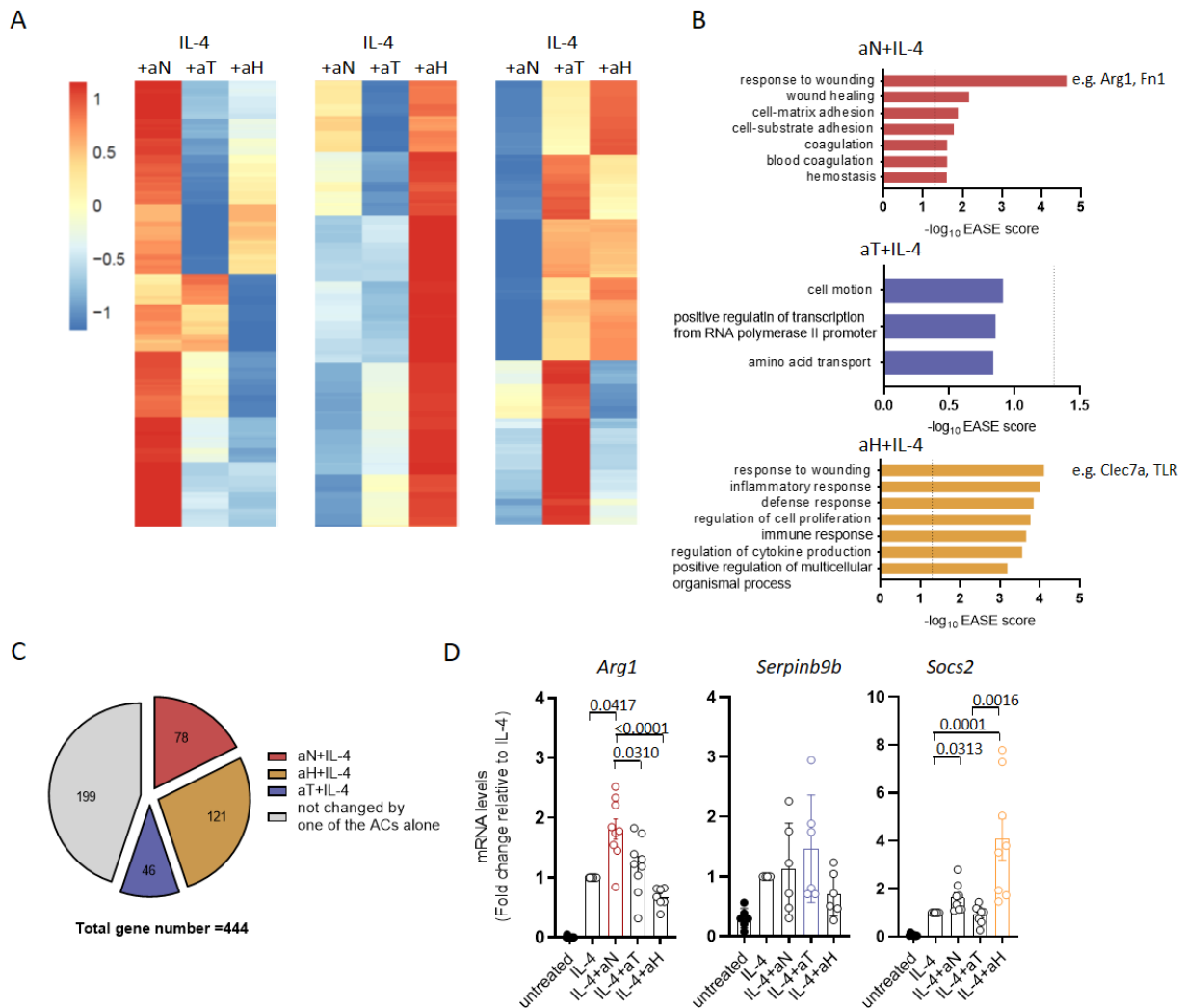


Fig. 13: IL-4-induced transcriptional profile of macrophages is dependent on the apoptotic cell they are phagocytosing.

(A) Heatmap displays differently expressed genes in macrophages treated with aN+IL-4, aT+IL-4 or aH+IL-4 analysed by RNA-seq. Genes are at least three times upregulated in the IL-4 sample compared to the untreated control. Depicted is the log₁₀ CPM (counts per million). RNA from 3 independent experiments are pooled. (B) Gene ontology assessment of genes which are highly upregulated in either aN+IL-4 or aT+IL-4 or aH+IL-4 (scaled score >1, with a negative score for the other samples). Dotted line represents p<0.05. (C) Numbers of differently expressed genes which are only induced in one of the conditions (aN+IL-4 red, T+IL-4, blue or aH+IL-4, orange). Grey area depicts the genes that are changed in their expression by more than one type of apoptotic cells (ACs) alone. (D) *Arg1*, *Socs2* and *Serpinb9b* mRNA levels in BMDMs either untreated or treated with IL-4 or aN, aT or aH prior to IL-4 stimulation. Each data point indicates one independent sample. n=6-8. Mean ± SEM, Kruskal-Wallis test resulted in (D) p= <0.0001; p= 0.5161; p= <0.0001 (left to right) followed by pairwise analysis conducted with Dunn's test between indicated samples. If not revised differently no significant changes were observed, ns: p>0.05.

The bulk sequencing analysis showed that aN shape macrophages' function towards a tissue-remodelling/anti-inflammatory one. aH are more prone to decrease the expression of these genes and shape the IL-4 response towards a more tolerogenic function. However, sensing of aT prior to IL-4 does not change the IL-4 response dramatically, instead small changes of some specific genes are seen in macrophages.

The analysis of the phagocytosis capacity, the function and the phenotype of macrophages revealed the impact of the original identity of an apoptotic cell on macrophages' heterogeneity. However, what the impact of the recognition and uptake of different apoptotic cells on macrophage function during an infection is has never been investigated so far. The next part of this work focuses on macrophages' heterogeneity and their phagocytosis capacity during an infection with *S. mansoni* a condition in which the anti-inflammatory/tissue remodelling phenotype of macrophages is necessary for host survival¹⁵⁴.

4.5 Macrophages' heterogeneity during *Schistosoma mansoni* infection is a consequence of phagocytosis of different apoptotic cells

Infection with *S. mansoni* first induces a type 1 immune response, followed by a switch to a type 2 immune response with upregulation of cytokines like IL-4 and IL-13¹⁴⁴. During disease progression, liver and colon damage occur, leading to an increase of apoptotic cells (see 1.4.2). To thoroughly study macrophages and the impact of phagocytosis of apoptotic cells during the infection with *S. mansoni*, single cell sequencing (scSeq) was performed. To this end, cells from the infected liver were isolated and CD11b⁺ cells were sorted, while excluding CD3⁺ T cells and CD11c⁺ DCs (Fig. 14A). Uniform manifold approximation and projection (UMAP) analysis to visualise the scSeq data revealed different clusters of cells (Fig. 14B). Briefly, cells that cluster closely together are more similar to each other than cells clustering apart from each other. To categorise the clusters, the expression of key markers for different cell types among the clusters were investigated (Fig. 14C). The expression intensity is depicted by the blue colour. The percentage of cells expressing the genes is defined by the circle size. In line with the sorting strategy, all clusters show a high expression of *Itgam*, the gene encoding the CD11b protein. Macrophage clusters 2, 3, 5 and 6 were defined by the expression of the classical macrophage markers *Cd14*, *Cd68* and *Adreg1* (encoding the protein F4/80). High expression of the genes *Killer cell lectin-like receptor subfamily a1 (Klra1)*, *Klrd1* and *Ncr1* (NKp46) is characteristic for NK cells¹⁸² (cluster 1). Although CD11c⁺ and Ly6G⁺ cells were excluded from the sorting, the UMAP analysis revealed contaminations with neutrophils. Neutrophils are defined by the expression of markers as *Ly6g*, *Neutrophilic granule protein (Ngp)* or *Lipocalin-2 (Lcn)* (cluster 7 and 9) and they acquire *C-X-C motif*

chemokine receptor 2 (*Cxcr2*) expression during the differentiation into mature neutrophils (cluster 8)¹⁸³, therefore immature neutrophils express low levels of *Cxcr2* (cluster 4)¹⁸³.

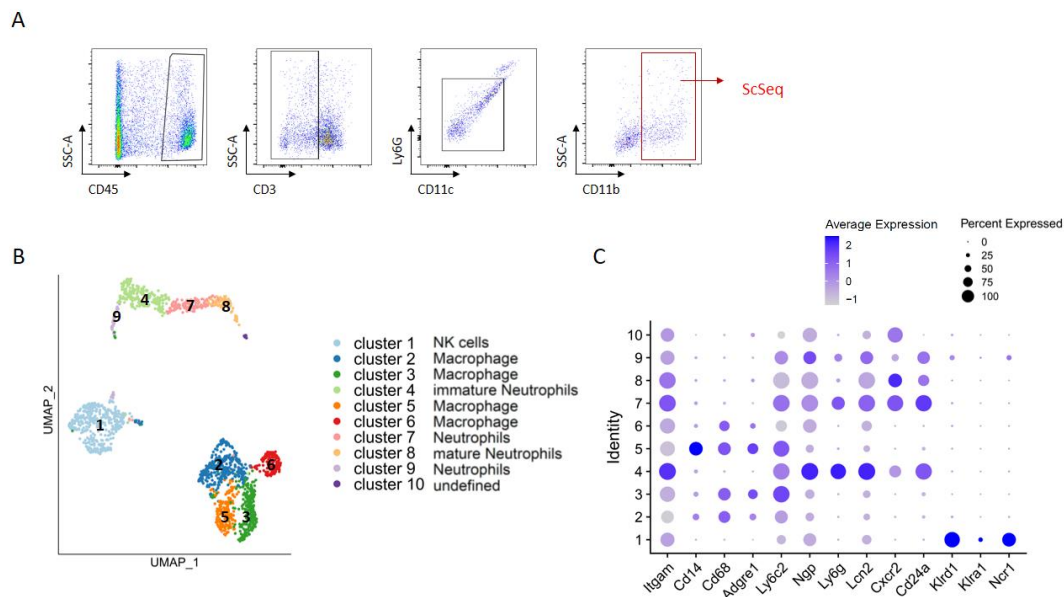


Fig. 14: Single cell sequencing (scSeq) of cells isolated from the liver of *S. mansoni*-infected mice reveals four distinct macrophage clusters.

(A) Mice were infected s.c. with 30 *Cercariae*. At week 14 p.i., livers were collected and CD11b⁺ cells isolated by FACS. CD3⁺ T-cells were excluded, as well as CD11c⁺ -DCs. CD11b⁺ cells were used for scSeq. Cells from 4 mice were pooled. (B) UMAP clustering of the sequenced CD11b⁺ cells. (C) Clusters are defined by the expression of *Itgam*, *Cd14*, *Cd68*, *Adgre1*, *Ly6c2*, *Ngp*, *Ly6g*, *Lcn*, *Cxcr2*, *Cd24a*, *Klrd1*, *Klra1* and *Ncr1*. Size of the circle shows the expression percentage of these inside the clusters, while the colour refers to the average expression per cluster.

To investigate whether the alteration of the four different macrophage clusters (2, 3, 5 and 6) in the scSeq is caused by the phagocytosis of different apoptotic cells, the bulk sequencing data were integrated in the scSeq data. To this end, the 50 selectively highest expressed genes in each sample (aH+IL-4, aT+IL-4 and aN+IL-4), were compared to the transcriptomic signature of macrophages in clusters 2, 3, 5 and 6. Based on these genes, expression of each individual cell from the scSeq was scaled to their compliance in the gene list. Scaled classification for each cell is depicted in the UMAP (Fig. 15A). Indeed, clusters 3 and 5 are enriched for the expression pattern characteristic of the aN+IL-4-induced transcriptomic signature *in vitro* (orange dots), while cluster 6 is enriched in gene expression observed in the aT+IL-4 sample (green dots). Gene expression associated with the phagocytosis of aH+IL-4 *in vitro* (blue dots) can be found broadly across all clusters. Furthermore, in each cluster the macrophages were analysed for their functional properties. The heatmap illustrates that each macrophage cluster has a specific gene expression profile. Genes associated with angiogenesis or tissue repair, such as *Kruppel-like factor 2* (*Klf2*), *Nuclear receptor 2a1* (*Nr2a1*) or *Thrombospondin 1* (*Thbs1*) or *Fn1* and *Fibrinogen-like protein 2* (*Fgl2*) are highly expressed in macrophages from clusters 5 and 3 respectively. Cluster 6 showed enrichment of phagocytosis

receptors like *Cd36* or *Cd300e*, while macrophages in cluster 2 expressed genes associated with antigen presentation like the *H2*-family or *Cd74*, which encodes for the histocompatibility antigen II. *Cd40*, a co-stimulatory molecule that plays a role in antigen presentation by activated APCs after binding to its ligand on the surface of e.g. T cells and is additionally necessary for macrophage induced B cell activation¹⁸⁴, is expressed in macrophages of this cluster (Fig. 15B).

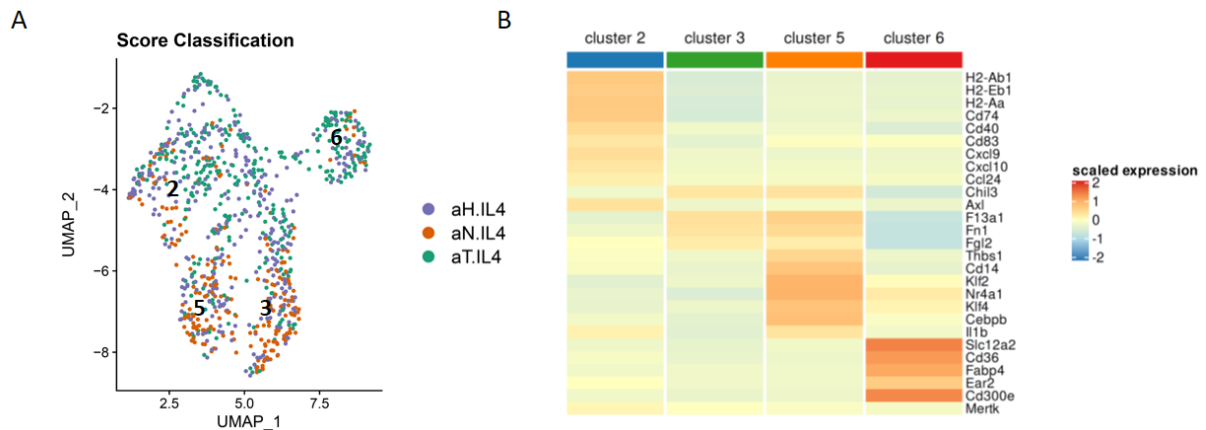


Fig. 15 Macrophage heterogeneity in mice infected with *S. mansoni* is driven by phagocytosis of different apoptotic cells.

(A) UMAP analysis of the combined bulk and scSeq data. Scored expression of the gene profiles from the bulk sequencing are shown integrated in the scSeq clusters. Orange dots refers to cells from the scSeq that expressed higher amounts of genes in compliance with BMDMs treated with aN+IL-4 *in vitro* rather than BMDMs treated with aT+IL-4 or aH+IL-4. Blue dots and green dots represents cells that either express more genes associated to BMDMs treated with aH+IL-4 or aT+IL-4, respectively. (B) Heatmap of a functional gene analysis of the four macrophage-clusters. Gene expression is shown as scaled expression.

These data displayed that during the infection with *S. mansoni*, sensing of apoptotic cells with various origins imprints macrophages' function and phenotype differentially. Taking into consideration that the characteristics of the macrophage clusters are associated with the phagocytosis of different apoptotic cells, the involvement of phagocytosis receptor expression was analysed by using a knock-out mouse for *Axl* and *Mertk*, thereby the impact of phagocytosis on the heterogeneity of macrophages during infection and analysing its effect on the disease outcome was further investigated.

4.6 Blocking phagocytosis during schistosomiasis reveals its impact on the function of macrophages

AXL and MERTK are tyrosine kinase receptors, important for the phagocytosis of apoptotic cells via recognition of PtdSer on the surface of apoptotic cells^{86,185} (see 1.2.1). To test if their genetic ablation in macrophages alters their function and the disease course, as described in *Nippostrongylus brasiliensis* infection⁹¹, mice with the genetic deletion of *Axl* and *Mertk* (*Csf1r-Cre⁺AM^{f/f}*) were infected with *S. mansoni*. Littermates without a Cre-promotor (*Csf1r-Cre⁻AM^{f/f}*) were used as controls.

Macrophages during the chronic phase of the disease (week 14 p.i) were analysed, where granuloma and fibrosis induction already took place. Liver and intestine represent focal points of damage during infection; to this end, liver macrophages as well as liver and colon tissue were collected for analysis of their phenotype and egg deposition. The blood was analysed to reveal liver damage and changes in cytokine production.

To verify that liver macrophages express *Axl* and *Mertk*, gene expression was investigated via qPCR. Mice with a knockout for *Axl* and *Mertk* were used as a negative control (Fig. 16). To this end, liver cells were isolated and macrophages obtained by cell-sorting. CD45⁻ cells and neutrophils (Ly6G⁺) were excluded. Ly6C⁻CD11b⁺F4/80⁺ expression defined non-infiltrating macrophages (left panel). No expression of *Axl* and *Mertk* was detectable in the *Csf1r* Cre⁺AM^{f/f} mice (right panel-red bar). Liver macrophages from *Csf1r*-Cre⁻AM^{f/f} mice (black bar) showed high expression of *Axl* and *Mertk* under homeostatic conditions.

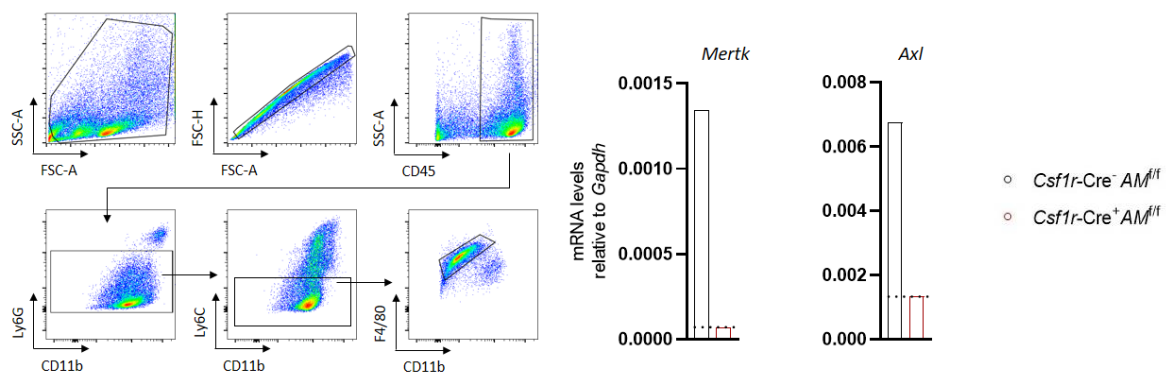


Fig. 16: Liver macrophages express high levels of *Axl* and *Mertk* in steady stage.

Flow cytograms reporting the sorting strategy of liver macrophages. Dead and single cells were excluded. Starting from CD45⁺ cells, neutrophils were excluded via Ly6G staining and Ly6C⁻CD11b⁺F4/80⁺ macrophages were sorted. mRNA levels of *Axl* and *Mertk* were analysed for *Csf1r*-Cre⁻AM^{f/f} (black bars) and *Csf1r*-Cre⁺AM^{f/f} (red bars) by qPCR. Dotted line indicates the basal expression of the knockout mice. Three mice were pooled to sort macrophages and to perform RNA isolation.

To analyse the impact of the absence of *Axl* and *Mertk* on apoptotic cell accumulation, the amount of apoptotic cells in the liver was evaluated by flow cytometry 14 weeks p.i. with *S. mansoni*. Apoptotic cells are defined by the expression of PtdSer, via staining with Annexin V. The apoptotic cells (Annexin V⁺) are further characterised based on their original identity. CD45⁺ cells are separated into T cells (CD3⁺), eosinophils (SiglecF⁺), neutrophils (Ly6G⁺CD11b⁺) and macrophages (either CD11b⁺F4/80⁺ or CD11b⁺F4/80⁻). CD45⁻ cells include all non-parenchymal cells of the liver, mainly hepatocytes. Red bars indicate apoptotic cells isolated from infected *Csf1r*-Cre⁺AM^{f/f} mice, while black bars indicate apoptotic cells from infected *Csf1r*-Cre⁻AM^{f/f} mice. In general, the overall number of apoptotic cells rose significantly during the infection in *Csf1r*-Cre⁺AM^{f/f} mice compared to *Csf1r*-Cre⁻AM^{f/f} mice (Fig. 17A).

In addition, the dotted line in panel A displays the amount of apoptotic cells in naïve mice. During the infection, a significant increase of apoptotic T cells and macrophages was detectable in the *Csf1r-Cre⁺AM^{f/f}* mice, while no significant change in the apoptotic cell numbers of neutrophils, eosinophils or CD45⁻ cells were observed comparing infected *Csf1r-Cre⁺AM^{f/f}* and *Csf1r-Cre⁻AM^{f/f}* mice (Fig. 17 B). However, CD45⁻ cells were slightly increased in infected *Csf1r-Cre⁺AM^{f/f}* mice.

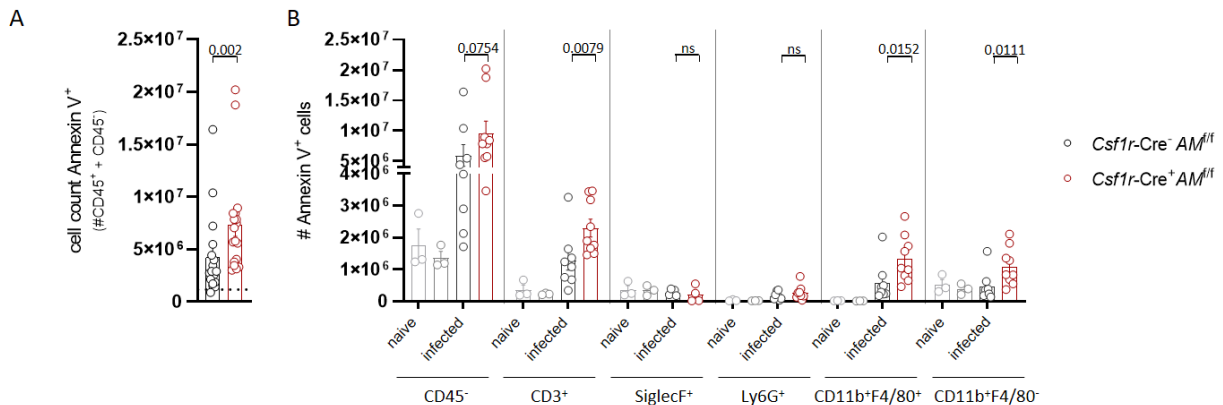


Fig. 17: Depletion of *Axl* and *Mertk* during the infection with *S. mansoni* results in accumulation of apoptotic cells in the liver.

Mice were infected with *S. mansoni*. Liver samples were collected 14 weeks p.i. Black bars indicate *Csf1r-Cre⁺Axl^{f/f}Mertk^{f/f}* mice; red bars indicate *Csf1r-Cre⁺Axl^{f/f}Mertk^{f/f}* mice. (A) Dotted line indicates amount of apoptotic cells in naïve mice. Absolute number of annexin V⁺ cells are depicted. (B) Cells are further divided into specific cell types. Annexin V⁺ hepatocytes (CD45⁻), T cells (CD3⁺), eosinophils (SiglecF⁺), neutrophils (Ly6G⁺) and macrophages (CD11b⁺F4/80⁺ and CD11b⁺F4/80⁻) are displayed. Each data point indicates one independent sample, n=3-9. Mean ± SEM, Mann-Whitney U test was exclusively performed between infected *Csf1r-Cre⁻AM^{f/f}* mice and infected *Csf1r-Cre⁺AM^{f/f}* mice, ns: p>0.05.

An accumulation of apoptotic cells was observed at 14 weeks p.i. in the liver. In addition, the data showed that in particular apoptotic macrophages and T cells accumulated in high numbers in the absence of *Axl* and *Mertk*.

Next, the impact of *Axl* and *Mertk*-dependent phagocytosis on the disease outcome was analysed (Fig. 18). With this objective, alanine aminotransferase (ALT) levels in the serum of infected mice were determined. ALT is an enzyme that is present in healthy livers. However, when liver damage occurs, ALTs are released into the bloodstream and can be detected in the serum¹⁸⁶. Infected mice showed an increase in ALT levels compared to the naïve controls, and most importantly, infected *Csf1r-Cre⁺AM^{f/f}* mice showed significantly elevated ALT levels in the serum compared to *Csf1r-Cre⁻AM^{f/f}* mice. The dotted line indicates ALT levels of age-matched naïve mice (Fig. 18A). In addition, the amount of parasite eggs inside the liver to assess disease severity was determined. Parasite eggs were counted after digestion of the liver tissue and calculated per gram liver tissue. Numbers of parasite eggs were elevated in *Csf1r-Cre⁺AM^{f/f}* mice compared to *Csf1r-Cre⁻AM^{f/f}* mice (Fig. 18B). A similar phenotype was observed in the amount of parasite eggs counted in the colons of *Csf1r-Cre⁺AM^{f/f}* and *Csf1r-Cre⁻AM^{f/f}*

mice (data not shown). Elevated ALT levels in combination with increased parasite egg numbers in the liver could favour granuloma formation and rearrangement of the ECM in the liver¹⁸⁷. To address this, liver histology sections were stained with siRed, a dye that stains collagen deposition in red. Representative histology pictures are displayed (Fig. 18C left). The quantification of positively stained granuloma structures and/or parasite eggs that were enclosed by a granuloma revealed that *Csf1r-Cre⁺AM^{f/f}* mice have a greater amount of siRed⁺ particles compared to *Csf1r-Cre⁻AM^{f/f}* mice (Fig. 18C right). Additionally, total liver RNA was analysed for the expression of enzymes that contribute to the rearrangement or the removal of excess ECM, like metalloprotease 14 (*Mmp14*) or inhibitors such as inhibitor of metalloproteases-1 (*Timp1*), as MMPs and TIMPs might be suppressed in fibrotic settings¹⁸⁸. In *Csf1r-Cre⁺AM^{f/f}* mice a significant decrease in the expression of both *Mmp14* and *Timp1*, compared to *Csf1r-Cre⁻AM^{f/f}* mice was observed (Fig. 18D).

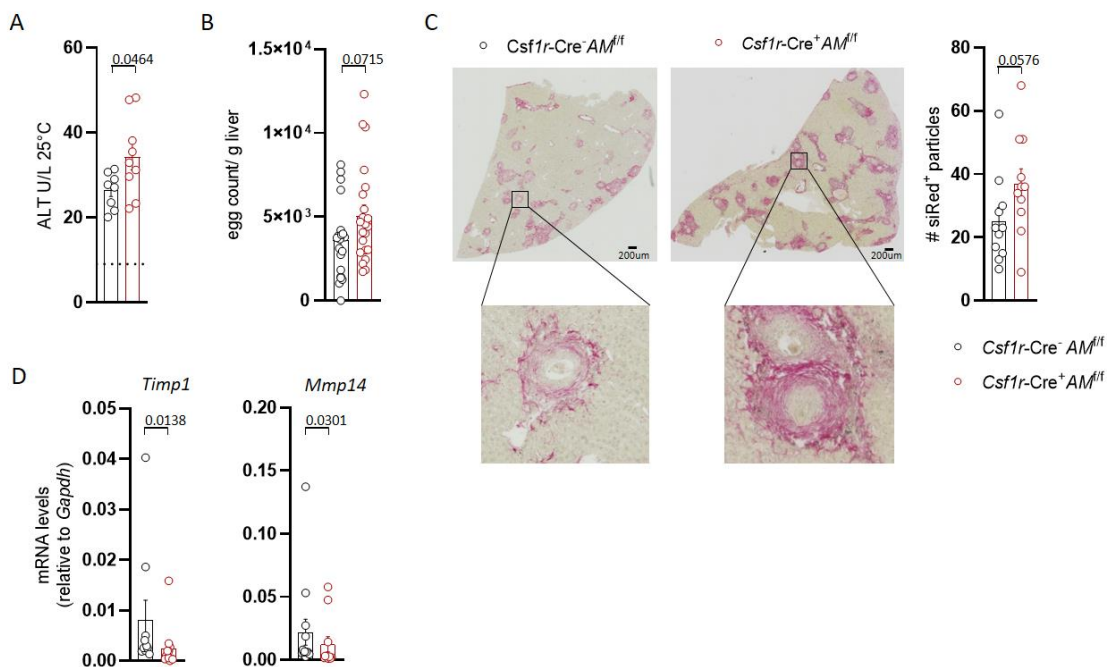


Fig. 18: Blockage of phagocytosis during the infection with *S. mansoni* leads to a more severe disease phenotype.

Mice were infected with *S. mansoni*. Tissue samples were collected 14 weeks p.i. Black bars indicate *Csf1r-Cre⁻AM^{f/f}* mice; red bars indicate *Csf1r-Cre⁺AM^{f/f}* mice. (A) ReflotronTM measurements of serum ALT levels. Dotted line indicates ALT levels in naïve mice. (B) Number of *S. mansoni* egg per gram of liver. (C) Representative images of liver section stained with siRed left. Scale bars indicates 200 μ m. Histology analysis of siRed positive particles per slide. One positive particle was defined by positive siRed stain, visible granuloma structure and/or egg detection. (D) mRNA levels of total liver RNA is shown for *Mmp14* and *Timp1*, as detected by qPCR. Each data point indicates one independent sample. n=8-23. Mean \pm SEM, Mann-Whitney *U* test, ns: p>0.05.

In summary, *Csf1r-Cre⁺AM^{f/f}* mice showed an a more severe disease pathology inside the liver compared to *Csf1r-Cre⁻AM^{f/f}* mice.

PBMCs isolated from patients with severe fibrosis showed enhanced cytokine production of IL-10, IL-13 and IL-5¹⁸⁹. This led to the question whether the impairment in *Axl* and *Mertk*-dependent phagocytosis alters the cytokine milieu. Based on this, the amount of IL-5, IL-13 and IL-10 in the serum of the mice were analysed. In addition, IL-4 production was investigated. Mice with a knockout for *Axl* and *Mertk* showed significantly elevated levels of IL-5, IL-13 and IL-10 compared to *Csf1r-Cre⁺AM^{fl/fl}*. A strong increase of IL-4 was additionally observed in the *Csf1r-Cre⁺AM^{fl/fl}* mice (Fig. 19), however not to a significant extent.

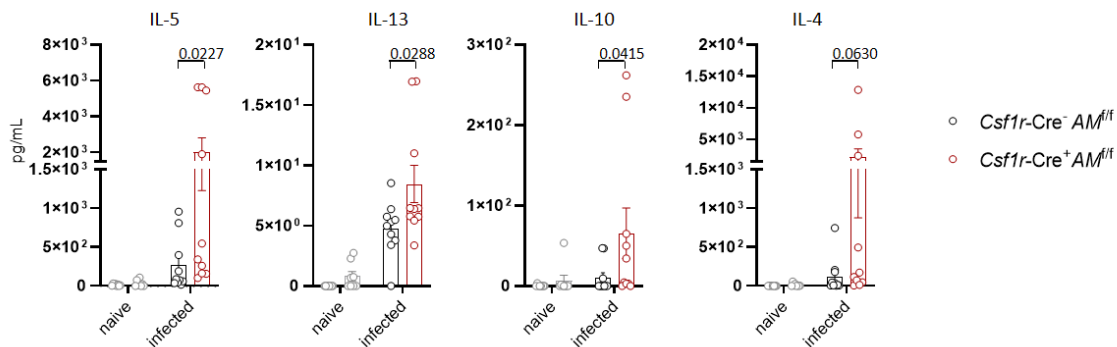


Fig. 19: Fibrosis-associated cytokines are enhanced in the serum of *Csf1r-Cre⁺AM^{fl/fl}* mice.

Mice were infected with *S. mansoni*. Serum samples were collected 14 weeks p.i. Black bars indicate *Csf1r-Cre⁻AM^{fl/fl}* mice; red bars indicate *Csf1r-Cre⁺AM^{fl/fl}* mice. IL-5, IL-13, IL-10 and IL-4 levels in the serum of infected or naïve mice. Each data point indicates one independent sample. n=10. Mean ± SEM, Mann-Whitney U test performed only in the infected group, ns: p>0.05.

To this end, the genetic ablation of *Mertk* and *Axl* in macrophages alters the cytokine expression during schistosomiasis. Impairment of phagocytosis might also affect the Th2 response of T cells. Since the intestine is the place of residence from the helminth, cells from the mesenteric lymph nodes were isolated from infected mice and stimulated in vitro with αCD3. Secretion of IL-4 and IL-13, which are prototypical marker of a type 2 immune response during *S. mansoni* infection, were evaluated by ELISA in the supernatant of lymph node cells. Comparable levels of IL-4 and IL-13 were detected in the supernatant after stimulation of cells from *Csf1r-Cre⁻AM^{fl/fl}* and *Csf1r-Cre⁺AM^{fl/fl}* mice (Fig. 20).

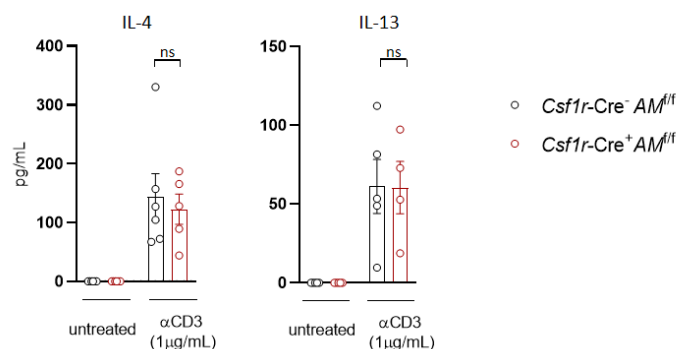


Fig. 20: Cytokine production from mesenteric lymph nodes is not altered in *Csf1r-Cre⁺AM^{fl/fl}* infected mice.

Mice were infected with *S. mansoni*. Black bars indicate *Csf1r-Cre⁻AM^{fl/fl}* mice; red bars indicate *Csf1r-Cre⁺AM^{fl/fl}* mice. Lymph nodes were collected 14 weeks p.i. IL-4 and IL-13 levels in unstimulated and stimulated cells from mesenteric lymph nodes are shown. Each data point indicates one independent sample. n=3-6. Mean ± SEM, Mann-Whitney U test. Test was exclusively performed between the infected samples, ns: p>0.05.

To assess if the impairment in apoptotic cell phagocytosis affects the phenotype of macrophages, they were analysed for their possible contribution to fibrosis. In this setting, cells from the pooled livers of five mice were isolated and then CD45⁺Ly6G⁻Ly6C⁻CD11b⁺F4/80⁺ macrophages obtained by FACS. As described previously, neutrophils were excluded by Ly6G⁺CD11b⁺ staining (Fig. 21A). mRNA level expression of *Arg1*, *Chil3*, *Il-1 β* , *Il-10* and *Timp1* was measured. *Arg1*, *Chil3*, *Il-1 β* and *Il-10* were analysed, as high expression levels are associated with fibrogenic processes in the chronic phase of the disease. *Timp1*, as described earlier, is a negative regulator for MMPs and alters ECM rearrangement. *Csf1r-Cre⁺AM^{f/f}* mice showed higher levels of *Arg1*, *Chil3*, *Il-1 β* and *Timp1* compared to the *Csf1r-Cre⁻AM^{f/f}* mice. In contrast to the cytokine production in the serum (Fig. 19), higher levels of *Il-10* in *Csf1r-Cre⁻AM^{f/f}* macrophages compared to *Csf1r-Cre⁺AM^{f/f}* macrophages were detected. All markers analysed were increased during infection compared to naive mice (Fig. 21B).

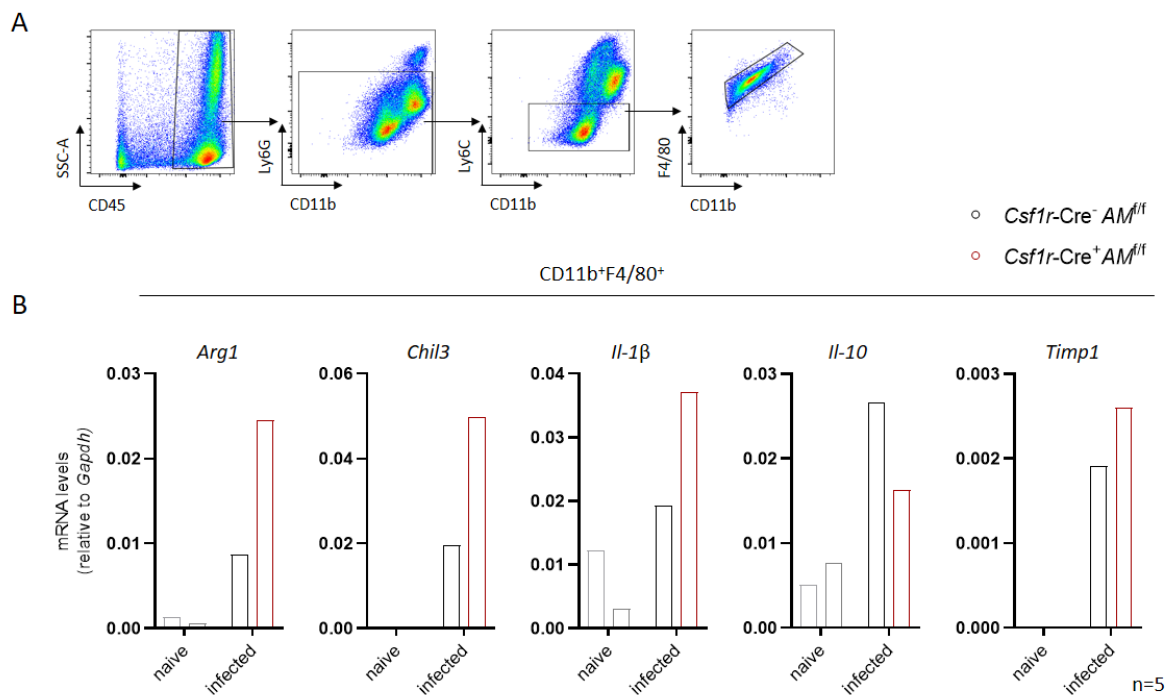


Fig. 21: Liver macrophages from *S. mansoni*-infected *Csf1r-Cre⁺AM^{f/f}* mice have an increase in fibrosis markers. Mice were infected with *S. mansoni*. Liver samples were collected 14 weeks post infection. (A) Representative flow cytograms show the sorting strategy. (B) mRNA levels of *Arg1*, *Chil3* and *IL1 β* , *Il-10* and *Timp1* in macrophages cell sorted from livers of naive and infected mice. Black bars indicate *Csf1r-Cre⁻AM^{f/f}* mice; red bars indicate *Csf1r-Cre⁺AM^{f/f}* mice. mRNA levels are detected by qPCR. Each column represents RNA from five pooled mice.

Analysis using the *Csf1r-Cre⁺AM^{f/f}* mice revealed that phagocytosis of apoptotic cells has a high impact on the function of macrophages during schistosomiasis and thereby contributes to the pathology of the disease. However, in general little is known about the therapeutic use of macrophages. Hence, in the next section, the focus laid on the therapeutic potential of macrophages, and how the uptake of

apoptotic cells with different original identities is shaping the response of macrophages and can pave the way for novel therapeutic approaches in the context of schistosomiasis.

4.7 The transfer of macrophages treated with apoptotic neutrophils *in vitro* is beneficial for the *Schistosoma mansoni*-infected host

Transfer of macrophages is reported to be beneficial for the host during *S. mansoni* infection¹⁶². However, it is not known whether the treatment with apoptotic cells can enhance the therapeutic potential of macrophages. Of special interest are macrophages treated *in vitro* with aN, because the previously obtained data suggest that these are the only cell population able to potentiate the tissue remodelling response of macrophages, which is described to be beneficial in the early phase of schistosomiasis¹⁴⁴. Besides aN, the impact of the transfer of macrophages treated with aT and aH was evaluated. With this objective, macrophages were pre-treated *in vitro* with either aN (M ϕ +aN), aT (M ϕ +aT) or aH (M ϕ +aH) and stimulated with IL-4. Transfer of macrophages was performed at week 6 and 7 p.i., at the onset of egg deposition and at the time point in which the Th1-Th2 switch occurs¹²⁷ (Fig. 22A). Control mice were infected but did not receive any macrophages. This provided the possibility to normalise the infection to a not-macrophage-altered infection, as the established infections might differ in their strength due to the fitness of the administered *cercariae* over independent experiments. In addition, transfer of macrophages without pre-priming of exogenous apoptotic cells still includes the effects of the uptake of apoptotic macrophages on living macrophages inside the culture. However, the effect of apoptotic macrophages on macrophages themselves is not point of focus in this study. To assess whether the transfer of macrophages treated with apoptotic cells has an influence on the liver damage, ALT levels in the serum of infected mice were measured. No differences between the mice receiving macrophages pre-cultured with aN, aT or aH were observed compared to infected control mice treated with PBS (Fig. 22B). Besides the measurement of ALT levels, the amount of parasite eggs provides information about the severity of the disease; to this end parasite eggs were counted inside the liver and colon. Parasite egg counts were normalised to control mice treated with PBS. In line with the observed minor changes in the ALT levels, there were only minor reductions in the amount of eggs detectable inside the liver after transfer of macrophages (Fig. 22C). However, a slight reduction in the number of eggs present in the livers of mice which received macrophages pre-treated with aN was observed compared to the PBS control. Macrophages pre-treated with aT or aH did not affect the number of eggs accumulated in the colon of recipient mice, in contrast injection of aN-pre-primed macrophages reduced the egg counts in the intestine significantly (Fig. 22C).

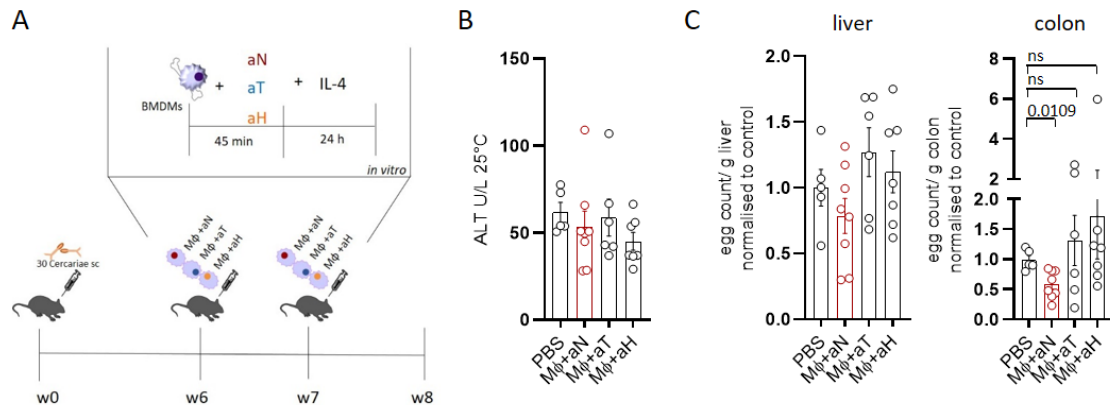


Fig. 22: Transfer of macrophages pre-treated *in vitro* with aN decreases the egg count in the colon of *S. mansoni*-infected mice.

(A) Schematic experimental model. Mice were infected with *S. mansoni*. At week 6 and 7 p.i. 1 Mio. macrophages pre-treated *in vitro* with either aN (red bars), aT or aH were transferred into the mice. Results were obtained 8 weeks p.i. (B) Reflotron™ measurements of serum ALT levels at week 8 p.i. (C) Number of *S. mansoni* eggs per gram of liver or gram of colon normalised to the PBS control. Each data point indicates one independent sample. n= 5-8. Mean ± SEM. Mann-Whitney U test, all samples were compared only to the PBS control. If not indicated no significance was reached for that graph, ns: p>0.05.

Egg-induced pathology can be altered by TGFβ release during the disease¹⁹⁰, therefore *Tgfβ* expression was measured in the colon. Reduced egg counts were accompanied by higher expression levels of *Tgfβ* in the colon from mice treated with aN-pre-primed macrophages compared to the controls. No changes were observed for mice treated with macrophages pre-cultured with aT or aH (Fig. 23). Parasite egg release might be favoured by ECM rearrangement. Taking that into consideration, *Mmp14* and *Timp1* expression were measured in the total colon tissue. The reduced egg count in the mice that received aN-pre-primed macrophages was accompanied by a slight increase of *Mmp14* expression. In contrast, transfer of macrophages did not alter the expression of *Timp1* in the colon compared to the PBS control.

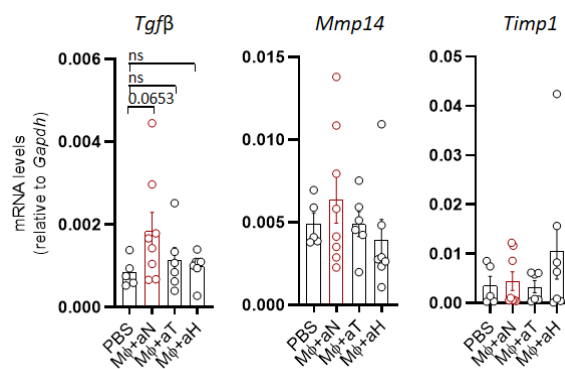


Fig. 23: Transfer of macrophages co-cultured *in vitro* with aN increases *Tgfβ* and *Mmp14* expression in the colon of *S. mansoni*-infected mice.

Mice were infected s.c. with *S. mansoni*. At week 6 and 7 p.i. 1 Mio macrophages pre-treated with either aN (red bars), aT or aH were transferred. Results were obtained 8 weeks p.i. mRNA levels of total colon RNA are shown for *Tgfβ*, *Mmp14* and *Timp1*, as detected by qPCR. Each data point indicates one independent sample. n=5-8. Mean ± SEM, Mann-Whitney U test, test refers exclusively to the PBS control. If not indicated no significance was reached for that graph, ns: p>0.05.

Even though the parasite egg counts in the liver were not altered, the phenotype of liver macrophages were analysed. Additionally, infiltration of CD3⁺ T cells and Ly6G⁺CD11b⁺ neutrophils in the liver were investigated by flow cytometry. Frequencies were normalised to the PBS-controls of each individual experiment. Transfer of macrophages pre-treated with aH significantly increased the frequency of CD3⁺ T cells in the liver, while no changes in the frequency of CD3⁺ T cells were observed in the mice receiving aN or aT compared to the control (Fig. 24A). The frequency of neutrophils (Ly6G⁺CD11b⁺) was not altered.

It has been described that anti-inflammatory macrophages expressing YM1 regulate granuloma formation, while ARG1 expression is, besides other functions, negatively associated with liver fibrosis modulation during schistosomiasis¹⁶⁵. Therefore, frequencies of YM1⁺ and ARG1⁺ macrophages in the liver were evaluated. Transfer of macrophages significantly increased the amount of YM1⁺ macrophages in all three groups compared to the control. ARG1⁺ macrophages were reduced in frequency in mice injected with macrophages pre-treated with aN. For the transfer of aT-pre-primed macrophages or aH-pre-primed macrophages no changes in the frequency of ARG1⁺ macrophages were observed in comparison to the control (Fig. 24B). These findings delineate how macrophage transfer affects the immune environment in the host. More precisely, donor macrophages were able to modulate host macrophage polarisation without affecting the infiltration of neutrophils and T cell infiltration in two of the conditions analysed.

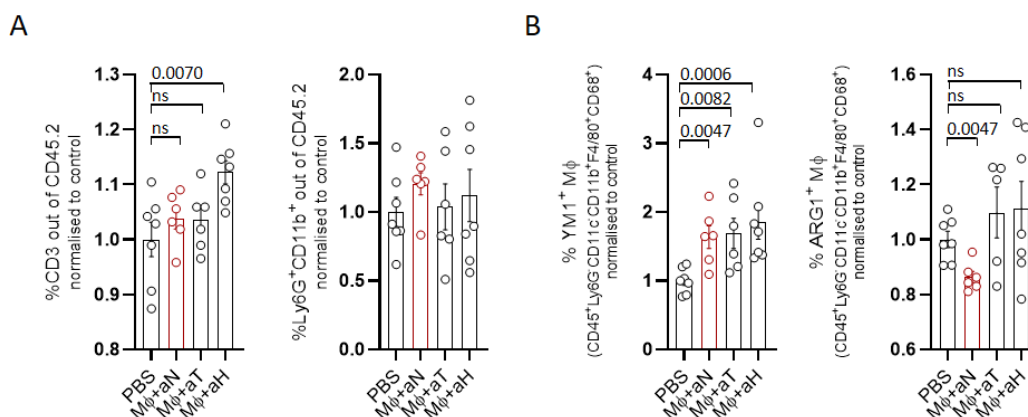


Fig. 24: Recipient mice showed lower amounts of ARG1⁺ macrophages after transfer of macrophages pre-treated with aN *in vitro*.

(A) Frequencies of CD3⁺ or Ly6G⁺ CD11b⁺ cells in the livers of the recipient mice. Data are normalised to the control. (B) Data depicting frequencies of YM1⁺ and ARG1⁺ macrophages isolated from the liver of the infected recipient mice. Each data point indicates one independent sample. n=5-8. Mean ± SEM. Mann-Whitney U test. Test refers exclusively to the PBS control. If not indicated differently, no significance was reached for that graph, ns: p>0.05.

In summary, the transfer of macrophages pre-treated with aN reduces the number of parasite egg in the intestine and the frequencies of ARG1⁺ macrophages in the liver, while this is not observed for aH-

pre-primed or aT-pre-primed macrophages. To provide comparability to human studies, investigations with patient samples were performed further.

4.8 Characterisation of phagocytosis receptor expression on human CD14⁺ monocytes during schistosomiasis

The impact of phagocytosis of apoptotic cells in humans with schistosomiasis is not yet known. To assess this, blood samples were collected from schistosomiasis-patients in Madagascar. Due to limited access to human samples, the following experiments were performed only with a small sample size and should therefore be considered as a prospective for further research. CD14⁺ cells, including monocytes and macrophages were isolated from PBMCs, due to low cell numbers, monocytes and macrophages could not be further analysed separately. RNA from CD14⁺ cells was extracted and mRNA levels of the phagocytic receptors *Axl* and *Mertk* were investigated. Additionally, the mRNA expression of the PtdSer-R *Cd36* was investigated (Fig. 25). As a control, samples from healthy controls (HC) were analysed. Due to limited sample availability, endemic samples (filled circles) are pooled with HC collected in Hamburg (open circles). An increase in the mRNA expression of all three phagocytosis receptors was observed; however, not to a significant extent. Notably, *Mertk* expression was only found in two of the patient samples. It might be taken into account that the expression of *Axl* seemed to be highly different in endemic and not endemic healthy controls.

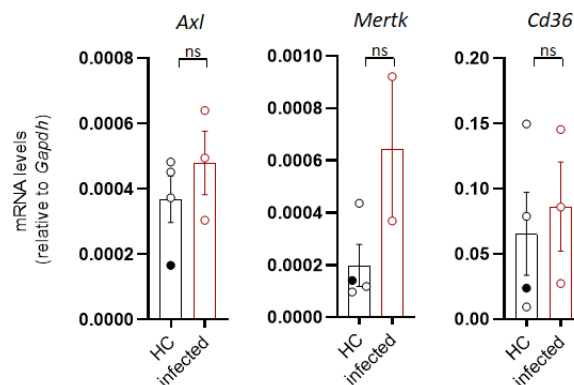


Fig. 25: CD14⁺ cells from patients with *S. mansoni* infection have an increased phagocytosis receptor expression.

mRNA expression for *Axl*, *Mertk* and *Cd36* from *S. mansoni*-infected patients (red bars) and healthy controls (black bars). Healthy controls were either endemic (filled dots) or not endemic (open circles). Each data point indicates one independent sample. n=3-4. Mean ± SEM. Mann-Whitney U test, ns: p>0.05.

The infection with *S. mansoni* altered the expression of phagocytic receptors in patients and indicates that, similar to the mice counterpart, apoptotic cells might be also relevant in the human context.

5 Discussion

Macrophages are important players of the innate immune response. Their phenotype and function are highly dependent on stimuli from the environment. Phagocytosis of apoptotic cells induces an immunosuppressive response in macrophages. In damage settings in the presence of IL-4 and IL-13, phagocytosis of apoptotic cells commits macrophages towards the acquisition of an anti-inflammatory/tissue remodelling phenotype. This study aimed to reveal the impact of phagocytosis of apoptotic cells with different identities on macrophages' function and phenotype. To this end, the response of macrophages after sensing different apoptotic cells was analysed. This approach was combined with murine *S. mansoni* infection as a model for a type 2 immune response, which was used to investigate whether *in vivo* phagocytosis of different apoptotic cell types also shapes macrophage heterogeneity and function.

The presented results demonstrated that the nature of the apoptotic cell phagocytosed imprints the transcriptome and thereby the functional heterogeneity of macrophages in an IL-4-enriched environment. It was discovered that during a chronic infection with *S. mansoni*, the capability of macrophages to control granuloma formation and parasite egg deposition depends on macrophages' phagocytosis via AXL and MERTK. Finally, it was shown that the reprogramming of macrophages, induced by the apoptotic cells phagocytosed, alters the infection outcome and the efficacy of their therapeutic potential.

5.1 Induction of the tissue remodelling phenotype is exclusive to apoptotic neutrophils

One of the main functions of macrophages is to phagocytose foreign, dead or damaged cells, including apoptotic cells^{1,174,191}. Many studies have been conducted to investigate the cross-talk between dying cells and macrophages^{77,191–193}. However, in most of these studies the focus was laid on the impact of different types of cell death (e.g. necrosis vs apoptosis), rather than the identity of the apoptotic cell¹⁹⁴. Furthermore, they often only used one type of apoptotic cell at the time, whereby mainly aN or aT are used for these studies^{70,91,113,195}. Along that line, apoptotic cells are described as a homogenous group of cells, defined by their apoptotic characteristics, such as PtdSer exposure, morphology changes, caspase activation or DNA fragmentation¹¹², rather than by their origin. However, when damage occurs, more than one cell type goes into apoptosis. In addition, different types of apoptotic cells accumulate depending on which and where the damage occurs. T cell apoptosis occurs in high numbers in autoimmune diseases¹⁹⁶, whereas in virus infections such as hepatitis or fatty liver disease, hepatocytes are the main cells that die¹⁹⁷. It is described in the literature that the amount of apoptotic

cells present affects the macrophage response¹⁹⁸; however, whether the accumulation of apoptotic cells with different identities distinctly alters the response of the corresponding phagocytic macrophages has not been investigated until now. The data presented in this thesis showed for the first time that the original identity of an apoptotic cell affects the macrophages' tissue remodelling response. The tissue remodelling phenotype of macrophages is characterised by the upregulation of genes that are associated with wound healing or tissue repair like *Fn1*, *Rentla*, *Ear2*, *Arg1* or *Chil3*⁴⁷ after the sensing of IL-4. In line with previous studies⁹¹, which showed that apoptotic cells could amplify the IL-4 response of macrophages, phagocytosis of aN potentiated the IL-4-induced gene expression in macrophages in the present study. Conversely and most strikingly, the uptake of aT or aH did not trigger the potentiation of the analysed tissue remodelling genes or proteins (Fig. 7). In addition, confirming that apoptotic cells with various origins differentially modulate macrophage phenotype *in vivo* revealed that only the administration of aN+IL-4, but not aT+IL-4 increased the frequency of tissue remodelling proteins on isolated peritoneal macrophages (Fig. 8). The presented results broadly support that apoptotic cells are actively shaping macrophages' response.

However, it might be, that the stage of apoptosis influences the response of macrophages, as the clearance of early apoptotic cells is favoured over late apoptotic cells¹⁹⁹. Here the stage of apoptosis could differ in the analysed aN, aT or aH and might explain why only aN are able to commit macrophages towards a tissue remodelling phenotype. Analysis of apoptotic characteristics for early and late stages of apoptosis of aH, aN or aT showed no differences in the amount of exposed PtdSer or the amount of DNA fragmentation as detected by Annexin V or TUNEL staining respectively (Fig. 5). During the early phase of apoptosis, DNA condensation occurs before DNA fragmentation. This is associated with the appearance of large DNA fragments of 50 - 300 kbp²⁰⁰ and displayed by few TUNEL⁺ cells. This is in contrast to the later stage of apoptosis where DNA fragmentation results in a characteristic DNA ladder pattern of 180 bp oligonucleosomes as seen by electrophoresis²⁰¹ and displayed by high frequencies of TUNEL⁺ cells.

Furthermore, the exposure of PtdSer on the surface of cells which still have an intact membrane defines early apoptotic cells¹¹². The recognition of PtdSer on the surface of apoptotic cells is the prototypical signal that induces their uptake by macrophages^{76,170,202,203}. In addition, PtdSer is a critical signal for the induction of a tissue remodelling response in macrophages^{91,128,204}. Indeed it has been shown that blocking the interaction between PtdSer exposed on the surface of apoptotic cells and the PtdSer-R on the surface of macrophages inhibited the upregulation of tissue remodelling gene expression in macrophages⁹¹. Therefore, changes in the frequencies of PtdSer between different apoptotic cell types could favour the uptake of one apoptotic cell type over another and thereby differentially alter the tissue remodelling phenotype of macrophages. Although the three apoptotic cell types do not differ in their amount of early apoptotic cells defined by their PtdSer exposure,

surprisingly only aN induced the tissue remodelling response in macrophages. In line with this, liposomes provided with PtdSer are not sufficient for the induction of the tissue remodelling gene expression in macrophages (Fig. 9). However, liposomes provided with higher amounts of PtdSer were phagocytosed the most, suggesting that the exposure of greater amounts of PtdSer by apoptotic cells leads to increased recognition and uptake of the apoptotic cells by macrophages. These findings demonstrate that, although PtdSer is an essential signal for shaping the phenotype of macrophages, an additional factor is necessary for the induction of the tissue remodelling response in macrophages.

Besides the stage of apoptosis, it can be hypothesised that the size and shape of the target affects macrophages' polarisation, as it influences their phagocytic capacity. The capability of macrophages to phagocytose particles is limited to a size over $0.5 \mu\text{m}^2$ and it has been described that the engulfment time increases with the size of the target^{74,205}.

More important than the size of the target for the phagocytic capacity of macrophages is the shape of the target cell^{74,206}. One of the main reasons why the shape of the target cell controls phagocytosis is the requirement of actin cytoskeleton reorganisation in macrophages in the initial phase of phagocytosis²⁰⁶. If the actin structure that is needed to move the phagocyte membrane over the particle cannot be created, phagocytosis will not be initiated, as observed for complex shapes²⁰⁶. Furthermore, the binding of the apoptotic cells to the macrophage might affect the response of the macrophages. This hypothesis is supported by findings showing that the binding of aN to macrophages differs from the binding of aT or aged erythrocytes. Besides the recognition of PtdSer, other factors modulate specifically the uptake of aN by macrophages, such as hydrogen ions and charged molecules on the surface of aN, a mechanism that has not been described for the uptake of aT⁷⁰. Although the shape of the apoptotic cells was not investigated in the present study, the living counterparts of the apoptotic cells give a hint that the shape and size of aH differs from the shape of aT and aN^{207,208}.

In addition, the analysis of the phagocytic capacity of macrophages revealed that macrophages phagocytose all investigated apoptotic cell types (aN, aT and aH). However, aH and aT are phagocytosed to a higher degree than aN (Fig. 6). A high frequency of aN were bound to macrophages, but not taken up. It might be that the cytoskeleton rearrangement needed for the phagocytosis of aN is more complex compared to the phagocytosis of other apoptotic cell types and therefore more aN than aH or aT are bound but not phagocytosed. However, this is doubtful, because neutrophils are one of the first cells that infiltrate after tissue damage and are constantly removed by macrophages²⁰⁹.

Therefore, it is tempting to speculate that the binding of aN is sufficient to initiate a response in the macrophages and thereby full aN phagocytosis might not be needed to specify macrophage function.

The selective induction of the tissue remodelling phenotype of macrophages by aN raised the hypothesis that aN-secreted factors are responsible for this observation. For example, apoptotic cells are able to produce TGF β ²¹⁰ and IL-10²¹¹ and it has been reported that released soluble mediators contribute to the response of macrophages after phagocytosis of the target¹⁷³; as IL-10 produced by apoptotic cells, can stimulate the IL-10 production of macrophages²¹². Small amounts of RNA which stay intact after apoptosis induction¹⁷³ can enable protein translation in the apoptotic cells. These translated proteins include histones, “find-me” signals or cytokines. For instance, released histone H1 after lung tissue damage induced IL-1 β production in macrophages²¹³ and emitted lactoferrin or IL-38 are able to negatively shape macrophages’ cytokine response by downregulation of IL-6 and IL-1 β production^{214,215}. Furthermore, extracellular vesicles are released from apoptotic cells and can promote TGF β production by macrophages²¹⁶.

The hypothesis that aN-secreted factors contributed to the tissue remodelling phenotype of macrophages was investigated through transcript analysis of macrophages after the transfer of cell supernatant from the aN-macrophages co-culture to the co-culture with aT. To this end, transferring the supernatant provided the same microenvironment in both co-cultures, excluding the type of apoptotic cells. Gene expression of *Ear2*, *Retnla* or *Chil3* did not change in macrophages that sensed aT in the presence of the aN-primed-supernatant compared to macrophages co-culture with aT in the absence of the aN-primed-supernatant (Fig. 10). This suggests that either no aN-secreted factor is accountable for the response induced in macrophages or a molecule secreted by the aT during the co-culture interfered with the effects of aN-primed supernatant on macrophages. Of note, factors which are bound to the aN were not transferred and therefore their effect on macrophage function cannot be dissected with the performed experiment. The supernatant was centrifuged before supplemented to the aT-macrophage co-culture to exclude cell contaminations. Equally, the aN-membrane-associated proteins were also removed from the supernatant. Additionally, disrupted membranes were not transferred either, as they are highly hydrophobic and likely to form aggregates that pellet together with the cells²¹⁷. Therefore, membrane-associated proteins such as iron channels, signal transducers or transmembrane domains like GPI anchors should still be considered as potential contributors to the aN-induced response of macrophages^{218,219}.

Further, as soluble mediators, the contribution of cytokines to the observed phenotype in macrophages in the present thesis was excluded as none of the analysed cytokines (IL-10, IL-6, IL-4, IL-5, IL-13, IL-1 β , TNF α and IFN γ) were detected in the three apoptotic cell cultures or in the macrophage culture after incubation with the apoptotic corpses. The analysed cytokines might be too diluted to be detected rather than not being produced at all, however the cell concentration in the culture (e.g. around 30 mio cells per mL aT culture) should be sufficient to produce quantifiable amounts of cytokines. Additionally, the supplemented IL-4 inside the culture was detected and

functioned as an internal control. After 48h of cell culture the produced cytokines might be already consumed by neighbouring cells inside the culture after binding to their receptors, and are therefore not detectable. Nonetheless, the absence of cytokine expression does not fully exclude their contribution, but rather proposes that they play a minor role in this setting.

The specificity of aN to induce a tissue remodelling phenotype in macrophages could not be explained by the secretion of selective soluble mediators. It was further hypothesised that specific neutrophil characteristics might contribute to the selective macrophage response. Neutrophils are the only cell type that produce NET structures²²⁰. During pathogen defence, neutrophils are recruited to the site of injury in high numbers to eliminate invading pathogens through the formation of NETs. Neutrophils do not only undergo NET formation if a pathogen is invading, but also under stress conditions, like reduced availability of nutrients, which can lead to the lethal form of NET production, defined as NETosis²²¹. Based on this, NET formation might occur in the aN culture, where fewer nutrients are available. The NET structure is composed of a network of DNA, enzymes like MPO and neutrophil elastase (NE). MPO is required for the formation of NETs as shown via its pharmacological inhibition^{177,222}. However, the experiments in which aN isolated from mice lacking *Mpo* were co-cultured with macrophages suggested no involvement of MPO or NET formation in the observed macrophage phenotype (Fig. 11). Even though it has been described that MPO plays a key role in NET-mediated microbial killing, MPO is not necessary in NET formation induced by bacteria²²². Citrullinated Histone H3, cell-free DNA or neutrophil elastase are additional NETosis markers. In appendicitis studies with mice and humans, elevated levels of all markers, including MPO, were found and correlated with disease severity²²³. Further studies from our group showed no alterations on the macrophage phenotype when free cell DNA was removed by treatment with DNase. Additionally, staining of citrullinated Histone H3 further supported the absence of NETs in the co-culture (unpublished master thesis data²²⁴). However, in order to fully exclude the involvement of NETs in the here described phenotype of macrophages, fluorescent microscopy should be used as an alternative method.

The obtained results suggest that neither soluble factors, nor the formation of NETs are responsible for the specific signature of macrophages after the co-culture with aN. Consequently, a cell-cell-contact is highly suggested to be necessary for shaping the response of macrophages. This might be represented by the interaction between the phagocytic receptors on macrophages and their ligands on the apoptotic cell surface, comparative to the well-described immunological synapse. The immunological synapse between the T cell receptor on T cells and the major histocompatibility complexes (MHCs) on the surface of the APC is a fundamental process²²⁵ in shaping the responses of both cells. Comparably, the engagement of phagocytosis ligands on the surface of apoptotic cells by

the phagocytosis receptors on the macrophages forms a phagocytic synapse²²⁶. Here, not only the identity of the apoptotic cell that supplies the ligands for the phagocytic synapse, but also the phagocytic receptor that is used by the macrophage to bind to the ligands and the strength of these interaction provide signals that could shape the response of the macrophage. In line with this, CD36, a PtdSer-R, is reported to be essential for the phagocytosis of *Plasmodium falciparum*-infected erythrocytes²²⁷ and thereby confirms that phagocytic receptors can favour the recognition and uptake of one apoptotic cell type over another. In addition, the interaction between the ligands and the chosen phagocytic receptors might trigger different signalling pathways inside the macrophage, dependent on the used phagocytic receptor type or bound apoptotic cells and this could specifically affect the polarisation of macrophages. Supporting this hypothesis, analysis of phagocytic receptor expressions in macrophages after phagocytosis of aN, aT or aH showed that macrophages express less *Cd36* and *Mertk* after co-culture with aH, while *Axl* expression was not altered (Fig. 12A), which suggest that the sensing of a selective apoptotic cells is affecting the expression of phagocytic receptors. However, a conclusion if a specific apoptotic cell favours one receptor over the other cannot be drawn from the conducted experiment and needs to be further investigated.

In addition to the type of phagocytic receptor engaged, the strength of the interaction between the ligand and the receptor at the phagocytic synapse might also modulate the response of the macrophages. Besides differences in the phagocytic receptor/ligand affinity, the amount of available bridging molecules could play a role. AXL and MERTK, for example, need the bridging molecules GAS6 and PROS1 to bind PtdSer exposed on the apoptotic cell surface²²⁸. Analysis of their expression in macrophages after phagocytosis of aN, aT and aH showed that the engulfment of aH decreased their expression of *Pros1* and *Gas6* (Fig. 12B). Furthermore, GAS6 and PROS1 can alter the immune response and are described to be upregulated in monocytes isolated from patients with multiple sclerosis (MS). Their expression was even further enhanced in MS patients with additional helminth infections²²⁹. This suggests that changes in the expression of GAS6 and PROS1 can affect the response of macrophages towards an apoptotic cell. In addition, an increase in bridging molecules might favour the binding capability of macrophages to PtdSer, which could additionally account for the modulation of the macrophage response. Consequently, it is tempting to hypothesise that the strength of the interaction at the phagocytic synapse or the type of phagocytic receptor engaged contributes to the tissue remodelling response of macrophages after sensing aN and IL-4.

5.2 The nature of an apoptotic cell modulates the function of macrophages

aH and aT did not have the capability to potentiate the tissue remodelling phenotype of macrophages, however the RNAseq analysis revealed that they affect the transcriptome of macrophages. While aN

induced a tissue remodelling gene profile in macrophages, aT phagocytosis limited the IL-4 response and engulfment of aH committed macrophages towards a tolerogenic function (Fig. 13). In line with this, genes like *Socs2*, *Socs3*, *Tlr8*, and regulatory genes for SOCS were upregulated in macrophages after aH phagocytosis. Genes of the *Socs* family are described to restrict pathology after hepatocyte injury, maintain homeostasis and are involved in macrophages' polarisation^{180,230}. SOCS2 functions as an inhibitor of hepatocyte proliferation in early stages of damage and promotes proliferation in the regenerative process²³⁰. Activation of the phagocytic receptors AXL, MERTK and TYRO3 by inflammatory stimulation through the interferon receptor induced the upregulation of SOCS1 and SOCS3 in macrophages, which actively suppress TLR signalling. Thereby macrophages regulate and restrict TLR-driven inflammatory responses^{231,232}. Additionally, SOCS1, but not SOCS3²³¹, is highly induced in allergy and anti-inflammatory macrophages. Furthermore, macrophages that phagocytosed aH are in all probability located in the liver. The tolerogenic function of these macrophages might be associated to the immune-prevalent status of the liver. It is the only organ which is able to regenerate itself and induces antigen-specific tolerance^{233,234}. Accordingly, the engulfment of aH might commit macrophages towards a tolerogenic function to maintain this immune privilege.

aT altered the lowest amount of IL-4-induced genes specifically (46 genes). Consistent with the previous described *in vitro* data (Fig. 7); aT did not decrease or potentiate the IL-4 response drastically. However, the sensing of aT appeared to restrict the IL-4 response, as genes that are involved in the regulation of the tissue remodelling response in macrophages are enriched. For instance *Ahnak*, a known tumour suppressor that potentiates TGF β signalling and thereby negatively regulates cell growth²³⁵, is one of the upregulated genes. The loss of *Ahnak* expression is associated with fewer anti-inflammatory macrophages in the adipose tissue²³⁶, but increased tissue remodelling alveolar macrophages in lung tumors²³⁷. Besides *Ahnak*, the expression of *Arnt2*, a gene involved in cell proliferation, amplified after aT phagocytosis in macrophages. *Arnt2* is one of the target genes of IL-10, which depends on PI3K signalling, and *Arnt2* is upregulated after signalling over the IL-10-PI3K axes. Both IL-10 and PI3K negatively regulate inflammatory responses in macrophages²³⁸. Accordingly, upregulation of *Arnt2* indicates that a restriction of inflammatory processes took place in these macrophages. Furthermore, *Rnase2a* expression was elevated after sensing of aT. *Rnase2a* functions as a chemoattractant for tissue macrophages²³⁹ and is expressed after IL-4, IL-13 and IL-33 stimulation of macrophages; cytokines which induce an anti-inflammatory signature in macrophages²⁴⁰. It possesses anti-viral properties, highlighting its role in viral defence²⁴¹. The transcriptomic signature acquired by macrophages upon phagocytosis of aT suggests that either aT clearance restricts the IL-4 response in macrophages or the phagocytosis of aT commits macrophages towards the acquisition of functions that are not regulated by IL-4 induced genes, such as an anti-viral or pathogen-eliminating response.

As expected from the *in vitro* results, aN phagocytosis induced genes in macrophages that are associated with tissue remodelling, wound healing and coagulation like *Arg1* or *Fn1*¹⁴⁹, which is in line with published data^{53,242}. Supporting these findings, *Pdcd1lg2* (PD-L2), which is specifically associated with anti-inflammatory macrophages with a monocyte origin¹⁴⁴, is only upregulated after aN phagocytosis. Moreover, recruitment of neutrophils in high numbers mainly takes place after the occurrence of damage, which might explain why macrophages that phagocytosed aN acquire a tissue remodelling phenotype and thereby are able to contribute to the healing of the damaged tissue.

In agreement with a recent discovery that showed transcriptome diversity of macrophages after phagocytosis of apoptotic cells¹⁷⁸, the provided data demonstrated that apoptotic cells should not be described as a homogenous population defined by morphological changes, but should rather be characterised by their original identity and their possibility to actively shape the response of macrophages. In line with this conclusion, it was recently discovered that apoptotic cells release metabolites like AMP, GTP or spermidine that affect the phenotype of macrophages¹⁷³. AMP for example can be degraded to adenosine, which inhibits TNF α production in macrophages (see 1.2.1). Therefore, the apoptotic cell content or produced factors should be contemplated to be involved in the response of macrophages and might distinguish one apoptotic cell from the other. Supporting the involvement of metabolites to drive macrophage responses, the RNAseq analysis revealed high induction of ATPases, ATP binding structures, AMP- or GTP-associated proteins and kinases for AMP and GTP in macrophages. However, this was observed independently of the type of apoptotic cell phagocytosed.

5.3 The phagocytosis of specific apoptotic cells drives macrophages' heterogeneity during infection with *Schistosoma mansoni*

To verify that the nature of an apoptotic cell shapes macrophages' heterogeneity and function upon phagocytosis, an infection model where different dying cells accumulate in a type 2-enriched environment was used. During the infection with *S. mansoni*, the immune response consists of two main phases (see 1.4.2): an initial Th1 response that is replaced by a Th2 response in later stages of the disease, when IL-4 levels and appearance of parasite antigens increase. The response of macrophages to IL-4 during the infection is critical to attenuate liver damage and intestinal inflammation. Loss of the IL4R α signalling increased hepatotoxicity²⁴³. Although initially pro-inflammatory macrophages appear during the infection, the shift in the immune response later leads to the accumulation of IL-4-responding macrophages. ScSeq analysis verified heterogeneity within the

macrophage populations present in the liver during the chronic phase of the infection. Four clusters of CD11b⁺ macrophages were indeed identified by the expression levels of e.g. *Cd68* and *Cd14* (Fig. 14). In addition, the ScSeq analysis revealed clusters of CD11b⁺ NK cells and neutrophils. NK cells are highly activated by *S. mansoni*²⁴⁴ and their CD11b expression ranges from low expression on NK cells in the bone marrow and lymph nodes to a high CD11b expression on NK cells from the blood, spleen, lung and liver and with increased cytotoxicity²⁴⁵. Antibody-dependent adherence and killing is mediated by NK cells during the infection with *S. mansoni*, but additionally by neutrophils as they can adhere to *schistosomula*²⁴⁶. Neutrophils are constantly recruited during the infection, which explains their appearance in different developmental stages in the liver as displayed in the UMAP analysis.

During invasion, *S. mansoni* is able to induce cell death²⁴⁷, a process also known for other parasites, e.g. *Trypanosoma brucei*, which induces apoptosis to reduce the fitness of the host and therefore enhance its own survival¹²². In the acute phase of *S. mansoni* infection, parasite migration and pro-inflammatory responses against the worm are accompanied by apoptosis. Increased FAS and FAS-L expression for example is mediated by *schistosomulae* traveling through the skin of the host²⁴⁷. During the chronic phase, the formation of granulomas around the eggs inside the liver or intestine drives the enclosed cells into apoptosis, thereby providing a source of apoptotic cells with different identities that are phagocytosed by macrophages⁷³⁻⁷⁵. In consistency with the literature^{168,249}, analysis of the accumulated apoptotic cells in the liver revealed an enrichment of apoptotic CD3⁺ cells. However, the analysis of the apoptotic cell origin also showed a diverse identity of these cells besides CD3⁺. Apoptotic CD11b⁺, CD45⁻ and Ly6G⁺ cells were additionally found in the liver (Fig. 17).

To verify the impact of apoptotic cells on macrophages during schistosomiasis, the transcriptional heterogeneity of macrophages was aligned to the phagocytosis transcript of aH, aN or aT obtained from the RNAseq (Fig. 15). As already described, in particular numerous of apoptotic CD3⁺ T cells were observed in the experimental setting and are described during the infection with *S. mansoni*^{247,250}; consequently, macrophages with a transcript similar to the ones up-taking aT *in vitro* are present. These macrophages showed less capability to potentiate or decrease the IL-4-induced genes *in vitro* and are hypothesised to be more associated with counteracting and restricting the IL-4 response. Accordingly, macrophages with an aT-phagocytosis-associated gene profile during the infection can be partially linked to a pro-homeostatic function by their expression of *Cx3cr1⁺Ccr2⁻Nr4a1⁺*²⁵¹.

In line with the aN-induced tissue remodelling response *in vitro*, macrophages that showed a gene profile related to the engulfment of aN upregulated genes like *Fn1* or *Klf4*. These genes are associated with tissue remodelling/anti-inflammatory^{53,252,253} macrophages and wound closure^{254,255} as seen by non-healing wound outcomes in mice with a lack of *Fn1*²⁵⁶.

Macrophages with a transcript that refers to the uptake of aH+IL-4 were found abundantly across all clusters. An explanation for this observation might be that the cells were isolated from infected livers and in the liver during schistosomiasis aH might outnumber other apoptotic cell types. To be able to clear this high amount of dying cells, aH might be phagocytosed by all macrophages present.

In general, scSeq is noisier than bulk RNAseq²⁵⁷ and because the obtained scSeq data only comprises a small amount of cells, results need to be interpreted carefully. Low cell numbers resulted from an exclusion of dying or stressed cells, which are characterised by high amounts of genes associated to chaperones and heat shock proteins.

5.4 AXL and MERTK engagement is necessary for the uptake of apoptotic CD3⁺ cells and controls egg deposition and granuloma formation during *Schistosoma mansoni*

To further support the hypothesis that the type of phagocytic receptors engaged by macrophages during phagocytosis might drive the uptake of selective apoptotic cell types, the expression of different phagocytic receptors in the various macrophage clusters was investigated. In particular, receptors that are described to modulate a tissue remodelling response in macrophages, such as AXL and MERTK, were of utmost interest^{85,86,185,258}. The importance of AXL and MERTK receptors on macrophages is reflected by their abundant expression in the liver under homeostatic conditions⁸⁷, which was also observed in the present thesis (Fig. 16). Analysis of their expression levels revealed that only macrophages in cluster 2 expressed *Axl* and *Mertk* at the same time (Fig. 15). A possible contribution of AXL and MERTK to the transcriptional and functional heterogeneity of macrophages in the tissue dependent on the recognition of selective apoptotic cell types has not been described so far. In addition, no connection between the type of phagocytosis receptor and the accumulation of a specific apoptotic cell type has been reported in the literature. Of note, apoptotic CD3⁺ T cells and CD11b⁺ cells accumulate in high numbers in the liver of *S. mansoni*-infected mice that carry the genetic ablation of AXL and MERTK in macrophages (Fig. 17) and might suggest for the first time a dependency of apoptotic CD3⁺ and CD11b⁺ cell clearance on the AXL and MERTK receptor. Furthermore, considering *i*) the accumulation of apoptotic CD3⁺ T cells in mice lacking the AXL and MERTK receptor, *ii*) the specific expression of *Axl* and *Mertk* in macrophage cluster 2 in the scSeq analysis and *iii*) the enrichment of genes associated with aT phagocytosis in cluster 2, this study further suggests that *Axl* and *Mertk*-expressing macrophages acquire a specific transcriptomic signature dependent on their phagocytosis of apoptotic CD3⁺ T cells.

T cell apoptosis is a known immune modulator in parasitic infections with e.g. *S. mansoni* or *T. cruzi*. Although the elimination of apoptotic CD8⁺ cells in *T. cruzi* infection dampens inflammation and prevents exacerbated pathology, it increases macrophages polarisation towards an anti-inflammatory phenotype and contributes to the persistence of the parasite²⁵⁹. Apoptosis of T cells during the infection with *S. mansoni* is linked to the switch from a Th1 to a Th2 immune response and thereby critical for the survival of the host²⁵⁰. An increase in T cell apoptosis during schistosomiasis was correlated with reduced T cell-induced immunopathology, as reflected by the smaller granuloma sizes observed in mice that had significantly high amounts of apoptotic CD4⁺ T cells²⁴⁹. Therefore, the numerous apoptotic CD3⁺ cells observed in the liver of *Csf1r-Cre⁺AM^{f/f}* mice could be beneficial for the host and reduce immunopathology. Briefly, the immunopathology of schistosomiasis appears in both the acute and the chronic phase of the disease. In the acute phase, high induction of pro-inflammatory cytokines (TNF α , IL-1 and IL-6) can be found in the host²⁶⁰. During the later stage of the disease, the production of eggs (around 100-300 eggs per day) results in an increased amount of SEA. *In vitro* administration of SEA to cultured T cells induces their apoptosis¹⁶⁶, while *in vivo* SEA is associated with the switch toward a type 2 immune response. This switch is mainly characterised by induction of Th2 cell polarisation and production of type 2 cytokines like IL-5, IL-4 or IL-13¹²⁹. In addition to this, the parasite eggs are partially released with the faeces or trapped in the vessels of the liver or intestine. There, they cause the development of granulomas in both organs and thereby induce fibrosis²⁴⁸. An increase in the amount of eggs or detected granulomas is thus associated with a severe pathology.

Analysis of the immunopathology in the present mouse-model showed a severe disease phenotype in *Csf1r-Cre⁺AM^{f/f}* mice, characterised by increased numbers of *S. mansoni* eggs in the liver and intestine, which were accompanied with higher ALT levels in the serum of these mice (Fig. 18). This is in contrast to the hypothesised beneficial effect of the accumulated CD3⁺ T cells. ALT levels are commonly used during the infection with *S. mansoni* to follow disease severity²⁶¹ and the increased ALT levels in the *Csf1r-Cre⁺AM^{f/f}* mice suggest an elevated liver damaged compared to the control.

Greater liver damage and higher parasite egg counts indicate formation of liver fibrosis¹²⁹. In line with this assumption, collagen deposition was enhanced in *Csf1r-Cre⁺AM^{f/f}* mice (Fig. 18). The reduced phagocytosis of apoptotic CD3⁺ cells, which is presumably due to the genetic ablation of *Axl* and *Mertk* and not due to enhanced T cell apoptosis, might neutralise the suggested beneficial effect of the increased apoptotic CD3⁺ cell numbers. However, it needs to be highlighted that the decrease in the immunopathology, reported in the literature, was specifically observed after CD4⁺ T cell apoptosis²⁴⁹. Here the accumulation of the CD4⁺ apoptotic cells was linked to reduce CD4⁺-mediated pathology, which was not investigated in detail in the present thesis. Nonetheless, IL-4 and IL-13 production of α CD3 stimulated cells from the mesenteric lymph node of mice with ablated AXL and MERTK was comparable to that of the WT (Fig. 20), which suggests that T cell function is not altered by the

impairment in phagocytosis. For a complete dissection of the T cell response in the liver, in which the severe immune pathology has been observed in the present thesis, further analysis of the liver draining lymph nodes should be performed. However, regarding the analysis on the mesenteric lymph nodes it is important to highlight that the intestine is the tissue in which the worm persists in the host for years, where parasite eggs constantly pass through the vessels of the intestine and where damage with a constant ongoing immune response to the parasite is induced²⁴⁸. Consequently, the immune response of the intestine should be additionally investigated in more detail.

The pathology during *S. mansoni* is not only defined by the amounts of eggs inside the liver or intestine. Several studies reported that increased cytokine production^{262,263} and an enhanced tissue remodelling phenotype in macrophages^{144,264} is associated with a severe pathology during the infection with *S. mansoni*. In line with the increased egg counts, *Csf1r-Cre⁺AM^{f/f}* mice consistently produced significantly more IL-5, IL-13 and IL-10 as detected in the serum as well as IL-4 to some extent (Fig. 19). Furthermore, macrophages from these mice showed an elevated tissue remodelling function, as defined by the augmented expression of *Chil3* and *Arg1*. Conversely, the same macrophages expressed lower levels of *Il-10* compared to *Csf1r-Cre⁻AM^{f/f}* mice (Fig. 21).

The contribution of cytokines to the disease phenotype of schistosomiasis has been broadly investigated. Mice that lack *Il-4*, *Il-10* and *Il-13* do not survive the acute phase of the infection^{152,265–267}. IL-13 activates fibrotic pathways in target cells⁶⁰, like collagen production²⁶⁸, and is therefore the key cytokine for the induction of liver fibrosis during schistosomiasis¹⁵¹. Loss of IL-13-producing T cells resulted in enhanced disease severity with fatal outcome in mice²⁶⁹. Concordantly, IL-13 levels correlated with the severity of the disease¹⁵² and in line with this, human patients with a severe degree of fibrosis during the infection with *S. mansoni* produced high amounts of IL-13, IL-10 and IL-5¹⁸⁹. Furthermore, mice lacking IL-5 developed smaller granulomas, reduced hepatic fibrosis and produced less IL-13 during the infection with *S. mansoni*²⁷⁰. Whereas, IL-10 is reported to increase the expression of IL-4R α on the surface of macrophages and thereby enhance the IL-4 sensibility of macrophages²⁷¹. However, it has been reported that not only macrophages, but also T cells and in particular Tregs produce IL-10 during schistosomiasis^{272,273} and their production of IL-10 contributed to reduced morbidity and prolonged survival of infected mice¹⁵⁸.

Although the *Csf1r-Cre⁺AM^{f/f}* mice showed a more severe phenotype, it can be hypothesised that the increased IL-10 levels detected in the serum of *Csf1r-Cre⁺AM^{f/f}* mice compared to *Csf1r-Cre⁻AM^{f/f}* mice, is partially produced by Tregs. Moreover, IL-10 is additionally reported to induce anti-fibrotic processes¹⁵⁹, which might explain the elevated IL-10 expression in macrophages from the *Csf1r-Cre⁻AM^{f/f}* mice with a none severe disease phenotype. In addition, this could explain the reduced levels of IL-10 expression in macrophages from *Csf1r-Cre⁺AM^{f/f}* mice that showed a severe disease phenotype.

In conjunction with the elevated expression of IL-13, IL-5 and IL-10 in the serum, the augmented expression of *Chil3* and *Arg1* in macrophages isolated from the liver of *Csf1r-Cre⁺AM^{f/f}* mice further supports the hypothesis that the lack of *Axl* and *Mertk* results in a severe disease phenotype. In line with the presented results, IL-10 is suggested to induce the expression of *Chil3* in macrophages during the infection and contribute to the control of hepatic granulomatous inflammation in the absence of IL-4 signalling²⁴³. Furthermore, reduced levels of IL-13 in *Il-5^{-/-}* mice were accompanied with decreased expression of the tissue remodelling genes *Chil3* and *Arg1* in macrophages²⁷⁰. Although ARG1 is beneficial for the host in the acute phase of schistosomiasis¹⁴⁸ and iNOS instead of ARG1 production in macrophages is associated with early death of the mice²⁴⁸, ARG1 is considered as one of the main drivers of hepatic damage and fibrosis in the chronic phase¹⁵⁶. Here, ARG1 contribute to fibrosis induction by converting L-arginine to L-ornithine that functions as a substrate for collagen synthesis. *Chil3* is reported to exacerbate liver fibrosis in tetrachloride-induced liver fibrosis²⁷⁴ or in patients with hepatitis B²⁷⁵ or hepatitis C²⁷⁶ and contributes to a severe pathology during the infection with *S. mansoni*. *Chil3* expression has been described to increase with the onset of egg release by the parasite and is modulated by the simultaneous sensing of IL-4 and uptake of *S. mansoni* hemozoin by macrophages²⁷⁷. *S. mansoni* uses the host's haemoglobin as a source for nutrients²⁷⁸. Toxic free heme is crystallised into hemozoin, comparable to the mechanism used by *Plasmodium* parasites^{279,280}. In contrast to the *plasmodium*, *S. mansoni* hemozoin interacts with the immune cells of the host in a type 2-enriched environment and directly interacts with the host immune cells by stimulating high expression of tissue remodelling markers in macrophages, as *Chil3* or *Arg1*²⁷⁷. The obtained findings provide the conclusion that the engagement of AXL and MERTK regulate liver fibrosis formation and egg deposition, thereby modulating the pathology during infection with *S. mansoni*.

5.5 MMP14 and TIMP1 contribute to the egg transition through the liver

A severe fibrosis phenotype has also been described to be caused by the expression/secretion of pro-inflammatory/pro-fibrogenic mediators, besides the excessive expression of genes that normally resolve tissue damage. IL-1 β is one of these mediators and is involved in the progression of liver injury to fibrosis²⁸¹. Consistently, *Csf1r-Cre⁺AM^{f/f}* macrophages express higher IL-1 β levels as *Csf1r-Cre⁻AM^{f/f}* macrophages (Fig. 21). Moreover, fibrosis is described as a process in which collagen-rich ECM deposition is enhanced in the liver¹⁸⁸. Macrophages are capable of remodelling matrix structures, either by producing MMPs and TIMPs or through activation of T cells and fibroblasts. Furthermore, IL-1 is suggested to stimulate MMP production^{248,282,283}. However, it is controversially discussed whether MMPs are under- or overexpressed in fibrotic settings. This might be explained by the fact that

individual MMPs are reported to perform unique functions in different *in vivo* settings, and these functions are not observable *in vitro*²⁸⁴. In the present settings, expression of *Mmp14* and *Timp1* was decreased in *Csf1r-Cre⁺AM^{f/f}* mice (Fig. 18). Therefore, a link between high IL-1 β levels and an increase of MMPs as suggested in the literature^{248,282,283} was not observed for MMP14 in the present setting. The role of both molecules during schistosomiasis is not completely understood yet. However, the obtained data suggests that MMPs or TIMPs might play a role in the transition of parasite eggs through the tissue by facilitating ECM degradation and reconstruction, therefore favouring parasite egg release. In line with this, the reduced *Mmp14* and *Timp1* expression could explain the increase in parasite egg numbers observed in *Csf1r-Cre⁺AM^{f/f}* mice compared to the *Csf1r-Cre⁻AM^{f/f}* mice.

Studies showed that cancer cells upregulate MMP14 production to enhance their extravasation of the tissue²⁸⁵, therefore strengthening the potential involvement of MMP14 in egg movement through the tissue. In addition, *Mmp14* seems to be beneficial for the host, considering that mice with an inducible *Mmp14* knock-out showed a fibrotic phenotype in the skin²⁸⁶. Although several studies described upregulation of *Mmp14* in models of lung fibrosis^{181,287}, an anti-fibrotic role of *Mmp14* is suggested in epithelial cells by regulating their proliferation²⁸⁸. The enhanced egg accumulation in combination with the severe immune pathology observed in *Csf1r-Cre⁺AM^{f/f}* mice with reduced *Mmp14* expression, suggests an anti-fibrotic role of MMP14 that could affect egg transition and removal in the analysed experimental setting. This function might be further synergised by TIMP1, as the expression of both molecules, *Timp1* and *Mmp14*, decreased simultaneously in mice with reduced amount of parasite egg in the tissue.

TIMP1 is an inhibitor of MMPs, and is upregulated in wound healing and ECM reconstruction²⁸⁹. It has anti-apoptotic properties as reported in patients with hepatocellular carcinoma²⁹⁰. As observed in the present study and described in the literature²⁹¹, *Timp1* is expressed by macrophages (Fig. 21) and other cells of the liver (Fig. 18), like HSC²⁹². Elevated levels of TIMP1 are associated with poor prognosis in cancer patients^{290,293}, while increased expression levels of *Timp1* are found in mice with liver fibrosis induced by carbon tetrachloride or bile duct ligation. However, in these models it has been described that *Timp1* is not essential for fibrosis formation²⁹⁰. In the context of *S. mansoni* infection, although *Timp1* expression peaks at the chronic, fibrotic stage of the disease¹⁸⁷, changes in fibrosis formation were not found in *Timp1^{-/-}* mice²⁹⁴, suggesting that TIMP1 is not directly linked to fibrosis induction in this model of damage either. In line with the observations about *Timp1*'s contribution to angiogenesis and vascular permeability^{284,291}, the results rather proposes an involvement of *Timp1* in *Mmp14*-induced parasite egg clearance and transition.

5.6 Apoptotic cells are able to shape the therapeutic potential of macrophages

Modulation of the activation/function of macrophages is of high interest in biomedicine. An imbalance of anti- and pro-inflammatory macrophages can result in chronic diseases as observed in multiple sclerosis²⁹⁵ or rheumatoid arthritis²⁹⁶. Altering macrophage function might contribute to the re-establishment of homeostasis in pathological settings. However, a safe and efficient method to reprogram macrophages *in vivo*, although broadly investigated, has not been described so far²⁹⁷. Attempts using modified mRNA^{298,299} or macrophage-specific peptides fused to pro-apoptotic stimuli³⁰⁰ showed promising results, but their applicability needs to be further addressed. Adoptive transfer of *in vitro*-reprogrammed macrophages can bypass this problem and autologous macrophage transfer alleviated pathology in liver cirrhosis patients³⁰¹. It is tempting to hypothesise that aN-reprogrammed macrophages have a beneficial effect on the host during schistosomiasis. Consistently, in models of liver damage the accumulation of aN is beneficial for the host by strengthening the tissue remodelling phenotype of macrophages and thereby limiting the disease severity³⁰². In addition, it is described that mice lacking the adaptor molecule STING showed elevated percentages of neutrophils, which correlated with reduced *S. mansoni* burden³⁰³. Although it has been reported that during schistosomiasis neutrophils are recruited in high numbers after 2-7 days, when the *schistosomulae* arrive at the pulmonary vasculature³⁰⁴, only low levels of aN were detected in the livers of the *S. mansoni*-infected mice at the analysed time point (14 weeks p.i.) (Fig. 17). This was observed independently of the lack of the phagocytic receptors AXL and MERTK. However, in line with *i*) the beneficial effects of tissue remodelling macrophages during the infection with *S. mansoni*¹⁴⁴, *ii*) the reduced worm burden triggered by elevated neutrophil frequencies³⁰³ and *iii*) the specific tissue remodelling response of macrophages after aN phagocytosis (see 4.2), transfer of macrophages reprogrammed *in vitro* with aN significantly reduced the parasite egg count in the intestine of infected mice. In contrast, this result was not achieved through the transfer of macrophages pre-primed with aH or aT *in vitro* (Fig. 22), which support the specific role of aN in macrophage priming.

Transfer of BMDMs has been described to be advantageous during schistosomiasis and reduced liver fibrosis during the chronic phase¹⁶². Contradictory to what has previously been published¹⁶², no overall beneficial effect of the macrophage transfer was found in the present thesis compared to mice that were infected but did not receive macrophages. However, the reduction in liver fibrosis was described in mice treated with praziquantel before BMDM transfer¹⁶². Here, the impact of the treatment cannot be neglected as the administration of praziquantel results in the death of the worm and therefore no new eggs are produced during the cell therapy and could interfere, as the worm itself, with the immune response.

The adoptive transfer of macrophages also modulated the phenotype of recipient macrophages in the liver. Frequencies of YM1⁺ recipient macrophages increased in all conditions analysed independently of the apoptotic cell priming *in vitro* (Fig. 24), confirming that the transfer of macrophages affects the YM1 expression and thereby might influence the polarisation of the macrophages of the recipient mice. In line with the described and already mentioned detrimental effect of ARG1¹⁵⁶ during the disease, only the transfer of aN-pre-primed macrophages reduced the frequency of ARG1⁺ recipient macrophages. Furthermore, the reduced egg counts in the intestine observed in these mice could directly result from the diminished frequencies in ARG1⁺ resident macrophages²⁴⁸. However, the decrease of ARG1⁺ macrophages was detected in the liver, where aN-pre-primed macrophages only slightly reduced the parasite egg count (Fig. 22). An influence of the hepatic macrophage polarisation by the gut microbiota along the liver-gut-axes is described in non-alcoholic fatty liver disease. Accordingly, it can be hypothesised that in the present experimental setting an influence along the gut-liver axes might also take place and could thereby connect the reduced ARG1⁺ macrophages in the liver with the reduced parasite egg numbers in the intestine.

In consistent with the previously discussed results (see 5.5) and the reduced amounts of parasitic eggs, mice receiving aN-pre-primed macrophages showed a slight increase in *Mmp14* expression in the colon (Fig. 23). These results could support the role of *Mmp14* in the parasite egg release. However, the here discussed phenotype was observed during the acute phase and not, as previously, in the chronic phase of the disease. If and how the transfer of macrophages has a therapeutic potential on the *Mmp14* expression and the amount of parasite eggs in the chronic-fibrotic phase of the infection should be further investigated, as the effect might be more prominent at later time points of the infection. In line with this, curative chemotherapy in mice revealed that the granuloma structure during an *S. mansoni* infection differs over the course of the infection. Granuloma structures were resolved after 2-4 months in infections that were established for no longer than 12 weeks. When a prolonged infection was induced in mice, the time needed for degradation of granulomas increased up to 4 months³⁰⁵. In human patients with schistosomal-hepatosplenic-diseases, granuloma degradation was obtained after 2-3 years^{305,306}. This suggests that the timing and structure of the granuloma might co-determine the expression level and the efficacy of MMP function.

In accordance with this hypothesis, *Timp1* expression was not altered by the transfer of macrophages during the acute phase of the disease, which suggests that the impact of *Timp1* expression on the parasite egg release might be restricted to the chronic phase of the infection.

Furthermore, mice that received aN pre-primed macrophages upregulated the expression of *Tgfb* in the colon (Fig. 23). It is described, that stimulation with SEA *in vitro* increased the expression of *Tgfb*

in α CD3-stimulated mesenteric lymph nodes¹⁹⁰ and macrophages²⁶⁴. This was associated with an anti-inflammatory phenotype of the phagocytes, characterised by IL-10 and CD206 (MMR-1) expression. Although known as a pro-fibrogenic factor¹⁴⁴, TGF β production by tissue remodelling macrophages reduced collateral tissue damage during the formation of the granuloma¹⁵⁶. Besides macrophages, Tregs respond to TGF β during *S. mansoni* infection. Their development is favoured by TGF β released from the intestine, and accordingly increased Treg proliferation in the gut was observed after SEA injection¹⁹⁰. Elevated numbers of Tregs are described to suppress enteric granulomas¹⁹⁰, which might suggest that the decreased number of parasite eggs in the intestine in mice receiving aN-pre-primed macrophages might result from the increased *Tgfb* expression in these mice.

Moreover, in mice that received aH-pre-primed macrophages, an elevated frequency of CD3⁺ cells was observed in the liver (Fig. 24) and might be a consequence of the transferred macrophages. As stated earlier (see. 5.2), aH shape macrophages towards a tolerogenic function; this might induce recruitment of Tregs to counteract the immune responses. On the contrary, mice that received aH-pre-primed macrophages did not show alteration in *Tgfb* expression, which further suggest that the elevated frequency of CD3⁺ cells in the liver did not result from proliferated Tregs.

5.7 The role of phagocytic receptor expression in human macrophages during schistosomiasis

Although the characteristics of murine and human macrophages are only partially comparable, the response of macrophages towards *S. mansoni* is similar in humans and mice^{132,156}. Human blood monocytes isolated from patients with schistosomiasis showed a higher affinity towards *schistosomula*, as mirrored by their increased adherence to the parasite, compared to monocytes isolated from uninfected individuals³⁰⁷. These results underline the importance of macrophages/monocytes in parasite clearance also in the human context.

So far, no study was conducted on how phagocytosis by human macrophages contributes to the pathology of *S. mansoni*. However, the limited human sample size analysed in this work does not allow a comprehensive conclusion. Nonetheless, CD14⁺ cells isolated from *S. mansoni*-infected patients showed an increased *Axl*, *Mertk* and *Cd36* expression compared to healthy controls (Fig. 25). Although not statistically significant, slight differences in the phagocytosis receptor expression between the two groups support the hypothesis that the uptake of apoptotic cells can contribute to *S. mansoni* pathology in the human setting; similar to what is described for the mouse counterpart in the present thesis. The identity of the apoptotic cells might differ among human individuals and thereby might favour tolerance against the parasite in some patients or resistance to the parasite in other patients. Tolerance against a parasite is characterised by the ability to limit the damage induced by the parasite,

while resistance towards a parasite reduce the parasite burden³⁰⁸. As shown in the mouse counterpart of the present thesis, macrophages that phagocytosed aN acquire a tissue remodelling function. This phenotype of macrophages limits the granulomatous response, enhances host survival¹⁵⁶ and is also described to limit disease severity in different damage models^{91,309}. Therefore, the phagocytosis of aN by human macrophages during schistosomiasis is suggested for the induction of tolerance against the parasite. Mice that were able to phagocytose apoptotic CD3⁺ or CD11b⁺ cells during the infection with *S. mansoni* showed fewer parasite eggs, which might suggest a capacity to limit parasite burden – translating this findings in the human context, the phagocytosis of apoptotic CD3⁺ or CD11b⁺ cells might induce host-resistance to the parasite. However, further investigations are needed to verify this hypothesis.

6 Future perspective

6.1 Dissection of the crosstalk between macrophages and apoptotic cells

The present thesis showed that the origin of the phagocytosed apoptotic cell actively shapes the transcriptomic and functional heterogeneity in macrophages, whereby only aN committed macrophages towards a tissue remodelling phenotype. However, the mechanism how apoptotic cells shape the macrophages response and in particular, the induction of a tissue remodelling function in macrophages modulated specifically by aN needs to be investigated further. Hence, additional experiments to dissect the crosstalk between apoptotic cells, in particular aN, and macrophages are needed.

With the obtained data, it can be concluded that soluble factors are not involved in the aN-driven response of macrophages, suggesting the requirement for a cell-cell contact. To further dissect this interaction, isolation of plasma membrane-associated proteins, like CECAM, and transmembrane domains like GPI anchors from aN should be performed. Analysis of the tissue remodelling genes and protein expression in macrophages after individual supplementation of the membrane components could clarify their involvement in the cellular and molecular interaction of the aN - macrophage crosstalk.

Furthermore, changes in the metabolome occurring in macrophages after apoptotic cell clearance are known¹⁷⁸. Therefore, the metabolic signatures of macrophages after apoptotic cell phagocytosis should be investigated. The alterations specifically induced by aN phagocytosis would be of special interest in this context. In particular, in tissue remodelling macrophages oxidative phosphorylation is favoured over glycolysis¹⁹². An analysis of changes within the oxidative phosphorylation process could reveal genes that commit the macrophage response after phagocytosis of different apoptotic cell types. For this purpose, the web-based application Ingenuity pathway analysis (Qiagen) might help to discover differentially expressed master regulators. In addition, using high performance liquid chromatography, the production of metabolites like ATP and ADP, which are known to modulate macrophage responses³¹⁰, could be measured. Their quantification might provide an explanation for the various modulation of the macrophages' response by apoptotic cells with different identities. In addition, the lipid and amino acid metabolism is highly affected by the polarisation of macrophages¹⁹². To this end, liquid chromatography–mass spectrometry analysis could be performed to compare the metabolome of macrophages that phagocytosed specific apoptotic cell types to non-phagocytic macrophages.

Live cell imaging enables the analysis of the dynamic process of phagocytosis, allowing further characterisation of the crosstalk between apoptotic cells and macrophages. This would help to identify phagocytic receptors that selectively recognise and uptake one specific apoptotic cell type, and could

be combined with analysis of the apoptotic cell-macrophage interaction using macrophages that lack specific phagocytosis receptors.

In addition, the engagement of various phagocytic receptors might activate different signalling pathways. With the help of a kinase assay, disparities in downstream signalling events after phagocytosis of selective apoptotic cells in macrophages can be analysed. Furthermore, the strength of the binding between the various apoptotic corpses and the phagocyte can be investigated by either a time-resolved competition assay or real-time cell binding assay^{311,312}. It would be of high interest to investigate whether it is the binding or the uptake of apoptotic cells that induce the specific response in macrophages. For instance, RNAseq of macrophages that are exposed to apoptotic cells in the presence of actin inhibitors, which inhibit the cytoskeleton rearrangement and phagocytosis of the apoptotic cell, but allow the binding to the apoptotic cell, should be performed.

With the aim to further investigate the impact of the nature of apoptotic cells on macrophages' function *in vivo*, two methods are proposed. Spatial transcriptomic technology allows the visualisation and simultaneous analysis of cell-cell interactions on tissue sections. Using liver granuloma sections, macrophages that are in close proximity to different apoptotic cells could be visualised and their transcriptome characterised and compared amongst each other.

Additionally, the use of reporter mice, in which specific cell types are labelled, enables the identification of macrophages that specifically uptake a selective type of apoptotic cells. Here, the Catchup transgenic mice or albumin (Alb)-CreERT/Rosa26-LsL-LacZ transgenic mice could be used to track neutrophils or hepatocytes, respectively. Similarly, mice in which specific cell types are not able to go into apoptosis could be used. For example, in the Ly6G-Cre x Caspase9^{f/f} mice, neutrophils are not able to go into apoptosis, which would allow an analysis of the macrophage response excluding the impact of aN phagocytosis.

6.2 The therapeutic potential of macrophages

The present study underlined the therapeutic potential of macrophages reprogrammed by the phagocytosis of apoptotic cells with different origins. The transfer of macrophages primed *in vitro* with aN affects the disease outcome in a model of *S. mansoni* infection. However, it remains unclear for how long the beneficial effects of the transferred aN-pre-primed macrophages are maintained in the recipient mice. To this end, kinetic experiments should be performed.

Analysis of changes in the granuloma composition and egg transition upon macrophage transfer is of high interest. Therefore, morphological analysis of the granuloma via histology and quantification of *Mmp14* and *Timp1* expression levels are highly suggested and should be performed side by side with

the kinetic experiments. In addition, this would allow further investigation of the impact of *Mmp14* and *Timp1* in parasite egg release and the therapeutic potential of macrophages on both molecules. Because adoptive transfer experiments were performed only during the acute phase of *S. mansoni* infection, injection of macrophages during the chronic phase should be performed and is of special interest, as the constant inflammation induced by the parasite leads to fibrosis formation at later stages of the disease. To this end, factors that are involved in fibrosis formation and liver damage, besides *Mmp14* and *Timp1*, should additionally be investigated. It is indeed of particular interest to understand whether altering the macrophage composition in the damaged tissue might re-establish liver homeostasis. Recently, new methods like the chimeric antigen receptors for phagocytosis (CAR-P)³¹³ were developed for cell therapy. This method could be used to instruct macrophages to uptake specific apoptotic cell targets at different time points during the infection.

6.3 The impact of phagocytosis on human macrophages

The expression pattern of phagocytic receptors and bridging molecules expressed on monocytes in the blood of *S. mansoni*-infected patients is of high interest. Because of this, complementary protein analysis should be performed with a higher sample size. In addition, analysis of ALT levels or cytokine production in the serum of infected patients might reveal a correlation between phagocytic receptor expression, the amount of liver damage and the stage of the immune response. Comparable to the RNAseq analysis of murine macrophages, transcriptome analysis of human macrophages upon phagocytosis of different apoptotic cells might reveal functional differences of human macrophages depending on the apoptotic cell phagocytosed. With this aim, phagocytosis assays with different apoptotic cells, as conducted for the murine macrophages, should be performed. Analysis of various polarisation markers and phagocytosis receptors on human macrophages on protein and gene level would be highly valuable. These experiments would further provide a deeper understanding of the similarity or discrepancy between the macrophage response in mice and humans.

7 References

- [1] Hirayama, D.; Nakase, H.; Iida, T.; Nakase, H. The Phagocytic Function of Macrophage-Enforcing Innate Immunity and Tissue Homeostasis. *Int. J. Mol. Sci.* **2018**, *19*, 92. <https://doi.org/10.3390/ijms19010092>.
- [2] Stryer. *Stryer*, 7 th.; Springer Spektrum, **2013**.
- [3] Abbas, A. K.; Lichtman, A. H.; Pillai, S.; Baker, D. L. Cellular and Molecular Immunology. *Elsevier* **2017**, No. January, 267–301. <https://doi.org/10.1016/B978-1-4160-3123-9.50020-6>.
- [4] Fultz, R.; Engevik, M. A.; Shi, Z.; Hall, A.; Herrmann, B.; Ganesh, B. P.; Major, A.; Haag, A.; Mori-Akiyama, Y.; Versalovic, J. Phagocytosis by Macrophages Depends on Histamine H2 Receptor Signaling and Scavenger Receptor 1. *Microbiologyopen* **2019**, *8*, e908. <https://doi.org/10.1002/mbo3.908>.
- [5] Murphy; P.Travers; M.Walport. *Janeway Immunologie*, 7th ed.; **2009**.
- [6] Spellberg, B.; Edwards, J. E. Type 1/Type 2 Immunity in Infectious Diseases. *Clin. Infect. Dis.* **2001**, *32*, 76–102. <https://doi.org/10.1086/317537>.
- [7] Koyasu, S.; Moro, K. Type 2 Innate Immune Responses and the Natural Helper Cell. *Immunology* **2011**, *132*, 475–481. <https://doi.org/10.1111/j.1365-2567.2011.03413.x>.
- [8] Morel, P. A.; Butterfield, L. H. Dendritic Cell Control of Immune Responses. *Front. Immunol.* **2015**, *6*. <https://doi.org/10.3389/fimmu.2015.00042>.
- [9] Vivier, E.; Tomasello, E.; Baratin, M.; Walzer, T.; Ugolini, S. Functions of Natural Killer Cells. *Nat. Immunol.* **2008**, *9*, 503–510. <https://doi.org/10.1038/ni1582>.
- [10] Moretta, L.; Ferlazzo, G.; Bottino, C.; Vitale, M.; Pende, D.; Mingari, M. C.; Moretta, A. Effector and Regulatory Events during Natural Killer-Dendritic Cell Interactions. *Immunol. Rev.* **2006**, *214*, 219–228. <https://doi.org/10.1111/j.1600-065X.2006.00450.x>.
- [11] Elhelu, M. A. The Role of Macrophages in Immunology. *J. Natl. Med. Assoc.* **1983**, *75*, 314–317.
- [12] van de Laar, L.; Saelens, W.; De Prijck, S.; Martens, L.; Scott, C. L.; Van Isterdael, G.; Hoffmann, E.; Beyaert, R.; Saeys, Y.; Lambrecht, B. N.; Guillems, M. Yolk Sac Macrophages, Fetal Liver, and Adult Monocytes Can Colonize an Empty Niche and Develop into Functional Tissue-Resident Macrophages. *Immunity* **2016**, *44*, 755–768. <https://doi.org/10.1016/j.immuni.2016.02.017>.
- [13] Wynn, T. a.; Chawla, A.; Pollard, J. W. Origins and Hallmarks of Macrophages: Development, Homeostasis, and Disease. *Nature* **2013**, *496*, 445–455. <https://doi.org/10.1038/nature12034>.Origins.
- [14] Yona, S.; Kim, K. W.; Wolf, Y.; Mildner, A.; Varol, D.; Breker, M.; Strauss-Ayali, D.; Viukov, S.; Guillems, M.; Misharin, A.; Hume, D. A.; Perlman, H.; Malissen, B.; Zelzer, E.; Jung, S. Fate Mapping Reveals Origins and Dynamics of Monocytes and Tissue Macrophages under Homeostasis. *Immunity* **2013**, *38*, 79–91. <https://doi.org/10.1016/j.immuni.2012.12.001>.
- [15] Krenkel, O.; Tacke, F. Liver Macrophages in Tissue Homeostasis and Disease. *Nat. Rev. Immunol.* **2017**, *17*, 306–321. <https://doi.org/10.1038/nri.2017.11>.
- [16] Takahashi, K.; Yamamura, F.; Naito, M. Differentiation, Maturation, and Proliferation of Macrophages in the Mouse Yolk Sac: A Light-Microscopic, Enzyme-Cytochemical, Immunohistochemical, and Ultrastructural Study. *J. Leukoc. Biol.* **1989**, *45*, 87–96. <https://doi.org/10.1002/jlb.45.2.87>.
- [17] Okabe, Y. Molecular Control of the Identity of Tissue-Resident Macrophages. *Int. Immunol.* **2018**, *30*, 485–491. <https://doi.org/10.1093/intimm/dxy019>.
- [18] Kolter, J.; Feuerstein, R.; Zeis, P.; L€E, T.; Prinz, M.; Correspondence, P. H.; Hagemeyer, N.; Paterson, N.; D’errico, P.; Baasch, S.; Amann, L.; Masuda, T.; L€O Sslein, A.; Gharun, K.; Meyer-Luehmann, M.; Waskow, C.; Franzke, C.-W.; Gr€E, D.; Henneke, P. A Subset of Skin Macrophages Contributes to the Surveillance and Regeneration of Local Nerves Article A Subset of Skin Macrophages Contributes to the Surveillance and Regeneration of Local Nerves. *Immunity* **2019**, *50*, 1482-1497.e7. <https://doi.org/10.1016/j.immuni.2019.05.009>.
- [19] Greter, M.; Lelios, I.; Pelczar, P.; Hoeffel, G.; Price, J.; Leboeuf, M.; Kündig, T. M.; Frei, K.; Ginhoux, F.; Merad, M.; Becher, B. Stroma-Derived Interleukin-34 Controls the Development

- and Maintenance of Langerhans Cells and the Maintenance of Microglia. *Immunity* **2012**, *37*, 1050–1060. <https://doi.org/10.1016/j.immuni.2012.11.001>.
- [20] Wang, Y.; Szretter, K. J.; Vermi, W.; Gilfillan, S.; Rossini, C.; Cella, M.; Barrow, A. D.; Diamond, M. S.; Colonna, M. IL-34 Is a Tissue-Restricted Ligand of CSF1R Required for the Development of Langerhans Cells and Microglia. *Nat. Immunol.* **2012**, *13*, 753–760. <https://doi.org/10.1038/ni.2360>.
- [21] Satpathy, A. T.; Wu, X.; Albring, J. C.; Murphy, K. M. Re(de)Fining the Dendritic Cell Lineage. *Nat. Immunol.* **2012**, *13*, 1145–1154. <https://doi.org/10.1038/ni.2467>.
- [22] Ginhoux, F.; Guilliams, M. Tissue-Resident Macrophage Ontogeny and Homeostasis. *Immunity* **2016**, *44*, 439–449. <https://doi.org/10.1016/j.immuni.2016.02.024>.
- [23] Davies, L. C.; Taylor, P. R. Tissue-Resident Macrophages: Then and Now. *Immunology* **2015**, *144*, 541–548. <https://doi.org/10.1111/imm.12451>.
- [24] Langlet, C.; Tamoutounour, S.; Henri, S.; Luche, H.; Ardouin, L.; Grégoire, C.; Malissen, B.; Guilliams, M. CD64 Expression Distinguishes Monocyte-Derived and Conventional Dendritic Cells and Reveals Their Distinct Role during Intramuscular Immunization. *J. Immunol.* **2012**, *188*, 1751–1760. <https://doi.org/10.4049/jimmunol.1102744>.
- [25] Cecchini, M. G.; Dominguez, M. G.; Mocci, S.; Wetterwald, A.; Felix, R.; Fleisch, H.; Chisholm, O.; Hofstetter, W.; Pollard, J. W.; Stanley, E. R. Role of Colony Stimulating Factor-1 in the Establishment and Regulation of Tissue Macrophages during Postnatal Development of the Mouse. *Development* **1994**, *120*, 1357–1372.
- [26] Dai, X. M.; Ryan, G. R.; Hapel, A. J.; Dominguez, M. G.; Russell, R. G.; Kapp, S.; Sylvestre, V.; Stanley, E. R. Targeted Disruption of the Mouse Colony-Stimulating Factor 1 Receptor Gene Results in Osteopetrosis, Mononuclear Phagocyte Deficiency, Increased Primitive Progenitor Cell Frequencies, and Reproductive Defects. *Blood* **2002**, *99*, 111–120. <https://doi.org/10.1182/blood.V99.1.111>.
- [27] Chitu, V.; Stanley, E. R. Colony-Stimulating Factor-1 in Immunity and Inflammation. *Curr. Opin. Immunol.* **2006**, *18*, 39–48. <https://doi.org/10.1016/j.coi.2005.11.006>.
- [28] Li, Q.; Barres, B. A. Microglia and Macrophages in Brain Homeostasis and Disease. *Nat. Rev. Immunol.* **2018**, *18*, 225–242. <https://doi.org/10.1038/nri.2017.125>.
- [29] Wang, S.; Ye, Q.; Zeng, X.; Qiao, S. Functions of Macrophages in the Maintenance of Intestinal Homeostasis. *J. Immunol. Res.* **2019**, *2019*, 8. <https://doi.org/10.1155/2019/1512969>.
- [30] Schridde, A.; Bain, C. C.; Mayer, J. U.; Montgomery, J.; Pollet, E.; Denecke, B.; Milling, S. W. F.; Jenkins, S. J.; Dalod, M.; Henri, S.; Malissen, B.; Pabst, O.; McL Mowat, A. Tissue-Specific Differentiation of Colonic Macrophages Requires TGF β Receptor-Mediated Signaling. *Mucosal Immunol.* **2017**, *10*, 1387–1399. <https://doi.org/10.1038/mi.2016.142>.
- [31] Lavin, Y.; Winter, D.; Blecher-Gonen, R.; David, E.; Keren-Shaul, H.; Merad, M.; Jung, S.; Amit, I. Tissue-Resident Macrophage Enhancer Landscapes Are Shaped by the Local Microenvironment. *Cell* **2014**, *159*, 1312–1326. <https://doi.org/10.1016/j.cell.2014.11.018>.
- [32] Bonnardel, J.; T'Jonck, W.; Gaublomme, D.; Browaeys, R.; Scott, C. L.; Martens, L.; Vanneste, B.; De Prijck, S.; Nedospasov, S. A.; Kremer, A.; Van Hamme, E.; Borghgraef, P.; Toussaint, W.; De Bleser, P.; Mannaerts, I.; Beschin, A.; van Grunsven, L. A.; Lambrecht, B. N.; Taghon, T.; Lippens, S.; Elewaut, D.; Saeys, Y.; Guilliams, M. Stellate Cells, Hepatocytes, and Endothelial Cells Imprint the Kupffer Cell Identity on Monocytes Colonizing the Liver Macrophage Niche. *Immunity* **2019**, *51*, 638–654.e9. <https://doi.org/10.1016/j.immuni.2019.08.017>.
- [33] Lopez, B. G.; Tsai, M. S.; Baratta, J. L.; Longmuir, K. J.; Robertson, R. T. *Characterization of Kupffer Cells in Livers of Developing Mice*; **2011**. <https://doi.org/10.1186/1476-5926-10-2>.
- [34] Sakai, M.; Troutman, T. D.; Seidman, J. S.; Ouyang, Z.; Spann, N. J.; Abe, Y.; Ego, K. M.; Bruni, C. M.; Deng, Z.; Schlachetzki, J. C. M.; Nott, A.; Bennett, H.; Chang, J.; Vu, B. C. T.; Pasillas, M. P.; Link, V. M.; Texari, L.; Heinz, S.; Thompson, B. M.; McDonald, J. G.; Geissmann, F.; Glass, C. K. Liver-Derived Signals Sequentially Reprogram Myeloid Enhancers to Initiate and Maintain Kupffer Cell Identity. *Immunity* **2019**, *51*, 1–16. <https://doi.org/10.1016/j.immuni.2019.09.002>.
- [35] Mass, E.; Ballesteros, I.; Farlik, M.; Halbritter, F.; Günther, P.; Crozet, L.; Jacome-Galarza, C. E.;

- Händler, K.; Klughammer, J.; Kobayashi, Y.; Gomez-Perdiguero, E.; Schultze, J. L.; Beyer, M.; Bock, C.; Geissmann, F. Specification of Tissue-Resident Macrophages during Organogenesis. *Science (80-.)*. **2016**, *353*, aaf4238. <https://doi.org/10.1126/science.aaf4238>.
- [36] Biswas, S. K.; Mantovani, A. Orchestration of Metabolism by Macrophages. *Cell Metab.* **2012**, *15*, 432–437. <https://doi.org/10.1016/j.cmet.2011.11.013>.
- [37] Chinnery, H. R.; McMenemy, P. G.; Dando, S. J. Macrophage Physiology in the Eye. *Pflugers Archiv European Journal of Physiology*, **2017**, *469*, 501–515. <https://doi.org/10.1007/s00424-017-1947-5>.
- [38] Wynn, T. A.; Chawla, A.; Pollard, J. W. Macrophage Biology in Development, Homeostasis and Disease. *Nature* **2013**, *496*, 445–455. <https://doi.org/10.1038/nature12034>.
- [39] Bosurgi, L.; Brunelli, S.; Rigamonti, E.; Monno, A.; Manfredi, A. A.; Rovere-Querini, P. Vessel-Associated Myogenic Precursors Control Macrophage Activation and Clearance of Apoptotic Cells. *Clin. Exp. Immunol.* **2015**, *179*, 62–67. <https://doi.org/10.1111/cei.12356>.
- [40] Mosser, D. M.; Hamidzadeh, K.; Goncalves, R. Macrophages and the Maintenance of Homeostasis. *Cell. Mol. Immunol.* **2020**, *18*, 579–587. <https://doi.org/10.1038/s41423-020-00541-3>.
- [41] Wynn, T. A.; Vannella, K. M. Macrophages in Tissue Repair, Regeneration, and Fibrosis. *Immunity* **2016**, *44*, 450–462. <https://doi.org/10.1016/j.immuni.2016.02.015>.
- [42] Halterman, J. A.; Moo Kwon, H.; Wamhoff, B. R. Tonicity-Independent Regulation of the Osmosensitive Transcription Factor Tonebp (NFAT5). *Am. J. Physiol. - Cell Physiol.* **2012**, *302*, C1–C8. <https://doi.org/10.1152/ajpcell.00327.2011>.
- [43] Guillot, A.; Tacke, F. Liver Macrophages: Old Dogmas and New Insights. *Hepatol. Commun.* **2019**, *3*, 730–743. <https://doi.org/10.1002/hep4.1356>.
- [44] Stein, M.; Keshav, S.; Harris, N.; Gordon, S. Interleukin 4 Potently Enhances Murine Macrophage Mannose Receptor Activity: A Marker of Alternative Immunologic Macrophage Activation. *J. Exp. Med.* **1992**, *176*, 287–292. <https://doi.org/10.1084/jem.176.1.287>.
- [45] Murray, P. J.; Allen, J. E.; Biswas, S. K.; Fisher, E. A.; Gilroy, D. W.; Goerdt, S.; Gordon, S.; Hamilton, J. A.; Ivashkiv, L. B.; Lawrence, T.; Locati, M.; Mantovani, A.; Martinez, F. O.; Mege, J. L.; Mosser, D. M.; Natoli, G.; Saeij, J. P.; Schultze, J. L.; Shirey, K. A.; Sica, A.; Suttles, J.; Udalova, I.; vanGinderachter, J. A.; Vogel, S. N.; Wynn, T. A. Macrophage Activation and Polarization: Nomenclature and Experimental Guidelines. *Immunity* **2014**, *41*, 14–20. <https://doi.org/10.1016/j.immuni.2014.06.008>.
- [46] Martinez, F. O.; Gordon, S. The M1 and M2 Paradigm of Macrophage Activation : Time for Reassessment. **2014**, *13*, 1–13. <https://doi.org/10.12703/P6-13>.
- [47] Gordon, S.; Martinez, F. O. Alternative Activation of Macrophages: Mechanism and Functions. *Immunity* **2010**, *32*, 593–604. <https://doi.org/10.1016/j.immuni.2010.05.007>.
- [48] Mills, C. D.; Kincaid, K.; Alt, J. M.; Heilman, M. J.; Hill, A. M. M-1/M-2 Macrophages and the Th1/Th2 Paradigm. *J. Immunol.* **2000**, *164*, 6166–6173. <https://doi.org/10.4049/jimmunol.164.12.6166>.
- [49] Mantovani, A.; Biswas, S. K.; Galdiero, M. R.; Sica, A.; Locati, M. Macrophage Plasticity and Polarization in Tissue Repair and Remodelling. *J. Pathol.* **2013**, *229*, 176–185. <https://doi.org/10.1002/path.4133>.
- [50] Mantovani, A.; Sica, A.; Locati, M. Macrophage Polarization Comes of Age. *Immunity* **2005**, *23*, 344–346. <https://doi.org/10.1016/j.immuni.2005.10.001>.
- [51] Fleetwood, A. J.; Dinh, H.; Cook, A. D.; Hertzog, P. J.; Hamilton, J. A. GM-CSF- and M-CSF-Dependent Macrophage Phenotypes Display Differential Dependence on Type I Interferon Signaling. *J. Leukoc. Biol.* **2009**, *86*, 411–421. <https://doi.org/10.1189/jlb.1108702>.
- [52] Louis, C.; Cook, A. D.; Lacey, D.; Fleetwood, A. J.; Vlahos, R.; Anderson, G. P.; Hamilton, J. A. Specific Contributions of CSF-1 and GM-CSF to the Dynamics of the Mononuclear Phagocyte System. *J. Immunol.* **2015**, *195*, 134–144. <https://doi.org/10.4049/jimmunol.1500369>.
- [53] Jablonski, K. A.; Amici, S. A.; Webb, L. M.; Ruiz-Rosado, J. de D.; Popovich, P. G.; Partida-Sanchez, S.; Guerau-De-arellano, M. Novel Markers to Delineate Murine M1 and M2 Macrophages. *PLoS*

- One* **2015**, *10*, 5–11. <https://doi.org/10.1371/journal.pone.0145342>.
- [54] chen, yongwen; Feng, Z.; Diao, B.; Wang, R.; Wang, G.; Wang, C.; Tan, Y.; Liu, L.; Wang, C.; Liu, Y.; Liu, Y.; Yuan, Z.; Ren, L.; Wu, Y. The Novel Severe Acute Respiratory Syndrome Coronavirus 2 (SARS-CoV-2) Directly Decimates Human Spleens and Lymph Nodes. *medRxiv* **2020**, *2*, 2020.03.27.20045427. <https://doi.org/10.1101/2020.03.27.20045427>.
- [55] Gieseck, R. L.; Wilson, M. S.; Wynn, T. A. Type 2 Immunity in Tissue Repair and Fibrosis. *Nat. Rev. Immunol.* **2018**, *18*, 62–76. <https://doi.org/10.1038/nri.2017.90>.
- [56] Rodrigues, M.; Kosaric, N.; Bonham, C. A.; Gurtner, G. C. Wound Healing: A Cellular Perspective. *Physiol. Rev.* **2019**, *99*, 665–706. <https://doi.org/10.1152/physrev.00067.2017>.
- [57] Mokarram, N.; Bellamkonda, R. V. A Perspective on Immunomodulation and Tissue Repair. *Ann. Biomed. Eng.* **2014**, *42*, 338–351. <https://doi.org/10.1007/s10439-013-0941-0>.
- [58] Loke, P.; Nair, M. G.; Parkinson, J.; Guiliano, D.; Blaxter, M.; Allen, J. E. IL-4 Dependent Alternatively-Activated Macrophages Have a Distinctive in Vivo Gene Expression Phenotype. *BMC Immunol.* **2002**, *3*, 1–11. <https://doi.org/10.1186/1471-2172-3-7>.
- [59] Kuroda, E.; Ho, V.; Ruschmann, J.; Antignano, F.; Hamilton, M.; Rauh, M. J.; Antov, A.; Flavell, R. A.; Sly, L. M.; Krystal, G. SHIP Represses the Generation of IL-3-Induced M2 Macrophages by Inhibiting IL-4 Production from Basophils. *J. Immunol.* **2009**, *183*, 3652–3660. <https://doi.org/10.4049/jimmunol.0900864>.
- [60] Gieseck, R. L.; Ramalingam, T. R.; Hart, K. M.; Vannella, K. M.; Cantu, D. A.; Lu, W. Y.; Ferreira-González, S.; Forbes, S. J.; Vallier, L.; Wynn, T. A. Interleukin-13 Activates Distinct Cellular Pathways Leading to Ductular Reaction, Steatosis, and Fibrosis. *Immunity* **2016**, *45*, 145–158. <https://doi.org/10.1016/j.immuni.2016.06.009>.
- [61] Ramalingam, T. R.; Pesce, J. T.; Sheikh, F.; Cheever, A. W.; Mentink-Kane, M. M.; Wilson, M. S.; Stevens, S.; Valenzuela, D. M.; Murphy, A. J.; Yancopoulos, G. D.; Urban, J. F.; Donnelly, R. P.; Wynn, T. A. Unique Functions of the Type II Interleukin 4 Receptor Identified in Mice Lacking the Interleukin 13 Receptor A1 Chain. *Nat. Immunol.* **2008**, *9*, 25–33. <https://doi.org/10.1038/ni1544>.
- [62] Arandjelovic, S.; Ravichandran, K. S. Phagocytosis of Apoptotic Cells in Homeostasis. *Nat Immunol* **2015**, *16*, 907–917. <https://doi.org/10.1038/ni.3253>. Phagocytosis.
- [63] Metchnikoff, E. Lecture of the Comparative of Pathology in Inflammation. **1992**, No. d, 409–412.
- [64] Tauber, A. I. Metchnikoff and the Phagocytosis Theory. **2003**, *4*.
- [65] Metchnikoff, E. Immunity in infective diseases <https://catalog.hathitrust.org/Record/001582230> (accessed Apr 15, 2020).
- [66] Gordon, S. Phagocytosis: The Legacy of Metchnikoff. *Cell* **2016**, *166*, 1065–1068. <https://doi.org/10.1016/j.cell.2016.08.017>.
- [67] Majno, G.; Joris, I. Apoptosis, Oncosis, and Necrosis: An Overview of Cell Death. *Am. J. Pathol.* **1995**, *146*, 3–15.
- [68] Gordon, S. Phagocytosis: An Immunobiologic Process. *Immunity* **2016**, *44*, 463–475. <https://doi.org/10.1016/j.immuni.2016.02.026>.
- [69] Freeman, S. A.; Grinstein, S. Phagocytosis : Receptors , Signal Integration , and the Cytoskeleton Integration , and the Cytoskeleton. *Immunol. Rev.* **2014**, *262*, 193–215. <https://doi.org/10.1111/imr.12212>.
- [70] Savill, J. S.; Henson, P. M.; Haslett, C. Phagocytosis of Aged Human Neutrophils by Macrophages Is Mediated by a Novel 'charge-Sensitive' recognition Mechanism. *J. Clin. Invest.* **1989**, *84*, 1518–1527. <https://doi.org/10.1172/JCI114328>.
- [71] Janeway, C. a; Medzhitov, R. Innate Immune Recognition. *Annu. Rev. Immunol.* **2002**, *20*, 197–216. <https://doi.org/10.1146/annurev.immunol.20.083001.084359>.
- [72] Abbas, A. K.; Lichtman, A. H.; Pillai, S.; Baker, D. L. Cellular and Molecular Immunology. *Elsevier* **2017**, *9*, 267–301. <https://doi.org/10.1016/B978-1-4160-3123-9.50020-6>.
- [73] Elliott, M. R.; Ravichandran, K. S. Clearance of Apoptotic Cells: Implications in Health and Disease. *J. Cell Biol.* **2010**, *189*, 1059–1070. <https://doi.org/10.1083/jcb.201004096>.

- [74] Paul, D.; Achouri, S.; Yoon, Y. Z.; Herre, J.; Bryant, C. E.; Cicuta, P. Phagocytosis Dynamics Depends on Target Shape. *Biophys. J.* **2013**, *105*, 1143–1150. <https://doi.org/10.1016/j.bpj.2013.07.036>.
- [75] Rosales, C.; Uribe-Querol, E. Phagocytosis: A Fundamental Process in Immunity. *Biomed Res. Int.* **2017**, *2017*, 1–18. <https://doi.org/10.1155/2017/9042851>.
- [76] Bosurgi, L.; Hughes, L. D.; Rothlin, C. V.; Ghosh, S. Death Begets a New Beginning. *Immunol. Rev.* **2017**, *280*, 8–25. <https://doi.org/10.1111/jmr.12585>.
- [77] Gregory, C. D.; Brown, S. B. Apoptosis: Eating Sensibly. *Nat. Cell Biol.* **2005**, *7*, 1061–1063. <https://doi.org/10.1038/ncb1205-1061>.
- [78] Grimsley, C.; Ravichandran, K. S. Cues for Apoptotic Cell Engulfment: Eat-Me, Don't Eat-Me and Come-Get-Me Signals. *Trends Cell Biol.* **2003**, *13*, 648–656. <https://doi.org/10.1016/j.tcb.2003.10.004>.
- [79] Krysko, D. V.; Ravichandran, K. S.; Vandenabeele, P. Macrophages Regulate the Clearance of Living Cells by Calreticulin. *Nat. Commun.* **2018**, *9*, 9–11. <https://doi.org/10.1038/s41467-018-06807-9>.
- [80] Fadok, V. A.; Voelker, D. R.; Campbell, P. A.; Cohen, J. J.; Bratton, D. L.; Henson, P. M. Exposure of Phosphatidylserine on the Surface of Apoptotic Lymphocytes Triggers Specific Recognition and Removal by Macrophages. *J. Immunol.* **1992**, *148*, 2207–2216.
- [81] Lai, C.; Lemke, G. An Extended Family of Protein-Tyrosine Kinase Genes Differentially Expressed in the Vertebrate Nervous System. *Neuron* **1991**, *6*, 691–704. [https://doi.org/10.1016/0896-6273\(91\)90167-X](https://doi.org/10.1016/0896-6273(91)90167-X).
- [82] Nishi, C.; Toda, S.; Segawa, K.; Nagata, S. Tim4- and MerTK-Mediated Engulfment of Apoptotic Cells by Mouse Resident Peritoneal Macrophages. *Mol. Cell. Biol.* **2014**, *34*, 1512–1520. <https://doi.org/10.1128/mcb.01394-13>.
- [83] Yanagihashi, Y.; Segawa, K.; Maeda, R.; Nabeshima, Y. ichi; Nagata, S. Mouse Macrophages Show Different Requirements for Phosphatidylserine Receptor Tim4 in Efferocytosis. *Proc. Natl. Acad. Sci. U. S. A.* **2017**, *114*, 8800–8805. <https://doi.org/10.1073/pnas.1705365114>.
- [84] Nagata, S. Apoptosis and Clearance of Apoptotic Cells. *Annu. Rev. Immunol.* **2018**, *36*, 489–517. <https://doi.org/10.1146/annurev-immunol-042617-053010>.
- [85] Zagórska, P. G.; Lew, E. D.; Dransfield, I.; Lemke, G. Diversification of TAM Receptor Function. *Nat Immunol* **2014**, *15*, 920–928. <https://doi.org/10.1038/ni.2986>.
- [86] Rothlin, C. V.; Carrera-Silva, E. A.; Bosurgi, L.; Ghosh, S. TAM Receptor Signaling in Immune Homeostasis. *Annu. Rev. Immunol.* **2015**, *33*, 355–391. <https://doi.org/10.1146/annurev-immunol-032414-112103>.
- [87] Zagórska, A.; Través, P. G.; Jiménez-García, L.; Strickland, J. D.; Oh, J.; Tapia, F. J.; Mayoral, R.; Burrola, P.; Copple, B. L.; Lemke, G. Differential Regulation of Hepatic Physiology and Injury by the TAM Receptors Axl and Mer. *Life Sci. Alliance* **2020**, *3*, e20200694 1-15. <https://doi.org/10.26508/LSA.20200694>.
- [88] Subramanian, M.; Hayes, C. D.; Thome, J. J.; Thorp, E.; Matsushima, G. K.; Herz, J.; Farber, D. L.; Liu, K.; Lakshmana, M.; Tabas, I. An AXL/LRP-1/RANBP9 Complex Mediates DC Efferocytosis and Antigen Cross-Presentation in Vivo. *J. Clin. Invest.* **2014**, *124*, 1296–1308. <https://doi.org/10.1172/JCI72051>.
- [89] A-Gonzalez, N.; Bensinger, S. J.; Hong, C.; Beceiro, S.; Bradley, M. N.; Zelcer, N.; Deniz, J.; Ramirez, C.; Díaz, M.; Gallardo, G.; Ruiz de Galarreta, C.; Salazar, J.; Lopez, F.; Edwards, P.; Parks, J.; Andujar, M.; Tontonoz, P.; Castrillo, A. Apoptotic Cells Promote Their Own Clearance and Immune Tolerance through Activation of the Nuclear Receptor LXR. *Immunity* **2009**, *31*, 245–258. <https://doi.org/10.1016/j.immuni.2009.06.018>.
- [90] Rahman, Z. S. M.; Shao, W.-H.; Khan, T. N.; Zhen, Y.; Cohen, P. L. Impaired Apoptotic Cell Clearance in the Germinal Center by Mer-Deficient Tingible Body Macrophages Leads to Enhanced Antibody-Forming Cell and Germinal Center Responses. *J. Immunol.* **2010**, *185*, 5859–5868. <https://doi.org/10.4049/jimmunol.1001187>.
- [91] Bosurgi, L.; Cao, Y. G.; Cabeza-Cabrerizo, M.; Tucci, A.; Hughes, L. D.; Kong, Y.; Weinstein, J. S.;

- Licon-Limon, P.; Schmid, E. T.; Pelorosso, F.; Gagliani, N.; Craft, J. E.; Flavell, R. A.; Ghosh, S.; Rothlin, C. V. Macrophage Function in Tissue Repair and Remodeling Requires IL-4 or IL-13 with Apoptotic Cells. *Science* (80-.). **2017**, *356*, 1072–1076. <https://doi.org/10.1126/science.aai8132>.
- [92] BioRender. Created with BioRender.com.
- [93] Voll, R. E.; Herrmann, M.; Roth, E. A.; Stach, C.; Kalden, J. R.; Girkontaite, I. Immunosuppressive Effects of Apoptotic Cells. *Nature* **1997**, *390*, 350–351. <https://doi.org/10.1038/37022>.
- [94] A-Gonzalez, N.; Quintana, J. A.; García-Silva, S.; Mazariegos, M.; González de la Aleja, A.; Nicolás-Ávila, J. A.; Walter, W.; Adrover, J. M.; Crainiciuc, G.; Kuchroo, V. K.; Rothlin, C. V.; Peinado, H.; Castrillo, A.; Ricote, M.; Hidalgo, A.; de la Aleja, A. G.; Nicolás-Ávila, J. A.; Walter, W.; Adrover, J. M.; Crainiciuc, G.; Kuchroo, V. K.; Rothlin, C. V.; Peinado, H.; Castrillo, A.; Ricote, M.; Hidalgo, A. Phagocytosis Imprints Heterogeneity in Tissue-Resident Macrophages. *J. Exp. Med.* **2017**, *214*, 1281–1296. <https://doi.org/10.1084/jem.20161375>.
- [95] Murphy, P. S.; Wang, J.; Bhagwat, S. P.; Munger, J. C.; Janssen, W. J.; Wright, T. W.; Elliott, M. R. CD73 Regulates Anti-Inflammatory Signaling between Apoptotic Cells and Endotoxin-Conditioned Tissue Macrophages. *Cell Death Differ.* **2017**, *24*, 559–570. <https://doi.org/10.1038/cdd.2016.159>.
- [96] Antonioli, L.; Pacher, P.; Vizi, E. S.; Haskó, G. CD39 and CD73 in Immunity and Inflammation. *Trends Mol. Med.* **2016**, *19*, 355–367. <https://doi.org/10.1016/j.molmed.2013.03.005>.
- [97] Cohen, H. B.; Briggs, K. T.; Marino, J. P.; Ravid, K.; Robson, S. C.; Mosser, D. M. TLR Stimulation Initiates a CD39-Based Autoregulatory Mechanism That Limits Macrophage Inflammatory Responses. *Blood* **2013**, *122*, 1935–1945. <https://doi.org/10.1182/blood-2013-04-496216>.
- [98] Tibrewal, N.; Wu, Y.; D’Mello, V.; Akakura, R.; George, T. C.; Varnum, B.; Birge, R. B. Autophosphorylation Docking Site Tyr-867 in Mer Receptor Tyrosine Kinase Allows for Dissociation of Multiple Signaling Pathways for Phagocytosis of Apoptotic Cells and down-Modulation of Lipopolysaccharide-Inducible NF-KB Transcriptional Activation. *J. Biol. Chem.* **2008**, *283*, 3618–3627. <https://doi.org/10.1074/jbc.M706906200>.
- [99] Golpon, H. A.; Fadok, V. A.; Taraseviciene-Stewart, L.; Scerbavicius, R.; Sauer, C.; Welte, T.; Henson, P. M.; Voelkel, N. F. Life after Corpse Engulfment: Phagocytosis of Apoptotic Cells Leads to VEGF Secretion and Cell Growth. *FASEB J.* **2004**, *18*, 1716–1718. <https://doi.org/10.1096/fj.04-1853fje>.
- [100] Fadok, V. A.; Bratton, D. L.; Konowal, A.; Freed, P. W.; Westcott, J. Y.; Henson, P. M.; Bratton, D. L.; Konowal, A.; Freed, P. W.; Westcott, J. Y.; Henson, P. M. Macrophages That Have Ingested Apoptotic Cells in Vitro Inhibit Proinflammatory Cytokine Production through Autocrine/Paracrine Mechanisms Involving TGF- β , PGE₂, and PAF. *J. Clin. Invest.* **1998**, *101*, 890–898. <https://doi.org/10.1172/JCI1112>.
- [101] Szondy, Z.; Sarang, Z.; Kiss, B.; Garabuczi, É.; Köröskényi, K. Anti-Inflammatory Mechanisms Triggered by Apoptotic Cells during Their Clearance. *Front. Immunol.* **2017**, *8*, 909–919. <https://doi.org/10.3389/fimmu.2017.00909>.
- [102] Huynh, M.-L. N.; Fadok, V. A.; Henson, P. M. Phosphatidylserine-Dependent Ingestion of Apoptotic Cells Promotes TGF-B1 Secretion and the Resolution of Inflammation. *J. Clin. Invest.* **2002**, *109*, 41–50. <https://doi.org/10.1172/jci200211638>.
- [103] Szondy, Z.; Garabuczi, É.; Joós, G.; Tsay, G. J.; Sarang, Z. Impaired Clearance of Apoptotic Cells in Chronic Inflammatory Diseases: Therapeutic Implications. *Front. Immunol.* **2014**, *5*. <https://doi.org/10.3389/fimmu.2014.00354>.
- [104] Hughes, L. D.; Bosurgi, L.; Ghosh, S.; Rothlin, C. V. Chronicles of Cell Death Foretold: Specificities in the Mechanism of Disposal. *Front. Immunol.* **2017**, *8*, 1–8. <https://doi.org/10.3389/fimmu.2017.01743>.
- [105] Nagata, S.; Hanayama, R.; Kawane, K. Autoimmunity and the Clearance of Dead Cells. *Cell* **2010**, *140*, 619–630. <https://doi.org/10.1016/j.cell.2010.02.014>.
- [106] Barclay, A. N.; van den Berg, T. K. The Interaction Between Signal Regulatory Protein Alpha (SIRP α) and CD47: Structure, Function, and Therapeutic Target. *Annu. Rev. Immunol.* **2014**,

- 32, 25–50. <https://doi.org/10.1146/annurev-immunol-032713-120142>.
- [107] Zhao, X. W.; Van Beek, E. M.; Schornagel, K.; Van Der Maaden, H.; Van Houdt, M.; Otten, M. A.; Finetti, P.; Van Egmond, M.; Matozaki, T.; Kraal, G.; Birnbaum, D.; Van Elsas, A.; Kuijpers, T. W.; Bertucci, F.; Van Den Berg, T. K. CD47-Signal Regulatory Protein- α (SIRP α) Interactions Form a Barrier for Antibody-Mediated Tumor Cell Destruction. *Proc. Natl. Acad. Sci. U. S. A.* **2011**, *108*, 18342–18347. <https://doi.org/10.1073/pnas.1106550108>.
- [108] Lv, Z.; Bian, Z.; Shi, L.; Niu, S.; Ha, B.; Tremblay, A.; Li, L.; Zhang, X.; Paluszynski, J.; Liu, M.; Zen, K.; Liu, Y. Loss of Cell Surface CD47 Clustering Formation and Binding Avidity to SIRP α Facilitate Apoptotic Cell Clearance by Macrophages. *J. Immunol.* **2015**, *195*, 661–671. <https://doi.org/10.4049/jimmunol.1401719>.
- [109] Kerr, J. F. R.; Wyllie, A. H.; Curriet, A. R. Apoptosis: A Basic Biological Phenomenon with Wideranging Implications in Tissue Kinetics. *Br. J. Cancer* **1972**, *26*, 239.
- [110] Häcker, G. Apoptosis in Infection. *Microbes Infect.* **2018**, *20*, 552–559. <https://doi.org/10.1016/j.micinf.2017.10.006>.
- [111] Henson, P. M.; Bratton, D. L.; Fadok, V. A. Apoptotic Cell Removal. *Curr. Biol.* **2001**, *11*, 795–805. [https://doi.org/10.1016/S0960-9822\(01\)00474-2](https://doi.org/10.1016/S0960-9822(01)00474-2).
- [112] Saraste, A.; Pulkki, K. Morphologic and Biochemical Hallmarks of Apoptosis. *Cardiovasc. Res.* **2000**, *45*, 528–537.
- [113] Wyllie, A. H.; Morris, R. G.; Smith, A. L.; Dunlop, D. Chromatin Cleavage in Apoptosis: Association with Condensed Chromatin Morphology and Dependence on Macromolecular Synthesis. *J. Pathol.* **1984**, *142*, 67–77. <https://doi.org/10.1002/path.1711420112>.
- [114] Morris, R. G.; Hargreaves, A. D.; Duvall, E.; Wyllie, A. H. Hormone-Induced Cell Death: 2. Surface Changes in Thymocytes Undergoing Apoptosis. *Am. J. Pathol.* **1984**, *115*, 426–436.
- [115] Creagh, E. M.; Conroy, H.; Martin, S. J. Caspase-Activation Pathways in Apoptosis and Immunity. *Immunol. Rev.* **2003**, *193*, 10–21. <https://doi.org/10.1034/j.1600-065X.2003.00048.x>.
- [116] Fulda, S.; Debatin, K. M. Extrinsic versus Intrinsic Apoptosis Pathways in Anticancer Chemotherapy. *Oncogene* **2006**, *25*, 4798–4811. <https://doi.org/10.1038/sj.onc.1209608>.
- [117] Loreto, C.; La Rocca, G.; Anzalone, R.; Caltabiano, R.; Vespasiani, G.; Castorina, S.; Ralph, D. J.; Celtek, S.; Musumeci, G.; Giunta, S.; Djinic, R.; Basic, D.; Sansalone, S. The Role of Intrinsic Pathway in Apoptosis Activation and Progression in Peyronie’s Disease. *Biomed Res. Int.* **2014**, *2014*. <https://doi.org/10.1155/2014/616149>.
- [118] Elmore, S. Apoptosis: A Review of Programmed Cell Death. *Toxicol. Pathol.* **2007**, *35*, 495–516. <https://doi.org/10.1080/01926230701320337>.
- [119] Walczak, H.; Krammer, P. H. The CD95 (APO-1/Fas) and the TRAIL (APO-2L) Apoptosis Systems. *Exp. Cell Res.* **2000**, *256*, 58–66. <https://doi.org/10.1006/excr.2000.4840>.
- [120] Scaffidi, C.; Fulda, S.; Srinivasan, A.; Friesen, C.; Li, F.; Tomaselli, K. J.; Debatin, K. M.; Krammer, P. H.; Peter, M. E. Two CD95 (APO-1/Fas) Signaling Pathways. *EMBO J.* **1998**, *17*, 1675–1687. <https://doi.org/10.1093/emboj/17.6.1675>.
- [121] Segawa, K.; Kurata, S.; Yanagihashi, Y.; Brummelkamp, T. R.; Matsuda, F.; Nagata, S. Caspase-Mediated Cleavage of Phospholipid Flippase for Apoptotic Phosphatidylserine Exposure. *Science (80-.)*. **2014**, *344*, 1164–1168. <https://doi.org/10.1126/science.1252809>.
- [122] Bienvenu, A. L.; Gonzalez-Rey, E.; Picot, S. Apoptosis Induced by Parasitic Diseases. *Parasites and Vectors* **2010**, *3*, 106. <https://doi.org/10.1186/1756-3305-3-106>.
- [123] Klotz, C.; Frevert, U. Plasmodium Yoelii Sporozoites Modulate Cytokine Profile and Induce Apoptosis in Murine Kupffer Cells. *Int. J. Parasitol.* **2008**, *38*, 1639–1650. <https://doi.org/10.1016/j.ijpara.2008.05.018>.
- [124] WHO. Schistosomiasis-WHO Report <https://www.who.int/news-room/fact-sheets/detail/schistosomiasis> (accessed Jan 11, 2021).
- [125] WHO. Schistosomiasis. *World Heal. Organ.* **2020**.
- [126] WHO. WHO | Schistosomiasis <https://www.who.int/schistosomiasis/en/> (accessed Apr 29, 2020).
- [127] Hams, E.; Aviello, G.; Fallon, P. G. The Schistosoma Granuloma: Friend or Foe? *Front. Immunol.*

- 2013**, *4*, 1–8. <https://doi.org/10.3389/fimmu.2013.00089>.
- [128] Siqueira, L. da P.; Fontes, D. A. F.; Aguilera, C. S. B.; Timóteo, T. R. R.; Ângelos, M. A.; Silva, L. C. P. B. B.; de Melo, C. G.; Rolim, L. A.; da Silva, R. M. F.; Neto, P. J. R. Schistosomiasis: Drugs Used and Treatment Strategies. *Acta Trop.* **2017**, *176*, 179–187. <https://doi.org/10.1016/j.actatropica.2017.08.002>.
- [129] Schwartz, C.; Fallon, P. G. Schistosoma “Eggs-Iting” the Host: Granuloma Formation and Egg Excretion. *Front. Immunol.* **2018**, *9*, 2492. <https://doi.org/10.3389/fimmu.2018.02492>.
- [130] Nelwan, M. L. Schistosomiasis: Life Cycle, Diagnosis, and Control. *Curr. Ther. Res.* **2019**, *91*, 5–9. <https://doi.org/10.1016/j.curtheres.2019.06.001>.
- [131] Schwartz, C.; Fallon, P. G. Schistosoma “Eggs-Iting” the Host: Granuloma Formation and Egg Excretion. *Front. Immunol.* **2018**, *9*, 2492. <https://doi.org/10.3389/fimmu.2018.02492>.
- [132] Burke, M. L.; Jones, M. K.; Gobert, G. N.; Li, Y. S.; Ellis, M. K.; McManus, D. P. Immunopathogenesis of Human Schistosomiasis. *Parasite Immunol.* **2009**, *31*, 163–176. <https://doi.org/10.1111/j.1365-3024.2009.01098.x>.
- [133] Nono, J. K.; Ndlovu, H.; Aziz, N. A.; Mpotje, T.; Hlaka, L.; Brombacher, F. Host Regulation of Liver Fibroproliferative Pathology during Experimental Schistosomiasis via Interleukin-4 Receptor Alpha. *PLoS Negl. Trop. Dis.* **2017**, *11*. <https://doi.org/10.1371/journal.pntd.0005861>.
- [134] Gagea, M.; Yan, J.; Satelli, A.; Mitra, A.; Mishra, L.; Xueqing, X.; Hunter, C. A.; Li, S. IL-30 (IL27p28) Attenuates Liver Fibrosis through Inducing NKG2D-Rae1 Interaction between NKT and Activated Hepatic Stellate Cells in Mice. *Hepatology* **2014**, *60*, 2027–2039. <https://doi.org/10.1002/hep.27392>.
- [135] An, P.; Wei, L. L.; Zhao, S.; Sverdlov, D. Y.; Vaid, K. A.; Miyamoto, M.; Kuramitsu, K.; Lai, M.; Popov, Y. V. Hepatocyte Mitochondria-Derived Danger Signals Directly Activate Hepatic Stellate Cells and Drive Progression of Liver Fibrosis. *Nat. Commun.* **2020**, *11*, 2362. <https://doi.org/10.1038/s41467-020-16092-0>.
- [136] Costain, A. H.; MacDonald, A. S.; Smits, H. H. Schistosome Egg Migration: Mechanisms, Pathogenesis and Host Immune Responses. *Front. Immunol.* **2018**, *9*, 3042. <https://doi.org/10.3389/fimmu.2018.03042>.
- [137] Kumkate, S.; Jenkins, G. R.; Paveley, R. A.; Hogg, K. G.; Mountford, A. P. CD207+ Langerhans Cells Constitute a Minor Population of Skin-Derived Antigen-Presenting Cells in the Draining Lymph Node Following Exposure to Schistosoma Mansoni. *Int. J. Parasitol.* **2007**, *37*, 209–220. <https://doi.org/10.1016/j.ijpara.2006.10.007>.
- [138] Paveley, R. A.; Aynsley, S. A.; Turner, J. D.; Bourke, C. D.; Jenkins, S. J.; Cook, P. C.; Martinez-Pomares, L.; Mountford, A. P. The Mannose Receptor (CD206) Is an Important Pattern Recognition Receptor (PRR) in the Detection of the Infective Stage of the Helminth Schistosoma Mansoni and Modulates IFN γ Production. *Int. J. Parasitol.* **2011**, *41*, 1335–1345. <https://doi.org/10.1016/j.ijpara.2011.08.005>.
- [139] Cook, P. C.; Aynsley, S. A.; Turner, J. D.; Jenkins, G. R.; Van Rooijen, N. Multiple Helminth Infection of the Skin Causes Lymphocyte Hypo-Responsiveness Mediated by Th2 Conditioning of Dermal Myeloid Cells. *PLoS Pathog* **2011**, *7*, 1001323. <https://doi.org/10.1371/journal.ppat.1001323>.
- [140] Von Lichtenberg, F.; Sher, A.; McIntyre, S. A Lung Model of Schistosome Immunity in Mice. *Am. J. Pathol.* **1977**, *87*, 105–124.
- [141] Torben, W.; Ahmad, G.; Zhang, W.; Nash, S.; Le, L.; Karmakar, S.; Siddiqui, A. A. Role of Antibody Dependent Cell Mediated Cytotoxicity (ADCC) in Sm-P80-Mediated Protection against Schistosoma Mansoni. *Vaccine* **2012**, *30*, 6753–6758. <https://doi.org/10.1016/j.vaccine.2012.09.026>.
- [142] Ariyaratne, A.; Finney, C. A. M. Eosinophils and Macrophages within the Th2-Induced Granuloma: Balancing Killing and Healing in a Tight Space. *Infect. Immun.* **2019**, *87*. <https://doi.org/10.1128/IAI.00127-19>.
- [143] Peng, H.; Zhang, Q.; Li, X.; Liu, Z.; Shen, J.; Sun, R.; Wei, J.; Zhao, J.; Wu, X.; Feng, F.; Zhong, S.; Sun, X.; Wu, Z. IL-33 Contributes to Schistosoma Japonicum-Induced Hepatic Pathology through

- Induction of M2 Macrophages. *Sci. Rep.* **2016**, *6*, 1–11. <https://doi.org/10.1038/srep29844>.
- [144] Souza, C. O. S.; Gardinassi, L. G.; Rodrigues, V.; Faccioli, L. H. Monocyte and Macrophage-Mediated Pathology and Protective Immunity During Schistosomiasis. *Front. Microbiol.* **2020**, *11*, 9. <https://doi.org/10.3389/fmicb.2020.01973>.
- [145] Nascimento, M.; Huang, S. C.; Smith, A.; Everts, B.; Lam, W.; Bassity, E.; Gautier, E. L.; Randolph, G. J.; Pearce, E. J. Ly6Chi Monocyte Recruitment Is Responsible for Th2 Associated Host-Protective Macrophage Accumulation in Liver Inflammation Due to Schistosomiasis. *PLoS Pathog.* **2014**, *10*, e1004282. <https://doi.org/10.1371/journal.ppat.1004282>.
- [146] Fernandes, J. S.; Araujo, M. I.; Lopes, D. M.; Da Paixão De Souza, R.; Carvalho, E. M.; Santos Cardoso, L. Monocyte Subsets in Schistosomiasis Patients with Periportal Fibrosis. **2014**. <https://doi.org/10.1155/2014/703653>.
- [147] Borthwick, L. A.; Barron, L.; Hart, K. M.; Vannella, K. M.; Thompson, R. W.; Oland, S.; Cheever, A.; Sciruba, J.; Ramalingam, T. R.; Fisher, A. J.; Wynn, T. A. Macrophages Are Critical to the Maintenance of IL-13-Dependent Lung Inflammation and Fibrosis. *Mucosal Immunol.* **2016**. <https://doi.org/10.1038/mi.2015.34>.
- [148] Herbert, D. R.; Orekov, T.; Roloson, A.; Ilies, M.; Perkins, C.; O'Brien, W.; Cederbaum, S.; Christianson, D. W.; Zimmermann, N.; Rothenberg, M. E.; Finkelman, F. D. Arginase I Suppresses IL-12/IL-23p40-Driven Intestinal Inflammation during Acute Schistosomiasis. *J. Immunol.* **2010**, *184*, 6438–6446. <https://doi.org/10.4049/jimmunol.0902009>.
- [149] Pesce, J. T.; Ramalingam, T. R.; Mentink-Kane, M. M.; Wilson, M. S.; Kasmi, K. C. E.; Smith, A. M.; Thompson, R. W.; Cheever, A. W.; Murray, P. J.; Wynn, T. A. Arginase-1-Expressing Macrophages Suppress Th2 Cytokine-Driven Inflammation and Fibrosis. *PLoS Pathog.* **2009**, *5*, e1000371. <https://doi.org/10.1371/journal.ppat.1000371>.
- [150] Nair, M. G.; Du, Y.; Perrigoue, J. G.; Zaph, C.; Taylor, J. J.; Goldschmidt, M.; Swain, G. P.; Yancopoulos, G. D.; Valenzuela, D. M.; Murphy, A.; Karow, M.; Stevens, S.; Pearce, E. J.; Artis, D. Alternatively Activated Macrophage-Derived RELM- α Is a Negative Regulator of Type 2 Inflammation in the Lung. *J. Exp. Med.* **2009**, *206*, 937–952. <https://doi.org/10.1084/jem.20082048>.
- [151] Kaviratne, M.; Hesse, M.; Leusink, M.; Cheever, A. W.; Davies, S. J.; McKerrow, J. H.; Wakefield, L. M.; Letterio, J. J.; Wynn, T. A. IL-13 Activates a Mechanism of Tissue Fibrosis That Is Completely TGF- β Independent. *J. Immunol.* **2004**, *173*, 4020–4029. <https://doi.org/10.4049/jimmunol.173.6.4020>.
- [152] Mutengo, M. M.; Mduluzza, T.; Kelly, P.; Mwansa, J. C. L.; Kwenda, G.; Musonda, P.; Chipeta, J. Low IL-6, IL-10, and TNF- α and High IL-13 Cytokine Levels Are Associated with Severe Hepatic Fibrosis in *Schistosoma mansoni* Chronically Exposed Individuals. *J. Parasitol. Res.* **2018**, *2018*. <https://doi.org/10.1155/2018/9754060>.
- [153] Herbert, D. R.; Orekov, T.; Perkins, C.; Rothenberg, M. E.; Finkelman, F. D. IL-4R α Expression by Bone Marrow-Derived Cells Is Necessary and Sufficient for Host Protection against Acute Schistosomiasis. *J. Immunol.* **2008**, *180*, 4948–4955. <https://doi.org/10.4049/jimmunol.180.7.4948>.
- [154] Herbert, D. R.; Hölscher, C.; Mohrs, M.; Arendse, B.; Schwegmann, A.; Radwanska, M.; Leeto, M.; Kirsch, R.; Hall, P.; Mossmann, H.; Claussen, B.; Förster, I.; Brombacher, F. Alternative Macrophage Activation Is Essential for Survival during Schistosomiasis and Downmodulates T Helper 1 Responses and Immunopathology. *Immunity* **2004**, *20*, 623–635. [https://doi.org/10.1016/S1074-7613\(04\)00107-4](https://doi.org/10.1016/S1074-7613(04)00107-4).
- [155] Vannella, K. M.; Barron, L.; Borthwick, L. A.; Kindrachuk, K. N.; Narasimhan, P. B.; Hart, K. M.; Thompson, R. W.; White, S.; Cheever, A. W.; Ramalingam, T. R.; Wynn, T. Incomplete Deletion of IL-4R α by LysMCre Reveals Distinct Subsets of M2 Macrophages Controlling Inflammation and Fibrosis in Chronic Schistosomiasis. *PLoS Pathog.* **2014**, *10*. <https://doi.org/10.1371/journal.ppat.1004372>.
- [156] Barron, L.; Wynn, T. A. Macrophage Activation Governs Schistosomiasis-Induced Inflammation and Fibrosis. *Eur. J. Immunol.* **2011**, *41*, 2509–2514. <https://doi.org/10.1002/eji.201141869>.

- [157] Sanin, D. E.; Mountford, A. P. Sm16, a Major Component of *Schistosoma Mansoni* Cercarial Excretory/Secretory Products, Prevents Macrophage Classical Activation and Delays Antigen Processing. *Parasites and Vectors* **2015**, *8*, 1. <https://doi.org/10.1186/s13071-014-0608-1>.
- [158] Hesse, M.; Piccirillo, C. A.; Belkaid, Y.; Prufer, J.; Mentink-Kane, M.; Leusink, M.; Cheever, A. W.; Shevach, E. M.; Wynn, T. A. The Pathogenesis of Schistosomiasis Is Controlled by Cooperating IL-10-Producing Innate Effector and Regulatory T Cells. *J. Immunol.* **2004**, *172*, 3157–3166. <https://doi.org/10.4049/jimmunol.172.5.3157>.
- [159] Kamdem, S. D.; Moyou-Somo, R.; Brombacher, F.; Nono, J. K. Host Regulators of Liver Fibrosis during Human Schistosomiasis. *Front. Immunol.* **2018**, *9*, 2781. <https://doi.org/10.3389/fimmu.2018.02781>.
- [160] Oliveira, S. C.; Sehrawat, S.; Stadecker, M. J.; Gong, Q.; Liu, C.; Zheng, B.; Zhang, J.; Chen, H.; Nie, H.; Miller, H. T Lymphocyte-Mediated Liver Immunopathology of Schistosomiasis. *Front. Immunol. | www.frontiersin.org* **2020**, *11*, 61. <https://doi.org/10.3389/fimmu.2020.00061>.
- [161] Girgis, N. M.; Gundra, U. M.; Ward, L. N.; Cabrera, M.; Frevert, U.; Loke, P. Ly6Chigh Monocytes Become Alternatively Activated Macrophages in Schistosome Granulomas with Help from CD4+ Cells. *PLoS Pathog.* **2014**, *10*. <https://doi.org/10.1371/journal.ppat.1004080>.
- [162] de Souza, V. C. A.; Moura, D. M. N.; de Castro, M. C. A. B.; Bozza, P. T.; de Almeida Paiva, L.; Fernandes, C. J. B.; Leão, R. L. C.; Lucena, J. P.; de Araujo, R. E.; de Melo Silva, A. J.; Figueiredo, R. C. B. Q.; de Oliveira, S. A. Adoptive Transfer of Bone Marrow-Derived Monocytes Ameliorates *Schistosoma Mansoni* -Induced Liver Fibrosis in Mice. *Sci. Rep.* **2019**, *9*, 1–11. <https://doi.org/10.1038/s41598-019-42703-y>.
- [163] Souza, C. O. S.; Espíndola, M. S.; Fontanari, C.; Prado, M. K. B.; Frantz, F. G.; Rodrigues, V.; Gardinassi, L. G.; Faccioli, L. H. CD18 Regulates Monocyte Hematopoiesis and Promotes Resistance to Experimental Schistosomiasis. *Front. Immunol.* **2018**, *9*, 1970. <https://doi.org/10.3389/fimmu.2018.01970>.
- [164] Wolde, M.; Laan, L. C.; Medhin, G.; Gadissa, E.; Berhe, N.; Tsegaye, A. Human Monocytes/Macrophage Inflammatory Cytokine Changes Following in Vivo and in Vitro *Schistosoma Mansoni* Infection. *J. Inflamm. Res.* **2020**, *13*, 35–43. <https://doi.org/10.2147/JIR.S233381>.
- [165] Rolot, M.; Dougall, A. M.; Javaux, J.; Lallemand, F.; Machiels, B.; Martinive, P.; Gillet, L.; Dewals, B. G.; M. Dougall, A.; Javaux, J.; Lallemand, F.; Machiels, B.; Martinive, P.; Gillet, L.; Dewals, B. G. Recruitment of Hepatic Macrophages from Monocytes Is Independent of IL-4R α but Is Associated with Ablation of Resident Macrophages in Schistosomiasis. *Eur. J. Immunol.* **2019**, *49*, 1067–1081. <https://doi.org/10.1002/eji.201847796>.
- [166] Carneiro-Santos, P.; Martins-Filho, O.; Alves-Oliveira, L. F.; Silveira, A. M. S.; Coura-Filho, P.; Viana, I. R. C.; Wilson, R. A.; Correa-Oliveira, R. Apoptosis: A Mechanism of Immunoregulation during Human Schistosomiasis *Mansoni*. *Parasite Immunol.* **2000**, *22*, 267–277. <https://doi.org/10.1046/j.1365-3024.2000.00294.x>.
- [167] Fallon, G. P.; Smith, P.; Dunne, D. W. Type 1 and Type 2 Cytokine-Producing CD4+ and CD8+ T Cells in Primary Antiphospholipid Syndrome. *Eur. J. Immunol.* **1998**, *28*, 1408–1416. <https://doi.org/10.1007/s00277-004-0910-7>.
- [168] Lundy, S. K.; Lerman, S. P.; Boros, D. L. Soluble Egg Antigen-Stimulated T Helper Lymphocyte Apoptosis and Evidence for Cell Death Mediated by FasL+ T and B Cells during Murine *Schistosoma Mansoni* Infection. *Infect. Immun.* **2001**, *69*, 271–280. <https://doi.org/10.1128/IAI.69.1.271-280.2001>.
- [169] Nagata, S.; Suzuki, J.; Segawa, K.; Fujii, T. Exposure of Phosphatidylserine on the Cell Surface. *Cell Death Differ.* **2016**, *23*, 952–961. <https://doi.org/10.1038/cdd.2016.7>.
- [170] Arienti, S.; Barth, N. D.; Dorward, D. A.; Rossi, A. G.; Dransfield, I. Regulation of Apoptotic Cell Clearance during Resolution of Inflammation. *Front. Pharmacol.* **2019**, *10*, 1–12. <https://doi.org/10.3389/fphar.2019.00891>.
- [171] Lastrucci, C.; Baillif, V.; Behar, A.; Saati, T. Al; Dubourdeau, M.; Maridonneau-Parini, I.; Cougoule, C. Molecular and Cellular Profiles of the Resolution Phase in a Damage-associated

- Molecular Pattern (DAMP)-mediated Peritonitis Model and Revelation of Leukocyte Persistence in Peritoneal Tissues. *FASEB J.* **2015**, *29*, 1914–1929. <https://doi.org/10.1096/fj.14-259341>.
- [172] Bosurgi, L.; Cao, Y. G.; Cabeza-Cabrerizo, M.; Tucci, A.; Hughes, L. D.; Kong, Y.; Weinstein, J. S.; Licona-Limon, P.; Schmid, E. T.; Pelorosso, F.; Gagliani, N.; Craft, J. E.; Flavell, R. A.; Ghosh, S.; Rothlin, C. V. Macrophage Function in Tissue Repair and Remodeling Requires IL-4 or IL-13 with Apoptotic Cells. *Science* (80-.). **2017**, *356*, 1072–1076. <https://doi.org/10.1126/science.aai8132>.
- [173] Medina, C. B.; Mehrotra, P.; Arandjelovic, S.; Perry, J. S. A.; Guo, Y.; Morioka, S.; Barron, B.; Walk, S. F.; Ghesquière, B.; Krupnick, A. S.; Lorenz, U.; Ravichandran, K. S. Metabolites Released from Apoptotic Cells Act as Tissue Messengers. *Nature* **2020**, *580*, 130–135. <https://doi.org/10.1038/s41586-020-2121-3>.
- [174] Filardy, A. A.; Pires, D. R.; Nunes, M. P.; Takiya, C. M.; Freire-de-Lima, C. G.; Ribeiro-Gomes, F. L.; DosReis, G. A. Proinflammatory Clearance of Apoptotic Neutrophils Induces an IL-12 Low IL-10 High Regulatory Phenotype in Macrophages. *J. Immunol.* **2010**, *185*, 2044–2050. <https://doi.org/10.4049/jimmunol.1000017>.
- [175] Yang, H.; Biermann, M. H.; Brauner, J. M.; Liu, Y.; Zhao, Y.; Herrmann, M. New Insights into Neutrophil Extracellular Traps: Mechanisms of Formation and Role in Inflammation. *Front. Immunol.* **2016**, *7*, 1–8. <https://doi.org/10.3389/fimmu.2016.00302>.
- [176] Metzler, K. D.; Goosmann, C.; Lubojemska, A.; Zychlinsky, A.; Papayannopoulos, V. Myeloperoxidase-Containing Complex Regulates Neutrophil Elastase Release and Actin Dynamics during NETosis. *Cell Rep.* **2014**, *8*, 883–896. <https://doi.org/10.1016/j.celrep.2014.06.044>.
- [177] Björnsdóttir, H.; Welin, A.; Michaëlsson, E.; Osla, V.; Berg, S.; Christenson, K.; Sundqvist, M.; Dahlgren, C.; Karlsson, A.; Bylund, J. Neutrophil NET Formation Is Regulated from the inside by Myeloperoxidase-Processed Reactive Oxygen Species. *Free Radic. Biol. Med.* **2015**, *89*, 1024–1035. <https://doi.org/10.1016/j.freeradbiomed.2015.10.398>.
- [178] Lantz, C.; Radmanesh, B.; Liu, E.; Thorp, E. B.; Lin, J. Single-Cell RNA Sequencing Uncovers Heterogenous Transcriptional Signatures in Macrophages during Efferocytosis. *Sci. Rep.* **2020**, *10*, 1433. <https://doi.org/10.1038/s41598-020-70353-y>.
- [179] Campbell, L.; Saville, C. R.; Murray, P. J.; Cruickshank, S. M.; Hardman, M. J. Local Arginase 1 Activity Is Required for Cutaneous Wound Healing. *J. Invest. Dermatol.* **2013**, *133*, 2461–2470. <https://doi.org/10.1038/jid.2013.164>.
- [180] McCormick, S. M.; Heller, N. M. Regulation of Macrophage, Dendritic Cell, and Microglial Phenotype and Function by the SOCS Proteins. *Front. Immunol.* **2015**, *6*, 549. <https://doi.org/10.3389/fimmu.2015.00549>.
- [181] Jung, M.; Shim, S.; Im, Y. Bin; Park, W. Bin; Yoo, H. S. Global Gene-Expression Profiles of Intracellular Survival of the BruAb2-1031 Gene Mutated Brucella Abortus in Professional Phagocytes, RAW 264.7 Cells. *BMC Microbiol.* **2018**, *18*, 1–14. <https://doi.org/10.1186/s12866-018-1223-7>.
- [182] Goh, W.; Huntington, N. D. Regulation of Murine Natural Killer Cell Development. *Front. Immunol.* **2017**, *8*, 130. <https://doi.org/10.3389/fimmu.2017.00130>.
- [183] Rosales, C. Neutrophil: A Cell with Many Roles in Inflammation or Several Cell Types? *Front. Physiol.* **2018**, *9*, 113. <https://doi.org/10.3389/fphys.2018.00113>.
- [184] Elgueta, R.; Benson, M. J.; De Vries, V. C.; Wasiuk, A.; Guo, Y.; Noelle, R. J. Molecular Mechanism and Function of CD40/CD40L Engagement in the Immune System. *Immunol. Rev.* **2009**, *229*, 152–172. <https://doi.org/10.1111/j.1600-065X.2009.00782.x>.
- [185] Grabcic, A. M.; Goenka, A.; Fife, M. E.; Fujimori, T.; Hussell, T. Axl and MerTK Receptor Tyrosine Kinases Maintain Human Macrophage Efferocytic Capacity in the Presence of Viral Triggers. *Eur. J. Immunol.* **2018**, *48*, 855–860. <https://doi.org/10.1002/eji.201747283>.
- [186] Giannini, E. G.; Testa, R.; Savarino, V. Liver Enzyme Alteration: A Guide for Clinicians. *CMAJ* **2005**, *172*, 367–379. <https://doi.org/10.1503/cmaj.1040752>.
- [187] Singh, K. P.; Gerard, H. C.; Hudson, A. P.; Boros, D. L. Dynamics of Collagen, MMP and TIMP

- Gene Expression during the Granulomatous, Fibrotic Process Induced by *Schistosoma Mansoni* Eggs. *Ann. Trop. Med. Parasitol.* **2004**, *98*, 581–593. <https://doi.org/10.1179/000349804225021316>.
- [188] Giannandrea, M.; Parks, W. C. Diverse Functions of Matrix Metalloproteinases during Fibrosis. *DMM Disease Models and Mechanisms*, **2014**, *7*, 193–203. <https://doi.org/10.1242/dmm.012062>.
- [189] Jesus, R. De; Miranda, D. G.; Miranda, R. G.; Arau, M. I.; Jesus, A. A. De; Silva, A.; Santana, L. B.; Pearce, E.; Carvalho, E. M.; Mmun, I. N. I. Association of Type 2 Cytokines with Hepatic Fibrosis in Human *Schistosoma Mansoni* Infection. *Infect. Immun.* **2004**, *72*, 3391–3397. <https://doi.org/10.1128/IAI.72.6.3391>.
- [190] Turner, J. D.; Jenkins, G. R.; Hogg, K. G.; Aynsley, S. A.; Paveley, R. A.; Cook, P. C.; Coles, M. C.; Mountford, A. P. CD4+CD25+ Regulatory Cells Contribute to the Regulation of Colonic Th2 Granulomatous Pathology Caused by Schistosome Infection. *PLoS Negl. Trop. Dis.* **2011**, *5*. <https://doi.org/10.1371/journal.pntd.0001269>.
- [191] Horst, A. K.; Tiegs, G.; Diehl, L. Contribution of Macrophage Efferocytosis to Liver Homeostasis and Disease. *Front. Immunol.* **2019**, *10*, 2670–2683. <https://doi.org/10.3389/fimmu.2019.02670>.
- [192] Viola, A.; Munari, F.; Sánchez-Rodríguez, R.; Scolaro, T.; Castegna, A. The Metabolic Signature of Macrophage Responses. *Front. Immunol.* **2019**, *10*, 1–16. <https://doi.org/10.3389/fimmu.2019.01462>.
- [193] Zumerle, S.; Cali, B.; Munari, F.; Angioni, R.; Di Virgilio, F.; Molon, B.; Viola, A. Intercellular Calcium Signaling Induced by ATP Potentiates Macrophage Phagocytosis. *Cell Rep.* **2019**, *27*, 1–10.e4. <https://doi.org/10.1016/j.celrep.2019.03.011>.
- [194] Hotchkiss, R. S.; Chang, K. C.; Grayson, M. H.; Tinsley, K. W.; Dunne, B. S.; Davis, C. G.; Osborne, D. F.; Karl, I. E. Adoptive Transfer of Apoptotic Splenocytes Worsens Survival, Whereas Adoptive Transfer of Necrotic Splenocytes Improves Survival in Sepsis. *Proc. Natl. Acad. Sci. U. S. A.* **2003**, *100*, 6724–6729. <https://doi.org/10.1073/pnas.1031788100>.
- [195] Sándor, K.; Pallai, A.; Duró, E.; Legendre, P.; Couillin, I.; Sághy, T.; Szondy, Z. Adenosine Produced from Adenine Nucleotides through an Interaction between Apoptotic Cells and Engulfing Macrophages Contributes to the Appearance of Transglutaminase 2 in Dying Thymocytes. *Amino Acids* **2017**, *49*, 671–681. <https://doi.org/10.1007/s00726-016-2257-5>.
- [196] Gold, R.; Hartung, H. P.; Lassmann, H. T-Cell Apoptosis in Autoimmune Diseases: Termination of Inflammation in the Nervous System and Other Sites with Specialized Immune-Defense Mechanisms. *Trends Neurosci.* **1997**, *20*, 399–404. [https://doi.org/10.1016/S0166-2236\(97\)01079-5](https://doi.org/10.1016/S0166-2236(97)01079-5).
- [197] Cao, L.; Quan, X. B.; Zeng, W. J.; Yang, X. O.; Wang, M. J. Mechanism of Hepatocyte Apoptosis. *J. Cell Death* **2016**, *9*, 19–29. <https://doi.org/10.4137/JCD.S39824>.
- [198] Elliott, M. R.; Ravichandran, K. S. The Dynamics of Apoptotic Cell Clearance. *Dev. Cell* **2016**, *38*, 147–160. <https://doi.org/10.1016/j.devcel.2016.06.029>.
- [199] Poon, I. K. H.; Hulett, M. D.; Parish, C. R. Molecular Mechanisms of Late Apoptotic/Necrotic Cell Clearance. *Cell Death Differ.* **2010**, *17*, 381–397. <https://doi.org/10.1038/cdd.2009.195>.
- [200] Oberhammer, F.; Wilson, J.; Dive, C.; Morris, I.; Hickman, J.; Wakeling, A.; Walker, P.; Sikorska, M. Apoptotic Death in Epithelial Cells: Cleavage of DNA to 300 and/or 50 Kb Fragments Prior to or in the Absence of Internucleosomal Fragmentation. *EMBO J.* **1993**, *12*, 3679–3684. <https://doi.org/10.1002/j.1460-2075.1993.tb06042.x>.
- [201] Wyllie, A. H.; Kerr, J. F. R.; Currie, A. R. Cell Death: The Significance of Apoptosis. *Int. Rev. Cytol.* **1980**, *68*, 251–306. [https://doi.org/10.1016/S0074-7696\(08\)62312-8](https://doi.org/10.1016/S0074-7696(08)62312-8).
- [202] Fadok, V. A.; De Cathelineau, A.; Daleke, D. L.; Henson, P. M.; Bratton, D. L. Loss of Phospholipid Asymmetry and Surface Exposure of Phosphatidylserine Is Required for Phagocytosis of Apoptotic Cells by Macrophages and Fibroblasts. *J. Biol. Chem.* **2001**, *276*, 1071–1077. <https://doi.org/10.1074/jbc.M003649200>.
- [203] Fadok, V. A.; Bratton, D. L.; Rose, D. M.; Pearson, A.; Ezekewitz, R. A. B.; Henson, P. M. A

- Receptor for Phosphatidylserine-Specific Clearance of Apoptotic Cells. *Nature* **2000**, *405*, 85–90. <https://doi.org/10.1038/35011084>.
- [204] Fadok, V. A.; Bratton, D. L.; Guthrie, L.; Henson, P. M. Differential Effects of Apoptotic Versus Lysed Cells on Macrophage Production of Cytokines: Role of Proteases. *J. Immunol.* **2001**, *166*, 6847–6854. <https://doi.org/10.4049/jimmunol.166.11.6847>.
- [205] Doshi, N.; Mitragotri, S.; Bereswill, S. Macrophages Recognize Size and Shape of Their Targets. *PLoS One* **2010**, *5*, 10051. <https://doi.org/10.1371/journal.pone.0010051>.
- [206] Champion, J. A.; Mitragotri, S. Role of Target Geometry in Phagocytosis. *Proc. Natl. Acad. Sci. U. S. A.* **2006**, *103*, 4930–4934. <https://doi.org/10.1073/pnas.0600997103>.
- [207] Meyer, D. J. The Liver. In *Canine and Feline Cytology*; Elsevier, **2016**; pp 259–283. <https://doi.org/10.1016/B978-1-4557-4083-3.00009-7>.
- [208] Hermida, M. D. R.; Malta, R.; De Santos, M. D. P. C.; Dos-Santos, W. L. C. Selecting the Right Gate to Identify Relevant Cells for Your Assay: A Study of Thioglycollate-Elicited Peritoneal Exudate Cells in Mice. *BMC Res. Notes* **2017**, *10*, 1–7. <https://doi.org/10.1186/s13104-017-3019-5>.
- [209] Casanova-Acebes, M.; Nicolás-Ávila, J. A.; Yao Li, J. L.; García-Silva, S.; Balachander, A.; Rubio-Ponce, A.; Weiss, L. A.; Adrover, J. M.; Burrows, K.; A-González, N.; Ballesteros, I.; Devi, S.; Quintana, J. A.; Crainiciuc, G.; Leiva, M.; Gunzer, M.; Weber, C.; Nagasawa, T.; Soehnlein, O.; Merad, M.; Mortha, A.; Ng, L. G.; Peinado, H.; Hidalgo, A. Neutrophils Instruct Homeostatic and Pathological States in Naive Tissues. *J. Exp. Med.* **2018**. <https://doi.org/10.1084/jem.20181468>.
- [210] Chen, W. J.; Frank, M. E.; Jin, W.; Wahl, S. M. TGF- β Released by Apoptotic T Cells Contributes to an Immunosuppressive Milieu. *Immunity* **2001**, *14*, 715–725. [https://doi.org/10.1016/S1074-7613\(01\)00147-9](https://doi.org/10.1016/S1074-7613(01)00147-9).
- [211] Gao, Y.; Herndon, J. M.; Zhang, H.; Griffith, T. S.; Ferguson, T. A. Antiinflammatory Effects of CD95 Ligand (FasL)-Induced Apoptosis. *J. Exp. Med.* **1998**, *188*, 887–896. <https://doi.org/10.1084/jem.188.5.887>.
- [212] Ip, W. K. E.; Hoshi, N.; Shouval, D. S.; Snapper, S.; Medzhitov, R. Anti-Inflammatory Effect of IL-10 Mediated by Metabolic Reprogramming of Macrophages. *Science (80-.)*. **2017**, *356*, 513–519. <https://doi.org/10.1126/science.aal3535>.
- [213] Fattahi, F.; Grailer, J. J.; Lu, H.; Dick, R. S.; Parlett, M.; Zetoune, F. S.; Nuñez, G.; Ward, P. A. Selective Biological Responses of Phagocytes and Lungs to Purified Histones. *J. Innate Immun.* **2017**, *9*, 300–317. <https://doi.org/10.1159/000452951>.
- [214] Mora, J.; Schlemmer, A.; Wittig, I.; Richter, F.; Putyrski, M.; Frank, A. C.; Han, Y.; Jung, M.; Ernst, A.; Weigert, A.; Brüne, B. Interleukin-38 Is Released from Apoptotic Cells to Limit Inflammatory Macrophage Responses. *J. Mol. Cell Biol.* **2016**, *8*, 426–438. <https://doi.org/10.1093/jmcb/mjw006>.
- [215] Cutone, A.; Rosa, L.; Lepanto, M. S.; Scotti, M. J.; Berlutti, F.; di Patti, M. C. B.; Musci, G.; Valenti, P. Lactoferrin Efficiently Counteracts the Inflammation-Induced Changes of the Iron Homeostasis System in Macrophages. *Front. Immunol.* **2017**, *8*, 705. <https://doi.org/10.3389/fimmu.2017.00705>.
- [216] Chen, H.; Kasagi, S.; Chia, C.; Zhang, D.; Tu, E.; Wu, R.; Zanvit, P.; Goldberg, N.; Jin, W.; Chen, W. J. Extracellular Vesicles from Apoptotic Cells Promote TGF β Production in Macrophages and Suppress Experimental Colitis. *Sci. Rep.* **2019**, *9*, 1–10. <https://doi.org/10.1038/s41598-019-42063-7>.
- [217] Jacquet, A. *Purification of Membrane Proteins*; **1990**. [https://doi.org/10.1016/0076-6879\(90\)82040-9](https://doi.org/10.1016/0076-6879(90)82040-9).
- [218] Lee, S. C.; Knowles, T. J.; Postis, V. L. G.; Jamshad, M.; Parslow, R. A.; Lin, Y. P.; Goldman, A.; Sridhar, P.; Overduin, M.; Muench, S. P.; Dafforn, T. R. A Method for Detergent-Free Isolation of Membrane Proteins in Their Local Lipid Environment. *Nat. Protoc.* **2016**, *11*, 1149–1162. <https://doi.org/10.1038/nprot.2016.070>.
- [219] Suski, J. M.; Lebiedzinska, M.; Wojtala, A.; Duszynski, J.; Giorgi, C.; Pinton, P.; Wieckowski, M. R. Isolation of Plasma Membrane-Associated Membranes from Rat Liver. *Nat. Protoc.* **2014**, *9*,

- 312–322. <https://doi.org/10.1038/nprot.2014.016>.
- [220] Martinod, K.; Witsch, T.; Farley, K.; Gallant, M.; Remold-O'Donnell, E.; Wagner, D. D. Neutrophil Elastase-Deficient Mice Form Neutrophil Extracellular Traps in an Experimental Model of Deep Vein Thrombosis. *J. Thromb. Haemost.* **2016**, *14*, 551–558. <https://doi.org/10.1111/jth.13239>.
- [221] Van Der Linden, M.; Westerlaken, G. H. A.; Van Der Vlist, M.; Van Montfrans, J.; Meyaard, L. Differential Signalling and Kinetics of Neutrophil Extracellular Trap Release Revealed by Quantitative Live Imaging. *Sci. Rep.* **2017**, *7*, 6529. <https://doi.org/10.1038/s41598-017-06901-w>.
- [222] Parker, H.; Winterbourn, C. C. Reactive Oxidants and Myeloperoxidase and Their Involvement in Neutrophil Extracellular Traps. *Front. Immunol.* **2012**, *3*, 1–6. <https://doi.org/10.3389/fimmu.2012.00424>.
- [223] Boettcher, M.; Esser, M.; Trah, J.; Klohs, S.; Mokhaberi, N.; Wenskus, J.; Trochimiuk, M.; Appl, B.; Reinshagen, K.; Raluy, L. P.; Klinke, M. Markers of Neutrophil Activation and Extracellular Traps Formation Are Predictive of Appendicitis in Mice and Humans: A Pilot Study. *Sci. Rep.* **2020**, *10*, 1–7. <https://doi.org/10.1038/s41598-020-74370-9>.
- [224] Kruff, B. Apoptotic Neutrophils and Their Selective Capacity to Drive a Tissue Remodelling Function in Macrophages, **2019**, unpublished.
- [225] Čemerski, S.; Shaw, A. Immune Synapses in T-Cell Activation. *Curr. Opin. Immunol.* **2006**, *18*, 298–304. <https://doi.org/10.1016/j.coi.2006.03.011>.
- [226] Barth, N. D.; Marwick, J. A.; Vendrell, M.; Rossi, A. G.; Dransfield, I. The “Phagocytic Synapse” and Clearance of Apoptotic Cells. *Front. Immunol.* **2017**, *8*, 1–9. <https://doi.org/10.3389/fimmu.2017.01708>.
- [227] McGilvray, I. D.; Serghides, L.; Kapus, A.; Rotstein, O. D.; Kain, K. C. Nonopsonic Monocyte/Macrophage Phagocytosis of Plasmodium Falciparum-Parasitized Erythrocytes: A Role for CD36 in Malarial Clearance. *Blood* **2000**, *96*, 3231–3240.
- [228] Myers, K. V.; Amend, S. R.; Pienta, K. J. Targeting Tyro3, Axl and MerTK (TAM Receptors): Implications for Macrophages in the Tumor Microenvironment. *Mol. Cancer* **2019**, *18*, 1–14. <https://doi.org/10.1186/s12943-019-1022-2>.
- [229] Ortiz Wilczyński, J. M.; Olexen, C. M.; Errasti, A. E.; Schattner, M.; Rothlin, C. V.; Correale, J.; Carrera Silva, E. A. GAS6 Signaling Tempers Th17 Development in Patients with Multiple Sclerosis and Helminth Infection. *PLoS Pathog.* **2020**, *16*, e1009176. <https://doi.org/10.1371/journal.ppat.1009176>.
- [230] Masuzaki, R.; Zhao, S.; Valerius, M. T.; Tsugawa, D.; Oya, Y.; Ray, K. C.; Karp, S. J. SOCS2 Balances Metabolic and Restorative Requirements during Liver Regeneration. *J. Biol. Chem.* **2016**, *291*, 3346–3358. <https://doi.org/10.1074/jbc.M115.703264>.
- [231] McCormick, S. M.; Gowda, N.; Fang, J. X.; Heller, N. M. Suppressor of Cytokine Signaling (SOCS)1 Regulates Interleukin-4 (IL-4)-Activated Insulin Receptor Substrate (IRS)-2 Tyrosine Phosphorylation in Monocytes and Macrophages via the Proteasome. *J. Biol. Chem.* **2016**, *291*, 20574–20587. <https://doi.org/10.1074/jbc.M116.746164>.
- [232] Rothlin, C. V.; Ghosh, S.; Zuniga, E. I.; Oldstone, M. B. A.; Lemke, G. TAM Receptors Are Pleiotropic Inhibitors of the Innate Immune Response. *Cell* **2007**, *131*, 1124–1136. <https://doi.org/10.1016/j.cell.2007.10.034>.
- [233] Racanelli, V.; Rehermann, B. The Liver as an Immunological Organ. *Hepatology*. John Wiley & Sons, Ltd February 1, 2006, pp S54–S62. <https://doi.org/10.1002/hep.21060>.
- [234] Parker, G. A.; Picut, C. A. Liver Immunobiology. *Toxicol. Pathol.* **2005**, *33*, 52–62. <https://doi.org/10.1080/01926230590522365>.
- [235] Lee, I. H.; Sohn, M.; Lim, H. J.; Yoon, S.; Oh, H.; Shin, S.; Shin, J. H.; Oh, S. H.; Kim, J.; Lee, D. K.; Noh, D. Y.; Bae, D. S.; Seong, J. K.; Bae, Y. S. Ahnak Functions as a Tumor Suppressor via Modulation of TGFβ/Smad Signaling Pathway. *Oncogene* **2014**, *33*, 4675–4684. <https://doi.org/10.1038/onc.2014.69>.
- [236] Shin, J. H.; Lee, S. H.; Kim, Y. N.; Kim, I. Y.; Kim, Y. J.; Kyeong, D. S.; Lim, H. J.; Cho, S. Y.; Choi, J.; Wi, Y. J.; Choi, J. H.; Yoon, Y. S.; Bae, Y. S.; Seong, J. K. AHNAK Deficiency Promotes Browning

- and Lipolysis in Mice via Increased Responsiveness to β -Adrenergic Signalling. *Sci. Rep.* **2016**, *6*, 1–10. <https://doi.org/10.1038/srep23426>.
- [237] Park, J. W.; Kim, I. Y.; Choi, J. W.; Lim, H. J.; Shin, J. H.; Kim, Y. N.; Lee, S. H.; Son, Y.; Sohn, M.; Woo, J. K.; Jeong, J. H.; Lee, C.; Soo Bae, Y.; Seong, J. K. Oncogenes and Tumor Suppressors AHNAK Loss in Mice Promotes Type II Pneumocyte Hyperplasia and Lung Tumor Development. **2018**. <https://doi.org/10.1158/1541-7786.MCR-17-0726>.
- [238] Antoniv, T. T.; Ivashkiv, L. B. Interleukin-10-Induced Gene Expression and Suppressive Function Are Selectively Modulated by the PI3K-Akt-GSK3 Pathway. *Immunology* **2011**, *132*, 567–577. <https://doi.org/10.1111/j.1365-2567.2010.03402.x>.
- [239] Yamada, K. J.; Barker, T.; Dyer, K. D.; Rice, T. A.; Percopo, C. M.; Garcia-Crespo, K. E.; Cho, S.; Lee, J. J.; Druey, K. M.; Rosenberg, H. F. Eosinophil-Associated Ribonuclease 11 Is a Macrophage Chemoattractant. *J. Biol. Chem.* **2015**, *290*, 8863–8875. <https://doi.org/10.1074/jbc.M114.626648>.
- [240] Cormier, S. A.; Yuan, S.; Crosby, J. R.; Protheroe, C. A.; Dimina, D. M.; Hines, E. M.; Lee, N. A.; Lee, J. J. TH2-Mediated Pulmonary Inflammation Leads to the Differential Expression of Ribonuclease Genes by Alveolar Macrophages. *Am. J. Respir. Cell Mol. Biol.* **2002**, *27*, 678–687. <https://doi.org/10.1165/rcmb.4882>.
- [241] Rosenberg, H. F. Eosinophil-Derived Neurotoxin (EDN/RNase 2) and the Mouse Eosinophil-Associated RNases (MEars): Expanding Roles in Promoting Host Defense. *Int. J. Mol. Sci.* **2015**, *16*, 15442–15455. <https://doi.org/10.3390/ijms160715442>.
- [242] Okabe, Y.; Medzhitov, R. Tissue-Specific Signals Control Reversible Program of Localization and Functional Polarization of Macrophages. *Cell* **2014**, *157*, 832–844. <https://doi.org/10.1016/j.cell.2014.04.016>.
- [243] Dewals, B. G.; Marillier, R. G.; Hoving, J. C.; Leeto, M.; Schwegmann, A.; Brombacher, F. IL-4R α -Independent Expression of Mannose Receptor and Ym1 by Macrophages Depends on Their IL-10 Responsiveness. *PLoS Negl. Trop. Dis.* **2010**, *4*. <https://doi.org/10.1371/journal.pntd.0000689>.
- [244] Attallah, A. M.; Lewis, F. A.; Urritia-Shaw, A.; Folks, T.; Yeatman, T. J. Natural Killer Cells (NK) and Antibody-Dependent Cell-Mediated Cytotoxicity (ADCC) Components of <i>Schistosoma mansoni</i> Infection. *Int. Arch. Allergy Immunol.* **1980**, *63*, 351–354. <https://doi.org/10.1159/000232649>.
- [245] Fu, B.; Wang, F.; Sun, R.; Ling, B.; Tian, Z.; Wei, H. CD11b and CD27 Reflect Distinct Population and Functional Specialization in Human Natural Killer Cells. *Immunology* **2011**, *133*, 350–359. <https://doi.org/10.1111/j.1365-2567.2011.03446.x>.
- [246] INCANI, R. N.; McLAREN, D. J. Neutrophil-Mediated Cytotoxicity to Schistosomula of *Schistosoma mansoni* in Vitro: Studies on the Kinetics of Complement and/or Antibody-Dependent Adherence and Killing. *Parasite Immunol.* **1981**, *3*, 107–126. <https://doi.org/10.1111/j.1365-3024.1981.tb00389.x>.
- [247] Chen, L.; Rao, K. V. N.; He, Y. X.; Ramaswamy, K. Skin-Stage Schistosomula of *Schistosoma mansoni* Produce an Apoptosis-Inducing Factor That Can Cause Apoptosis of T Cells. *J. Biol. Chem.* **2002**, *277*, 34329–34335. <https://doi.org/10.1074/jbc.M201344200>.
- [248] Pearce, E. J.; MacDonald, A. S. The Immunobiology of Schistosomiasis. *Nat. Rev. Immunol.* **2002**, *2*, 499–511. <https://doi.org/10.1038/nri843>.
- [249] Rutitzky, L. I.; Mirkin, G. A.; Stadecker, M. J. Apoptosis by Neglect of CD4 + Th Cells in Granulomas: A Novel Effector Mechanism Involved in the Control of Egg-Induced Immunopathology in Murine Schistosomiasis. *J. Immunol.* **2003**, *171*, 1859–1867. <https://doi.org/10.4049/jimmunol.171.4.1859>.
- [250] Estaquier, J.; Marguerite, M.; Sahuc, F.; Bessis, N.; Ameisen, C. A. and J. C. Interleukin-10 – Mediated T Cell Apoptosis during the T Helpertype 2 Cytokine Response in Murine *Schistosoma mansoni* Parasite Infection. *Eur. Cytokine Netw.* **1997**, *8*, 153–160.
- [251] Buscher, K.; Marcovecchio, P.; Hedrick, C. C.; Ley, K. Patrolling Mechanics of Non-Classical Monocytes in Vascular Inflammation. *Front. Cardiovasc. Med.* **2017**, *4*, 80.

- <https://doi.org/10.3389/fcvm.2017.00080>.
- [252] Liao, X.; Sharma, N.; Kapadia, F.; Zhou, G.; Lu, Y.; Hong, H.; Paruchuri, K.; Mahabeleshwar, G. H.; Dalmas, E.; Venteclaf, N.; Flask, C. A.; Kim, J.; Doreian, B. W.; Lu, K. Q.; Kaestner, K. H.; Hamik, A.; Clément, K.; Jain, M. K. Krüppel-like Factor 4 Regulates Macrophage Polarization. *J. Clin. Invest.* **2011**, *121*, 2736–2749. <https://doi.org/10.1172/JCI45444DS1>.
- [253] Tussiwand, R.; Everts, B.; Grajales-Reyes, G. E.; Kretzer, N. M.; Iwata, A.; Bagaitkar, J.; Wu, X.; Wong, R.; Anderson, D. A.; Murphy, T. L.; Pearce, E. J.; Murphy, K. M. Klf4 Expression in Conventional Dendritic Cells Is Required for T Helper 2 Cell Responses. *Immunity* **2015**, *42*, 916–928. <https://doi.org/10.1016/j.immuni.2015.04.017>.
- [254] Chung, A. S.; Gao, Q.; Kao, W. J. Either Integrin Subunit B1 or B3 Is Involved in Mediating Monocyte Adhesion, IL-1 β Protein and mRNA Expression in Response to Surfaces Functionalized with Fibronectin-Derived Peptides. *J. Biomater. Sci. Polym. Ed.* **2007**, *18*, 713–729. <https://doi.org/10.1163/156856207781034179>.
- [255] Bielefeld, K. A.; Amini-Nik, S.; Whetstone, H.; Poon, R.; Youn, A.; Wang, J.; Alman, B. A. Fibronectin and β -Catenin Act in a Regulatory Loop in Dermal Fibroblasts to Modulate Cutaneous Healing. *J. Biol. Chem.* **2011**, *286*, 27687–27697. <https://doi.org/10.1074/jbc.M111.261677>.
- [256] Patten, J.; Wang, K. Fibronectin in Development and Wound Healing. *Adv. Drug Deliv. Rev.* **2020**. <https://doi.org/10.1016/j.addr.2020.09.005>.
- [257] Yuan, G. C.; Cai, L.; Elowitz, M.; Enver, T.; Fan, G.; Guo, G.; Irizarry, R.; Kharchenko, P.; Kim, J.; Orkin, S.; Quackenbush, J.; Saadatpour, A.; Schroeder, T.; Shivdasani, R.; Tirosh, I. Challenges and Emerging Directions in Single-Cell Analysis. *Genome Biol.* **2017**, *18*, 84. <https://doi.org/10.1186/s13059-017-1218-y>.
- [258] Trahtemberg, U.; Mevorach, D. Apoptotic Cells Induced Signaling for Immune Homeostasis in Macrophages and Dendritic Cells. *Front. Immunol.* **2017**, *8*, 1356. <https://doi.org/10.3389/fimmu.2017.01356>.
- [259] Cabral-Piccin, M. P.; Guillermo, L. V. C.; Vellozo, N. S.; Filardy, A. A.; Pereira-Marques, S. T.; Rigoni, T. S.; Pereira-Manfro, W. F.; Dosreis, G. A.; Lopes, M. F. Apoptotic CD8 T-Lymphocytes Disable Macrophage-Mediated Immunity to Trypanosoma Cruzi Infection. *Cell Death Dis.* **2016**, *7*, e2232–e2232. <https://doi.org/10.1038/cddis.2016.135>.
- [260] De Jesus, A. R.; Silva, A.; Santana, L. B.; Magalhães, A.; De Jesus, A. A.; Pacheco de Almeida, R. P.; Rêgo, M. A. V.; Burattini, M. N.; Pearce, E. J.; Carvalho, E. M. Clinical and Immunologic Evaluation of 31 Patients with Acute Schistosomiasis Mansoni. *J. Infect. Dis.* **2002**, *185*, 98–105. <https://doi.org/10.1086/324668>.
- [261] Mansour, M. M.; Farid, Z.; Bassily, S.; Salah, L. H.; Watten, R. H. Serum Enzyme Tests in Hepatosplenic Schistosomiasis. *Trans. R. Soc. Trop. Med. Hyg.* **1982**, *76*, 109–111. [https://doi.org/10.1016/0035-9203\(82\)90032-3](https://doi.org/10.1016/0035-9203(82)90032-3).
- [262] Singh, K. P.; Gerard, H. C.; Hudson, A. P.; Boros, D. L. Differential Expression of Collagen, MMP, TIMP and Fibrogenic-Cytokine Genes in the Granulomatous Colon of Schistosoma Mansoni-Infected Mice. *Ann. Trop. Med. Parasitol.* **2006**, *100*, 611–620. <https://doi.org/10.1179/136485906X118530>.
- [263] Wolde, M. Human Monocytes / Macrophage In Fl Ammatory Cytokine Changes Following in Vivo and in Vitro Schistomam Manoni Infection. **2020**, 35–43.
- [264] Tang, H.; Liang, Y. B.; Chen, Z. Bin; Du, L. L.; Zeng, L. J.; Wu, J. G.; Yang, W.; Liang, H. P.; Ma, Z. F. Soluble Egg Antigen Activates M2 Macrophages via the STAT6 and PI3K Pathways, and Schistosoma Japonicum Alternatively Activates Macrophage Polarization to Improve the Survival Rate of Septic Mice. *J. Cell. Biochem.* **2017**, *118*, 4230–4239. <https://doi.org/10.1002/jcb.26073>.
- [265] Jankovic, D.; Kullberg, M. C.; Noben-Trauth, N.; Caspar, P.; Ward, J. M.; W.Cheever, A.; Paul, W. E.; Sher, A. Schistosome-Infected IL-4 Receptor Knockout (KO) Mice, in Contrast to IL-4 KO Mice, Fail to Develop Granulomatous Pathology While Maintaining the Same Lymphokine Expression Profile. *J. Immunol.* **1999**, *163*, 337–342. <https://doi.org/10.4049/jimmunol.1300235>.

- [266] Fallon, P. G.; Richardson, E. J.; McKenzie, G. J.; McKenzie, A. N. J. Schistosome Infection of Transgenic Mice Defines Distinct and Contrasting Pathogenic Roles for IL-4 and IL-13: IL-13 Is a Profibrotic Agent. *J. Immunol.* **2000**, *164*, 2585–2591. <https://doi.org/10.4049/jimmunol.164.5.2585>.
- [267] Hoffmann, K. F.; Cheever, A. W.; Wynn, T. A. IL-10 and the Dangers of Immune Polarization: Excessive Type 1 and Type 2 Cytokine Responses Induce Distinct Forms of Lethal Immunopathology in Murine Schistosomiasis. *J. Immunol.* **2000**, *164*, 6406–6416. <https://doi.org/10.4049/jimmunol.164.12.6406>.
- [268] Wynn, T. A. Fibrotic Disease and the TH1/TH2 Paradigm. *Nat. Rev. Immunol.* **2004**, *4*, 583–594. <https://doi.org/10.1038/nri1412>.
- [269] Schwartz, C.; Oeser, K.; Prazeres da Costa, C.; Layland, L. E.; Voehringer, D. T Cell-Derived IL-4/IL-13 Protects Mice against Fatal *Schistosoma mansoni* Infection Independently of Basophils. *J. Immunol.* **2014**, *193*, 3590–3599. <https://doi.org/10.4049/jimmunol.1401155>.
- [270] Reiman, R. M.; Thompson, R. W.; Feng, C. G.; Hari, D.; Knight, R.; Cheever, A. W.; Rosenberg, H. F.; Wynn, T. A. Interleukin-5 (IL-5) Augments the Progression of Liver Fibrosis by Regulating IL-13 Activity. *Infect. Immun.* **2006**, *74*, 1471–1479. <https://doi.org/10.1128/IAI.74.3.1471-1479.2006>.
- [271] Lang, R.; Patel, D.; Morris, J. J.; Rutschman, R. L.; Murray, P. J. Shaping Gene Expression in Activated and Resting Primary Macrophages by IL-10. *J. Immunol.* **2002**, *169*, 2253–2263. <https://doi.org/10.4049/jimmunol.169.5.2253>.
- [272] O'Garra, A.; Vieira, P. L.; Vieira, P.; Goldfeld, A. E. IL-10-Producing and Naturally Occurring CD4⁺Tregs: Limiting Collateral Damage. *J. Clin. Invest.* **2004**, *114*, 1372–1378. <https://doi.org/10.1172/JCI23215>.
- [273] Herbert, D. R.; Orekov, T.; Perkins, C.; Finkelman, F. D. IL-10 and TGF- β Redundantly Protect against Severe Liver Injury and Mortality during Acute Schistosomiasis. *J. Immunol.* **2008**, *181*, 7214–7220. <https://doi.org/10.4049/jimmunol.181.10.7214>.
- [274] Higashiyama, M.; Tomita, K.; Sugihara, N.; Nakashima, H.; Furuhashi, H.; Nishikawa, M.; Inaba, K.; Wada, A.; Horiuchi, K.; Hanawa, Y.; Shibuya, N.; Kurihara, C.; Okada, Y.; Nishii, S.; Mizoguchi, A.; Hozumi, H.; Watanabe, C.; Komoto, S.; Yamamoto, J.; Seki, S.; Miura, S.; Hokari, R. Chitinase 3-like 1 Deficiency Ameliorates Liver Fibrosis by Promoting Hepatic Macrophage Apoptosis. *Hepatol. Res.* **2019**, *49*, 1316–1328. <https://doi.org/10.1111/hepr.13396>.
- [275] Wang, L.; Liu, T.; Zhou, J.; You, H.; Jia, J. Changes in Serum Chitinase 3-like 1 Levels Correlate with Changes in Liver Fibrosis Measured by Two Established Quantitative Methods in Chronic Hepatitis B Patients Following Antiviral Therapy. *Hepatol. Res.* **2018**, *48*, E283–E290. <https://doi.org/10.1111/hepr.12982>.
- [276] Fontana, R. J.; Goodman, Z. D.; Dienstag, J. L.; Bonkovsky, H. L.; Naishadham, D.; Sterling, R. K.; Su, G. L.; Ghosh, M.; Wright, E. C.; Szabo, G.; Cormier, M.; Giansiracusa, D.; Kelley, M.; Reid, A. E.; Chung, R. T.; Molchen, W. A.; Di Giammarino, L.; Richtmyer, P.; Ford, E.; Shiffman, M. L.; Hofmann, C.; Smith, P.; Snow, K. K.; Curto, T. M.; Bell, M. C.; Seeff, L. B.; Robuck, P. R.; Hoofnagle, J. H.; Everhart, J. E. Relationship of Serum Fibrosis Markers with Liver Fibrosis Stage and Collagen Content in Patients with Advanced Chronic Hepatitis C. *Hepatology* **2008**, *47*, 789–798. <https://doi.org/10.1002/hep.22099>.
- [277] Truscott, M.; Evans, D. A.; Gunn, M.; Hoffmann, K. F. *Schistosoma mansoni* Hemozoin Modulates Alternative Activation of Macrophages via Specific Suppression of Retnla Expression and Secretion. *Infect. Immun.* **2013**, *81*, 133–142. <https://doi.org/10.1128/IAI.00701-12>.
- [278] Sun, J.; Li, C.; Wang, S. Organism-like Formation of *Schistosoma* Hemozoin and Its Function Suggest a Mechanism for Anti-Malarial Action of Artemisinin. *Sci. Rep.* **2016**, *6*, 1–10. <https://doi.org/10.1038/srep34463>.
- [279] Sullivan, D. J.; Gluzman, I. Y.; Goldberg, D. E. Plasmodium Hemozoin Formation Mediated by Histidine-Rich Proteins. *Science* (80-.). **1996**, *271*, 219–222. <https://doi.org/10.1126/science.271.5246.219>.
- [280] Nagaraj, V. A.; Sundaram, B.; Varadarajan, N. M.; Subramani, P. A.; Kalappa, D. M.; Ghosh, S. K.;

- Padmanaban, G. Malaria Parasite-Synthesized Heme Is Essential in the Mosquito and Liver Stages and Complements Host Heme in the Blood Stages of Infection. *PLoS Pathog.* **2013**, *9*, 1003522. <https://doi.org/10.1371/journal.ppat.1003522>.
- [281] Gieling, R. G.; Wallace, K.; Han, Y. P. Interleukin-1 Participates in the Progression from Liver Injury to Fibrosis. *Am. J. Physiol. - Gastrointest. Liver Physiol.* **2009**, *296*, 1324–1331. <https://doi.org/10.1152/ajpgi.90564.2008>.
- [282] Biswas, S. K.; Mantovani, A. Macrophage Plasticity and Interaction with Lymphocyte Subsets: Cancer as a Paradigm. *Nat. Immunol.* **2010**, *11*, 889–896. <https://doi.org/10.1038/ni.1937>.
- [283] Barron, L.; Wynn, T. A. Fibrosis Is Regulated by Th2 and Th17 Responses and by Dynamic Interactions between Fibroblasts and Macrophages. *Am. J. Physiol. - Gastrointest. Liver Physiol.* **2011**, *300*, G723–G728. <https://doi.org/10.1152/ajpgi.00414.2010>.
- [284] Gill, S. E.; Kassim, S. Y.; Birkland, T. P.; Parks, W. C. Mouse Models of MMP and TIMP Function. *Methods Mol. Biol.* **2010**, *622*, 31–52. https://doi.org/10.1007/978-1-60327-299-5_2.
- [285] Hotary, K. B.; Allen, E. D.; Brooks, P. C.; Datta, N. S.; Long, M. W.; Weiss, S. J. Membrane Type 1 Matrix Metalloproteinase Usurps Tumor Growth Control Imposed by the Three-Dimensional Extracellular Matrix. *Cell* **2003**, *114*, 33–45. [https://doi.org/10.1016/S0092-8674\(03\)00513-0](https://doi.org/10.1016/S0092-8674(03)00513-0).
- [286] Zigrino, P.; Brinckmann, J.; Niehoff, A.; Lu, Y.; Giebeler, N.; Eckes, B.; Kadler, K. E.; Mauch, C. Fibroblast-Derived MMP-14 Regulates Collagen Homeostasis in Adult Skin. *J. Invest. Dermatol.* **2016**, *136*, 1575–1583. <https://doi.org/10.1016/j.jid.2016.03.036>.
- [287] Cabrera, S.; Selman, M.; Lonzano-Bolaños, A.; Konishi, K.; Richards, T. J.; Kaminski, N.; Pardo, A. Gene Expression Profiles Reveal Molecular Mechanisms Involved in the Progression and Resolution of Bleomycin-Induced Lung Fibrosis. *Am. J. Physiol. - Lung Cell. Mol. Physiol.* **2013**, *304*. <https://doi.org/10.1152/ajplung.00320.2012>.
- [288] Atkinson, J. J.; Toennies, H. M.; Holmbeck, K.; Senior, R. M. Membrane Type 1 Matrix Metalloproteinase Is Necessary for Distal Airway Epithelial Repair and Keratinocyte Growth Factor Receptor Expression after Acute Injury. *Am. J. Physiol. - Lung Cell. Mol. Physiol.* **2007**, *293*. <https://doi.org/10.1152/ajplung.00028.2007>.
- [289] Brew, K.; Dinakarandian, D.; Nagase, H. Tissue Inhibitors of Metalloproteinases: Evolution, Structure and Function. *Biochim. Biophys. Acta - Protein Struct. Mol. Enzymol.* **2000**, *1477*, 267–283. [https://doi.org/10.1016/S0167-4838\(99\)00279-4](https://doi.org/10.1016/S0167-4838(99)00279-4).
- [290] Thiele, N. D.; Wirth, J. W.; Steins, D.; Koop, A. C.; Ittrich, H.; Lohse, A. W.; Kluwe, J. TIMP-1 Is Upregulated, but Not Essential in Hepatic Fibrogenesis and Carcinogenesis in Mice. *Sci. Rep.* **2017**, *7*. <https://doi.org/10.1038/s41598-017-00671-1>.
- [291] Zajac, E.; Schweighofer, B.; Kupriyanova, T. A.; Juncker-Jensen, A.; Minder, P.; Quigley, J. P.; Deryugina, E. I. Angiogenic Capacity of M1- and M2-Polarized Macrophages Is Determined by the Levels of TIMP-1 Complexed with Their Secreted ProMMP-9. *Blood* **2013**, *122*, 4054–4067. <https://doi.org/10.1182/blood-2013-05-501494>.
- [292] Torres, L.; García-Trevijano, E. R.; Rodríguez, J. A.; Carretero, M. V.; Bustos, M.; Fernández, E.; Eguinoa, E.; Mato, J. M.; Avila, M. A. Induction of TIMP-1 Expression in Rat Hepatic Stellate Cells and Hepatocytes: A New Role for Homocysteine in Liver Fibrosis. *Biochim. Biophys. Acta - Mol. Basis Dis.* **1999**, *1455*, 12–22. [https://doi.org/10.1016/S0925-4439\(99\)00049-6](https://doi.org/10.1016/S0925-4439(99)00049-6).
- [293] Holten-Andersen, M. N.; Stephens, R. W.; Nielsen, H. J.; Murphy, G.; Christensen, I. J.; Stetler-Stevenson, W.; Brünner, N. High Preoperative Plasma Tissue Inhibitor of Metalloproteinase-1 Levels Are Associated with Short Survival of Patients with Colorectal Cancer. *Clin. Cancer Res.* **2000**, *6*, 4292–4299.
- [294] Vaillant, B.; Chiaramonte, M. G.; Cheever, A. W.; Soloway, P. D.; Wynn, T. A. Regulation of Hepatic Fibrosis and Extracellular Matrix Genes by the Th Response: New Insight into the Role of Tissue Inhibitors of Matrix Metalloproteinases. *J. Immunol.* **2001**, *167*, 7017–7026. <https://doi.org/10.4049/jimmunol.167.12.7017>.
- [295] Chu, F.; Shi, M.; Zheng, C.; Shen, D.; Zhu, J.; Zheng, X.; Cui, L. The Roles of Macrophages and Microglia in Multiple Sclerosis and Experimental Autoimmune Encephalomyelitis. *J. Neuroimmunol.* **2018**, *318*, 1–7. <https://doi.org/10.1016/j.jneuroim.2018.02.015>.

- [296] Fukui, S.; Iwamoto, N.; Takatani, A.; Igawa, T.; Shimizu, T.; Umeda, M.; Nishino, A.; Horai, Y.; Hirai, Y.; Koga, T.; Kawashiri, S. Y.; Tamai, M.; Ichinose, K.; Nakamura, H.; Origuchi, T.; Masuyama, R.; Kosai, K.; Yanagihara, K.; Kawakami, A. M1 and M2 Monocytes in Rheumatoid Arthritis: A Contribution of Imbalance of M1/M2 Monocytes to Osteoclastogenesis. *Front. Immunol.* **2018**, *8*. <https://doi.org/10.3389/fimmu.2017.01958>.
- [297] Poltavets, A. S.; Vishnyakova, P. A.; Elchaninov, A. V.; Sukhikh, G. T.; Fatkhudinov, T. K. Macrophage Modification Strategies for Efficient Cell Therapy. *Cells* **2020**, *9*. <https://doi.org/10.3390/cells9061535>.
- [298] Zhang, F.; Parayath, N. N.; Ene, C. I.; Stephan, S. B.; Koehne, A. L.; Coon, M. E.; Holland, E. C.; Stephan, M. T. Genetic Programming of Macrophages to Perform Anti-Tumor Functions Using Targeted mRNA Nanocarriers. *Nat. Commun.* **2019**, *10*. <https://doi.org/10.1038/s41467-019-11911-5>.
- [299] Yi, X.; Zhang, J.; Zhuang, R.; Wang, S.; Cheng, S.; Zhang, D.; Xie, J.; Hu, W.; Liu, X.; Zhang, Y.; Ding, Y.; Zhang, Y. Silencing LAIR-1 in Human THP-1 Macrophage Increases Foam Cell Formation by Modulating PPAR γ and M2 Polarization. *Cytokine* **2018**, *111*, 194–205. <https://doi.org/10.1016/j.cyto.2018.08.028>.
- [300] Lee, C.; Jeong, H.; Bae, Y.; Shin, K.; Kang, S.; Kim, H.; Oh, J.; Bae, H. Targeting of M2-like Tumor-Associated Macrophages with a Melittin-Based pro-Apoptotic Peptide. *J. Immunother. Cancer* **2019**, *7*. <https://doi.org/10.1186/s40425-019-0610-4>.
- [301] Moroni, F.; Dwyer, B. J.; Graham, C.; Pass, C.; Bailey, L.; Ritchie, L.; Mitchell, D.; Glover, A.; Laurie, A.; Doig, S.; Hargreaves, E.; Fraser, A. R.; Turner, M. L.; Campbell, J. D. M.; McGowan, N. W. A.; Barry, J.; Moore, J. K.; Hayes, P. C.; Leeming, D. J.; Nielsen, M. J.; Musa, K.; Fallowfield, J. A.; Forbes, S. J. Safety Profile of Autologous Macrophage Therapy for Liver Cirrhosis. *Nat. Med.* **2019**, *25*, 1560–1565. <https://doi.org/10.1038/s41591-019-0599-8>.
- [302] Xu, R.; Huang, H.; Zhang, Z.; Wang, F. S. The Role of Neutrophils in the Development of Liver Diseases. *Cell. Mol. Immunol.* **2014**, *11*, 224–231. <https://doi.org/10.1038/cmi.2014.2>.
- [303] Souza, C.; Sanches, R. C. O.; Assis, N. R. G.; Marinho, F. V.; Mambelli, F. S.; Morais, S. B.; Gimenez, E. G. T.; Guimarães, E. S.; Castro, T. B. R.; Oliveira, S. C. The Role of the Adaptor Molecule STING during *Schistosoma Mansoni* Infection. *Sci. Rep.* **2020**, *10*, 1–14. <https://doi.org/10.1038/s41598-020-64788-6>.
- [304] Morais, S. B.; Figueiredo, B. C.; Assis, N. R. G.; Alvarenga, D. M.; de Magalhães, M. T. Q.; Ferreira, R. S.; Vieira, A. T.; Menezes, G. B.; Oliveira, S. C. *Schistosoma Mansoni* SmKI-1 Serine Protease Inhibitor Binds to Elastase and Impairs Neutrophil Function and Inflammation. *PLoS Pathog.* **2018**, *14*, e1006870. <https://doi.org/10.1371/journal.ppat.1006870>.
- [305] Andrade, Z. A.; Grimaud, J. A. Evolution of the Schistosomal Hepatic Lesions in Mice after Curative Chemotherapy. *Am. J. Pathol.* **1986**, *124*, 59–65.
- [306] Gomez, D. E.; De Lorenzo, M. S.; Alonso, D. F.; Andrade, Z. A. Expression of Metalloproteinases (MMP-1, MMP-2, and MMP-9) and Their Inhibitors (TIMP-1 and TIMP-2) in Schistosomal Portal Fibrosis. *Am. J. Trop. Med. Hyg.* **1999**, *61*, 9–13. <https://doi.org/10.4269/ajtmh.1999.61.9>.
- [307] Joseph, M.; Capron, A.; Butterworth, A. E.; Sturrock, R. F.; Houba, V. Cytotoxicity of Human and Baboon Mononuclear Phagocytes against *Schistosoma* in Vitro: Induction by Immune Complexes Containing IgE and *Schistosoma Mansoni* Antigens. *Clin. Exp. Immunol.* **1978**, *33*, 48–56.
- [308] Råberg, L.; Graham, A. L.; Read, A. F. Decomposing Health: Tolerance and Resistance to Parasites in Animals. *Philos. Trans. R. Soc. B Biol. Sci.* **2009**, *364*, 37–49. <https://doi.org/10.1098/rstb.2008.0184>.
- [309] Medzhitov, R.; Schneider, D. S.; Soares, M. P. Disease Tolerance as a Defense Strategy. *Science (80-.)* **2012**, *335*, 936–942. <https://doi.org/10.1126/science.1214935>.
- [310] Dubois-Colas, N.; Petit-Jentreau, L.; Barreiro, L. B.; Durand, S.; Soubigou, G.; Lecointe, C.; Klibi, J.; Rezaï, K.; Lokiec, F.; Coppée, J. Y.; Gicquel, B.; Tailleux, L. Extracellular Adenosine Triphosphate Affects the Response of Human Macrophages Infected with *Mycobacterium Tuberculosis*. *J. Infect. Dis.* **2014**, *210*, 824–833. <https://doi.org/10.1093/infdis/jiu135>.

- [311] Pollard, T. D. MBOC Technical Perspective: A Guide to Simple and Informative Binding Assays. *Mol. Biol. Cell* **2010**, *21*, 4061–4067. <https://doi.org/10.1091/mbc.E10-08-0683>.
- [312] Barta, P.; Volkova, M.; Dascalu, A.; Spiegelberg, D.; Trejtnar, F.; Andersson, K. Determination of Receptor Protein Binding Site Specificity and Relative Binding Strength Using a Time-Resolved Competition Assay. *J. Pharmacol. Toxicol. Methods* **2014**, *70*, 145–151. <https://doi.org/10.1016/j.vascn.2014.07.006>.
- [313] Morrissey, M. A.; Williamson, A. P.; Steinbach, A. M.; Roberts, E. W.; Kern, N.; Headley, M. B.; Vale, R. D. Chimeric Antigen Receptors That Trigger Phagocytosis. *Elife* **2018**, *7*. <https://doi.org/10.7554/eLife.36688>.